Domestication of environmental bacteria for biosensing applications

Thesis by
Elin M. Larsson

In Partial Fulfillment of the Requirements for the
Degree of
Doctor of Philosophy in Bioengineering

CALIFORNIA INSTITUTE OF TECHNOLOGY
Pasadena, California

2025
Defended April 14, 2025

Elin M. Larsson
ORCID: 0000-0003-1341-5937

ACKNOWLEDGEMENTS

Since first coming to Caltech in 2018 as an undergraduate researcher, I have had the privilege to interact with, and work alongside, extraordinary people. There are countless people I would like to thank for contributing to enriching my time at Caltech, but I am going to try to highlight a small fraction of people.

First, I'd like to thank the friends from the UK, Iceland, and Stockholm I met as an undergraduate researcher in the SURF program. Your support made me believe that the future was bright.

I'd also like to thank my lab mates in the Murray lab who welcomed me and made coming in to the lab a lot of fun. Rory, my SURF mentor, taught me everything I know about the day-to-day work in the lab. Thank you, Matt for using your superpower of knowing when someone needs to de-stress by laughing and making that happen. Manisha, I am going to miss your sense of humor, no-nonsense attitude, and intelligence. Alex, Andrey, Andy, Blade, Joe, Nikos, Yan, and others who I have crossed paths with in the lab — thank you for many laughs and conversations throughout the years.

Olivia, I am lucky to have gotten to be your mentor for a year where I got to learn as much from you as you did from me.

Miki, thank you for making my journey easier every time I needed help with lab-related business or when I needed to vent.

Mark and Reed have become more than colleagues. I am humbled by your kindness and support as well as the privilege to share important moments in our lives. Sam and Sarah, it has been truly wonderful to get to spend time with you, even when I was staying with you during the Eaton fire. I am grateful to you for your generosity and kindness during that time.

Kellan, I am so happy you agreed to become my gym buddy and thereby being a crucial part in me retaining my sanity in 4th and 5th year. I am sad we won't work on our gains anymore, but happy that we'll stay friends.

Carly, it's harder to make new friendships the older you get, and I am grateful our paths crossed by many random events aligning so that we could become colleagues and friends.

I'd like to thank members of the Newman lab where I have had many role models in science and beyond. Avi, my first mentor in the lab for your patience and endless advice that I have tried to take to heart. Darcy, who was my first wetlab mentor while rotating in the lab: your work ethic and rigor set the bar high day 1 and your kindness allowed me to make mistakes without feeling too bad about it. Steven taught me the power of communicating your science efficiently and clearly. Chelsey, who I was looking up to but too scared to talk to initially because of her radiating boss-vibes. I am grateful to have become friends with both you and your husband John. Thank you both for everything you taught me, in and out of the lab. Georgia, you taught me a lot about what it means to be a scientist, but I am the most grateful for you (and Sean) teaching me how to lift weights. Lev, I really admire you for truly caring about other people and always felt like I had someone I could talk to and be silly with in you.

Korbi and Richard, starting grad school at the same strange pandemic times created a special bond between us and I feel lucky that you two were the ones joining the lab at the same time as I did.

Amanda and Tess, it's been amazing to be able to support each other through this experience. Thank you for always being there and for challenging me to try new things during grad school.

Magnus, thank you for hosting me at the beginning of my PhD before the borders had reopened during the pandemic. You've remained a supportive mentor all the way from my undergrad years to this day. Daniel, you and Eoin were the first people who really inspired me to pursue microbiology. I will not forget that, nor will I forget your passion for teaching and your mentorship during my time at LTH.

Woody, thank you for hosting me for a summer rotation and encouraging me in the early days of my PhD. Hannah, I am so glad I got to meet you during this time to learn all I know about field work from you and become your friend.

I'd like to thank my committee members Jared Leadbetter, Bruce Hay, and Mengyi Cao for your feedback and support.

Dianne, thank you for taking a chance on me as your first Bioengineering graduate student. You have taught me so much about what it means to be a leader and a mentor. Your excitement about science shines through in every interaction. I will take that with me in my next steps.

Richard, I have so much to thank you for. Your faith in me changed the trajectory of my life and helped make me the scientist I am today. Thank you for your kindness, patience, and support through this long journey.

I'd like to thank my friends in Sweden for always making me feel like there was a candle lit inside my chest whenever I came to visit you during my time off. Daniel, Ella, Erik, and Frida, I am grateful to have met you in college and maintained friendships that I value deeply. Sara, Tommy, Andreas, Matilda, Per, Johanna, thank you for still putting up with me after all these years. Please keep it up. Fanny, I am incredibly lucky to know and share a friendship like ours that has shaped who I am in profound ways for the past 23 years. Thank you for being there through everything.

Thank you to my US aunts, uncles, cousins and their families for helping me out with various culture clashes and for always being up for adventures. I have enjoyed so much to spend time with you all.

Thank you to my family for your support and understanding that although I was far away, my heart was in the right place.

Last of all I would like to thank my husband John, for always believing in my resilience and strength in finishing this journey. Thank you for being my anchor and for making me laugh every single day even when it seemed impossible.

ABSTRACT

The field of synthetic biology has made impressive progress in the past 25 years, but is still lacking when it comes to our capability to predictably engineer organisms outside of a small group of lab model organisms. In this thesis, I present the efforts to domesticate two soil bacteria important in agriculture for biosensing. The first, *Pseudomonas synxantha*, a wheat-colonizing bacterium that helps fight off fungal disease, was engineered into a bioreporter for phosphorus limitation. We also made cell-free extract from this organism, to enable rapid characterization of genetic elements. For the second, *Xenorhabdus griffiniae*, we asked the question of whether this bacterium can sense the presence of its entomopathogenic nematode host *Steinernema hermaphroditum*. We learned that *X. griffiniae* is able to sense its host and we were able to build an early variant of a nematode reporter by first characterizing genetic elements in *X. griffiniae*.

PUBLISHED CONTENT AND CONTRIBUTIONS

1 Elin M. Larsson, Richard M. Murray, and Dianne K. Newman. "Engineering the soil bacterium *Pseudomonas synxantha* 2–79 into a ratiometric bioreporter for phosphorus limitation". *ACS Synthetic Biology* 13.1 (2024), pp. 384–393. DOI: 10.1021/acssynbio.3c00642.

2 Joseph T. Meyerowitz*, Elin M. Larsson*, and Richard M. Murray. "Development of cell-free transcription–translation Systems in three soil pseudomonads". *ACS Synthetic Biology* 13.2 (2024), pp. 530–537. DOI: 10.1021/acssynbio.3c00468.

TABLE OF CONTENTS

Chapter 1

INTRODUCTION

The microorganisms that live in the soil we walk on do amazing chemistry, and we only know a small fraction of what they are doing. From making compounds designed for warfare with other organisms to aiding themselves in surviving drought or nutrient and oxygen limitation, they have evolved strategies for thriving in the soil ecosystem. Many these organisms have even co-evolved to rely on each other for survival and quickly get rid of intruders trying to enter their niche. All of these interactions are enabled by the fact that sensing is happening so that a given organism can decide who is a friend and who is a foe and take proper action.

1.1 Why do we need sensing in biology?

The ability to know the localization and concentration of different molecules is a crucial part in understanding biological and environmental processes. Therefore, sensing coupled to a readable output is of great importance, both for fundamental understanding as well as a variety of direct applications. In medicine, we need to be able to understand drug metabolism and uptake in the gut [1] and how antibiotic resistance spreads in the environment and in the clinic [2]. Sensors for glucose levels are crucial for people with diabetes and enzyme-based, and immunological biosensors are critical in diagnostics. In the food and beverage industry, detection of toxins and contaminants ensure safe products for consumers.

In agriculture, we face an abundance of challenges regarding fertilizer and water use, plant-pathogen spread and degrading soil quality. Some of these challenges could benefit from solutions in sensing. Future developments in remote sensing could lead to irrigation and fertilizer application where it is needed [3]. Early detection of crop pests like root-knot nematodes could allow localized early intervention to stop spread. Lastly, addressing soil quality by determining the concentration of pollutants such as heavy metals and pesticides could allow decision-making for soil remediation.

1.2 Whole-cell biosensors and their applications

Whole-cell biosensors, or bioreporters, are living cells that report on the presence of analytes or a physical property like temperature [4] by converting the signal to

a readable output. These are different from microbial surface-display biosensors, where an enzyme is anchored to the cell surface. Here, it is the enzyme that is responsible for the sensing modality, not the bacterial cell itself. Another class of sensors is cell-free biosensors, which present many promising qualities but are limited by the lack of compartmentalization that living cells use to detect molecules in their environment.

In a brief history of this topic, the Ames test might be considered the first biosensor (1973) [5, 6] followed by the SOS chromotest (1982) [7], which are both used to determine if and at what concentration compounds are carcinogenic (Figure 1.1). The first GFP fusion (1994) enabled the study of gene expression and protein localization *in vivo* [8] and allowed the construction of early biosensors in bacteria. The field of synthetic biology as we know it today was born in 2000 with the work describing the construction of the repressilator [9] and the toggle switch [10]. Both of these combine biology and engineering to program living bacteria to behave in a predictable manner and have substantially accelerated the complexity of whole-cell biosensors today. Examples include biosensors for heavy metals [11, 12], pathogens [13] and crop-relevant nutrients [14]. All of these are based on direct sensing of ions or molecules, but one can also have other types of inputs, for example detection of specific DNA sequences [15, 16]. The outputs of these different sensors include colorimetry, fluorescence, luminescence, volatile gases [17] and sequencing-based outputs.

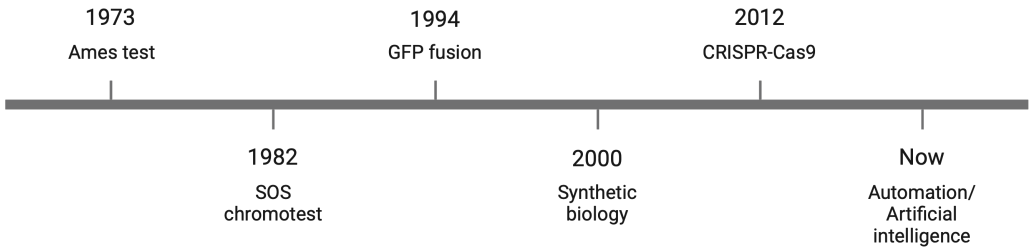

Figure 1.1: Significant milestones in biosensor development.

1.3 Why is "bio" significant for sensing?

There are other ways to sense molecules than using biological cells, for example by using electrochemistry or optics, and sometimes they are better, for example in terms of shelf-stability. Concerns that are remaining challenges for whole-cell biosensors include shelf-life, safe deployment/regulation concerns, loss of function

and limit of detection There are however several reasons why one might want to choose a whole-cell biosensor over other types of sensors.

Building a sensor in a living cell means that one can also couple the sensing to actuation. For example, one could couple sensing of a pathogen to production of an antibiotic, or the production of alkaline phosphatase in the rhizosphere upon sensing phosphorus limitation. This allows for localized action where it is needed. This ability to sense conditions at the microscale is particularly useful in heterogeneous environments like soils and the rhizosphere. The use of bacterial cells also means that one can sense, and possibly respond to, multiple inputs at a time. Bacteria are also able to sense the bioavailable fraction of molecules. For example, bacteria and plants in a soil that has large amounts of legacy phosphorus, phosphorus tightly bound to minerals and clays, might still experience phosphorus limitation if there is no bioavailable phosphorus that can be taken up from the environment. Chemical tests (Olson, Bray, and Mehlich-3) that are commonly used for determining phosphorus concentrations in soil [18–20], do not account for the fact that this phosphorus is unavailable to biology, and therefore need to be calibrated against plant productivity to be informative.

Another advantage is that bacteria are good at adjusting to their environment, meaning whole-cell biosensors allow some shifts in temperature, pH and moisture level. This might also mean that using bacterial cells, long-term monitoring in situ could become a reality. In this case, the bacteria can be coupled to electronics that can translate their signal to a readable output [21].

1.4 Sensors and actuators should be engineered into strains that naturally exist within the target environment

Although we can program bacteria to do certain tasks, we often overlook the fact that the lab-adjusted strains cannot stand a chance in the environmental context. Engineered *E. coli* bacteria die quickly compared to the native soil microbiome [22, 23]. First, this is suggesting that it might be beneficial to instead engineer bacteria from a specific niche and then re-introduce them. That way, the bacteria are adapted to the particular challenges in that environment. It can be fairly uncomplicated to do metabolic engineering to enable usage of a certain carbon source, but it is harder to engineer tolerance to pH, temperature and some toxins. Second, this is suggesting that the biosensors that are developed in the lab ought to be tested in a variety of conditions that are relevant to the environment they are to be deployed

in, whether that is the human gut or the rhizosphere. If all testing is done in shaken cultures where nutrients and oxygen are plentiful, we might miss the limitations of the designed biosensor.

1.5 Cell factories often benefit from using non-model chassis

Although model organisms like *E. coli* and *S. cerevisiae* have been extensively used in industry and are well-studied and easy to manipulate, the genetic diversity of microorganisms in soil could potentially offer solutions to many problems we are facing in sustainability and medicine today. Advancing computational biology approaches can help us explore this space to some degree through metagenomics. However, we will still need to validate the function of whatever we predict to be promising *in silico*. This becomes relevant in the context of cell-factories, biological cells that have been altered, using synthetic biology or metabolic engineering, to produce valuable products for different industries. As an example, *E. coli* does not have the metabolic capacity to make all chemicals we would want to produce at scale and is not tolerant to all feed-stocks nor conditions that can be common in large-scale fermenters. It's beneficial to have a strain that is tolerant to extreme pH because then we do not have to make sure the system is buffered. The same thing goes for temperature — if a strain can tolerate higher temperatures, money can be saved on cooling. Another aspect is the ability to use other carbon sources than glucose, both to lower feedstock costs, but also to avoid the direct competition with using feedstocks that could have been consumed by people. Therefore, using non-model, high-tolerance bacteria derived from the environment can be beneficial when developing cell factories for large-scale production.

1.6 "Domesticating" means different things to different audiences

When we think about the word "domesticate" the first thing that comes to mind might be domestication of farm animals like chickens or dairy-cows, or the domestication of insects like honey-bees or even food crops such as wheat. Molecular biologists and geneticists might think about the laboratory adaptation undergone by model organisms *Drosophila melanogaster* and *Caenorhabditis elegans* [24, 25]. Finally, microbiologists need to consider how bacteria adapt to growth in the laboratory [26]. However, the domestication of bacteria is not limited to the laboratory. The oldest type of microbial domestication is unarguably the use of microbes in fermentations for food preservation (Figure 1.2) [27]. In this simple case, microbes are passaged from one batch of fermentation to the next in order to inoculate each fresh batch.

During this type of passaging, the microbes naturally adapt to their growth habitat by altering their genetic composition, without human interference [28]. The next level of domestication might be considered the ability to take microbes from the environment and grow them under controlled conditions in the laboratory to enable studying them. This can include growing the bacteria by themselves in pure culture, or growing them in co-cultures with obligate partners required for growth. To be able to do this, we need knowledge about how to grow and preserve the bacteria in the lab. What nutrients are vital for their growth, what temperature and pH range and oxygen concentrations are acceptable? The last step of domestication after reliably being able to grow and store the bacteria in the lab is to be able to do genetic alterations. The definition of domestication in this thesis refers to the most complex end of this gradient. Not only do we want to be able to delete genes, but also engineer the bacteria to express exogenous genes in a predictable manner. This type of domestication opens the door for a wide variety of applications such as biosensors and cell factories, described above.

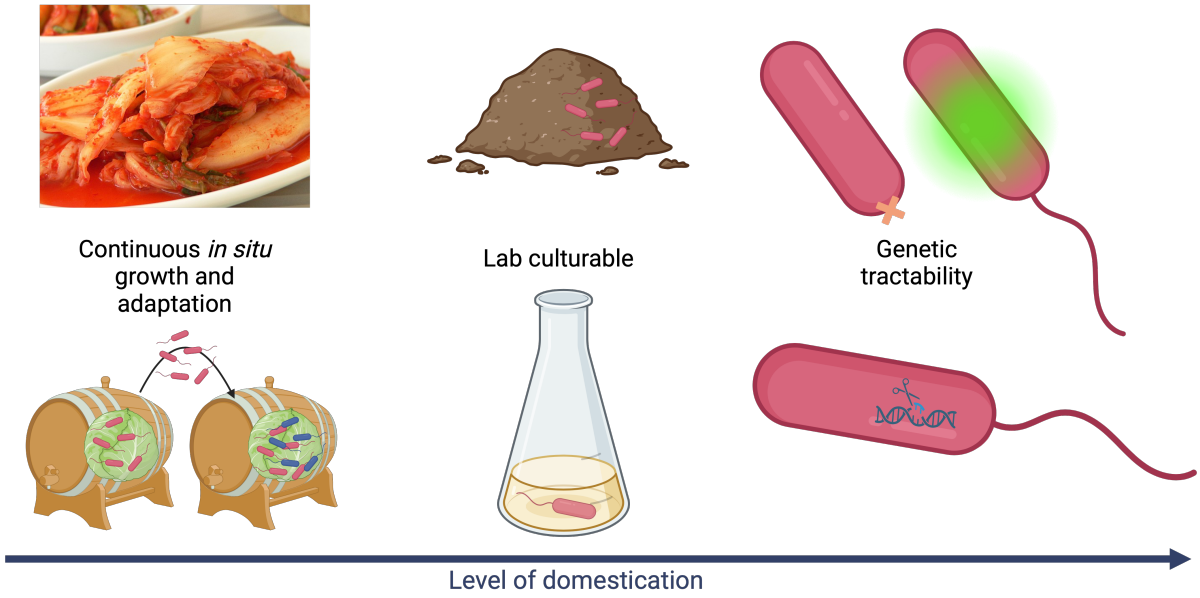

Figure 1.2: Domestication increased complexity.

Several companies were started to make the effort to harness these properties by domesticating environmental microbes for industrial use at scale. MicroByre (US) was aiming to make toolkits for non-model bacteria until going out of business in 2024. Cultivarum (US), Ginkgo Bioworks (US), Wild Microbes (US) and Evolutor

(UK) are still using synthetic biology, evolution, genetics, automation, and other approaches for strain engineering of microbes.

1.7 Challenges engineering non-model bacteria

First, a suitable chassis organism that is culturable under lab conditions must be selected. Then, a reliable transformation protocol of high enough efficiency must be developed to be used both for gene deletions and insertions. A common challenge to overcome when delivering foreign DNA is the cell's host defense system. If DNA can be delivered, we must be able to select for it, usually using antibiotic markers. This means that multi-resistant bacteria have fewer options to choose from in terms of resistance cassettes. Ideally, the ability to flip out antibiotic resistance cassettes is also possible when gene deletions or insertions on the chromosome are done. If the DNA is to be kept in the form of a plasmid, we also need to make sure that it can be maintained in the cell, i.e., that the origin of replication is compatible with the species we are working with. When working with non-model bacteria we face challenges such as differences in transcription/translation machinery, e.g., sigma factors vary between species [29], different termination mechanisms [30, 31], codon usage [32], and others. Another challenge is physiological compatibility of genetic parts and proteins, since the intracellular environment is different in bacteria from various habitats.

To be able to do genetic manipulations using synthetic biology and metabolic engineering, there are certain requirements that need to be met. Characterization of functional genetic parts must be done and the number of needed elements increases for more complex designs. For example identification and characterization of constitutive promoters, ribosome binding sites, fluorescent proteins (or other required coding sequences), terminators, integrases, degradation tags and non-leaky systems for transcription factor-based inducible expression might be required.

1.8 The *Pseudomonas* genus

Pseudomonads are gram-negative bacteria in the Gammaproteobacteria class. Their adaptability and metabolic diversity make them populate diverse niches such as chronic wounds, soil and the rhizosphere. They have also gained interest as industrial chassis due to their tolerance to toxic compounds that are common in low-cost feedstocks. *Pseudomonas putida* is one of the most well-studied "industrial" pseudomonad, *Pseudomonas aeruginosa* is the most well-studied human pathogen pseudomonad and *Pseudomonas fluorescens* is the most studied soil/plant associated

pseudomonad. The two latter make phenazines (phz), redox-active molecules that have antimicrobial properties as well as act as electron shuttles during oxygen-limited growth [33]. One species of interest for engineering is a close relative of *P. fluorescens*, *Pseudomonas synxantha*, a wheat-colonizing bacterium that produces the redox-active metabolite phenazine-1-carboxylic acid (PCA). *P. synxantha* lives on the plant roots where it releases PCA that protects the plant from disease [34]. In fact, a majority of wheat is colonized by phz+ species [35] highlighting the importance of these microbes to the health of the plant. We also know that the production of PCA is upregulated when the cells are limited for P. It is unclear why this is, but one potential explanation could be that these molecules also have the ability under certain conditions to liberate P from minerals through reductive dissolution [36]. In addition to being important for the wheat crop, *P. synxantha* is genetically tractable and non-pathogenic which are both important considerations for choosing a chassis to engineer.

1.9 The *Xenorhabdus* genus

Xenorhabdus spp. are gram-negative bacteria in the Gammaproteobacteria class. These bacteria are obligate symbionts of entomopathogenic (disease-causing in insects) nematodes in the *Steinernema* genus. The first species to be described was *Achromobacter nematophilus* (later *Xenorhabdus nematophila*) [37, 38].

Entomopathogenic nematodes infect many different insects and have therefore been suggested as potential replacements or supplements for chemical pesticides in agriculture [39, 40]. The bacterial symbiont sits in a compartment of the nematode intestine called the receptacle when the nematode is searching for an insect prey in the soil (Figure 1.3). Once an insect is found the nematode enters the insect through natural body openings and releases the bacteria through the mouth and anus. *Xenorhabdus* can then start to make a cocktail of toxins, enzymes (lipases and proteases), immunosuppressants and antimicrobials that help in killing, degrading and preserving the insect [41, 42]. After depleting the nutrients in the insect cadaver, the bacteria can recolonize the nematodes that disperse into the soil environment in search of a new insect larvae to infect.

Xenorhabdus griffiniae is the bacterial symbiont of *Steinernema hermaphroditum*, a consistently hermaphroditic entomopathogenic nematode. Although *X. griffiniae* is an obligate symbiont of *S. hermaphroditum* in the wild, they can be grown and

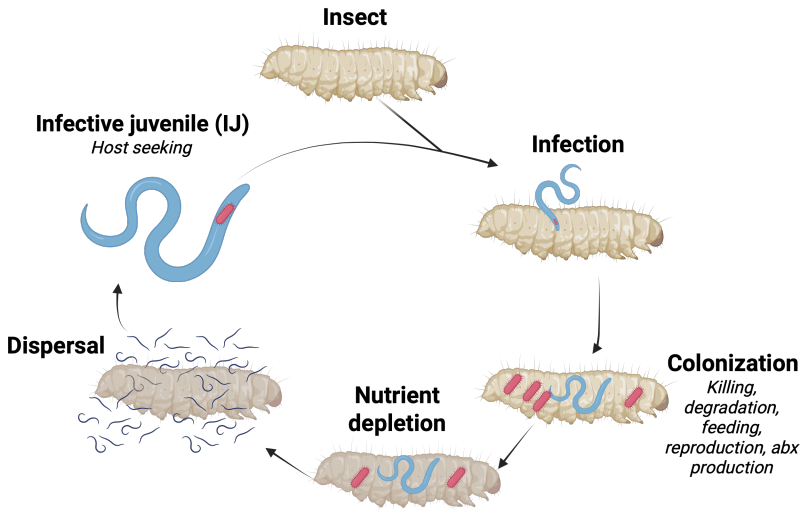

Figure 1.3: A simplified schematic of the *Steinernema-Xenorhabdus* life cycle.

studied independently in the lab. Both the bacteria and the nematode are genetically tractable.

1.10 Outline of thesis chapters

In Chapter 2, the bioengineering part of a larger multi-lab effort aiming to build a sensor for phosphorus limitation is presented. This work highlights the importance of making an effort to characterize performance under some of the variable conditions engineered bacteria face in a non-lab environment.

In Chapter 3, joint work with a former graduate student in the lab, Dr. Joseph Meyerowitz, making and characterizing cell-free extract made from three soil Pseudomonads and comparing that to gene expression *in vivo* is presented.

In Chapter 4, joint work with Caltech undergraduate student Olivia Wang building and characterizing a DNA part library for *Xenorhabdus griffiniae* to enable reliable strain engineering is presented.

In Chapter 5, the last project of my PhD, where I was trying to answer the question of whether a bacterial symbiont, *Xenorhabdus*, of an entomopatogenic nematode, *Sterinernema*, has the ability to sense and respond to the presence of its host is presented.

In Chapter 6, the initial steps towards constructing a "nematode reporter" are presented.

In Chapter 7, the conclusion of this thesis and the outlook and potential future directions of this work are outlined.

References

[1] Yuhua Li, Qiang Meng, Mengbi Yang, Dongyang Liu, Xiangyu Hou, Lan Tang, Xin Wang, Yuanfeng Lyu, Xiaoyan Chen, Kexin Liu, et al. "Current trends in drug metabolism and pharmacokinetics". *Acta Pharmaceutica Sinica B* 9.6 (2019), pp. 1113–1144.

[2] Elizabeth Peterson and Parjit Kaur. "Antibiotic resistance mechanisms in bacteria: Relationships between resistance determinants of antibiotic producers, environmental bacteria, and clinical pathogens". *Frontiers in Microbiology* 9 (2018), p. 2928.

[3] Robin Gebbers and Viacheslav I. Adamchuk. "Precision agriculture and food security". *Science* 327.5967 (2010), pp. 828–831.

[4] Lealia L. Xiong, Michael A. Garrett, Marjorie T. Buss, Julia A. Kornfield, and Mikhail G. Shapiro. "Tunable temperature-sensitive transcriptional activation based on lambda repressor". *ACS Synthetic Biology* 11.7 (2022), pp. 2518–2522.

[5] Bruce N. Ames, William E. Durston, Edith Yamasaki, and Frank D. Lee. "Carcinogens are mutagens: a simple test system combining liver homogenates for activation and bacteria for detection". *Proceedings of the National Academy of Sciences* 70.8 (1973), pp. 2281–2285.

[6] Bruce N. Ames, Frank D. Lee, and William E. Durston. "An improved bacterial test system for the detection and classification of mutagens and carcinogens". *Proceedings of the National Academy of Sciences* 70.3 (1973), pp. 782–786.

[7] Philippe Quillardet, Olivier Huisman, Richard D'ari, and Maurice Hofnung. "SOS chromotest, a direct assay of induction of an SOS function in Escherichia coli K-12 to measure genotoxicity." *Proceedings of the National Academy of Sciences* 79.19 (1982), pp. 5971–5975.

[8] Martin Chalfie, Yuan Tu, Ghia Euskirchen, William W. Ward, and Douglas C. Prasher. "Green fluorescent protein as a marker for gene expression". *Science* 263.5148 (1994), pp. 802–805.

[9] Michael B. Elowitz and Stanislas Leibler. "A synthetic oscillatory network of transcriptional regulators". *Nature* 403.6767 (2000), pp. 335–338.

[10] Timothy S. Gardner, Charles R. Cantor, and James J. Collins. "Construction of a genetic toggle switch in *Escherichia coli*". *Nature* 403.6767 (2000), pp. 339–342.

[11] Xiaoqiang Jia, Rongrong Bu, Tingting Zhao, and Kang Wu. "Sensitive and specific whole-cell biosensor for arsenic detection". *Applied and Environmental Microbiology* 85.11 (2019), e00694–19.

[12] Aziz Babapoor, Reza Hajimohammadi, Seyyed Mohammad Jokar, and Meysam Paar. “Biosensor design for detection of mercury in contaminated soil using rhamnolipid biosurfactant and luminescent bacteria”. *Journal of Chemistry* 2020 (2020), pp. 1–8.

[13] Ying Wu, Chien-Wei Wang, Dong Wang, and Na Wei. “A whole-cell biosensor for point-of-care detection of waterborne bacterial pathogens”. *ACS Synthetic Biology* 10.2 (2021), pp. 333–344.

[14] Kristen M. DeAngelis, Pingsheng Ji, Mary K. Firestone, and Steven E. Lindow. “Two novel bacterial biosensors for detection of nitrate availability in the rhizosphere”. *Applied and Environmental Microbiology* 71.12 (2005), pp. 8537–8547.

[15] Yu-Yu Cheng, Zhengyi Chen, Xinyun Cao, Tyler D Ross, Tanya G Falbel, Briana M Burton, and Ophelia S Venturelli. “Programming bacteria for multiplexed DNA detection”. *Nature communications* 14.1 (2023), p. 2001.

[16] Xuefei Angelina Nou and Christopher A. Voigt. “Sentinel cells programmed to respond to environmental DNA including human sequences”. *Nature Chemical Biology* 20.2 (2024), pp. 211–220.

[17] Hsiao-Ying Cheng, Caroline A. Masiello, Ilenne Del Valle, Xiaodong Gao, George N. Bennett, and Jonathan J. Silberg. “Ratiometric Gas Reporting: A Nondisruptive Approach To Monitor Gene Expression in Soils”. *ACS Synthetic Biology* 7.3 (2018), pp. 903–911.

[18] Sterling Robertson Olsen. *Estimation of available phosphorus in soils by extraction with sodium bicarbonate*. 939. US Department of Agriculture, 1954.

[19] Roger H. Bray. “Requirements for successful soil tests”. *Soil Science* 66.2 (1948), pp. 83–90.

[20] Adolf Mehlich. “Mehlich 3 soil test extractant: A modification of Mehlich 2 extractant”. *Communications in Soil Science and Plant Analysis* 15.12 (1984), pp. 1409–1416.

[21] Fatemeh Aghlmand, Chelsea Y. Hu, Saransh Sharma, Krishna Pochana, Richard M. Murray, and Azita Emami. “A 65-nm CMOS fluorescence sensor for dynamic monitoring of living cells”. *IEEE Journal of Solid-State Circuits* 58.11 (2023), pp. 3003–3019.

[22] Ghislaine Recorbet, Christine Picard, Philippe Normand, and Pascal Simonet. “Kinetics of the persistence of chromosomal DNA from genetically engineered *Escherichia coli* introduced into soil”. *Applied and Environmental Microbiology* 59.12 (1993), pp. 4289–4294.

[23] Ghislaine Recorbet, Catherine Robert, Alain Givaudan, Bernard Kudla, Phillipe Normand, and Geneviève Faurie. "Conditional suicide system of *Escherichia coli* released into soil that uses the *Bacillus subtilis sacB* gene". en. *Applied and Environmental Microbiology* 59.5 (May 1993), pp. 1361–1366. ISSN: 0099-2240, 1098-5336. DOI: 10.1128/aem.59.5.1361-1366.1993. URL: https://journals.asm.org/doi/10.1128/aem.59.5.1361-1366.1993 (visited on 11/30/2022).

[24] Craig E. Stanley and Rob J. Kulathinal. "Genomic signatures of domestication on neurogenetic genes in *Drosophila melanogaster*". *BMC Evolutionary Biology* 16 (2016), pp. 1–14.

[25] Mark G. Sterken, L. Basten Snoek, Jan E. Kammenga, and Erik C. Andersen. "The laboratory domestication of *Caenorhabditis elegans*". *Trends in Genetics* 31.5 (2015), pp. 224–231.

[26] Anna Knöppel, Michael Knopp, Lisa M. Albrecht, Erik Lundin, Ulrika Lustig, Joakim Näsvall, and Dan I. Andersson. "Genetic adaptation to growth under laboratory conditions in *Escherichia coli* and *Salmonella enterica*". *Frontiers in Microbiology* 9 (2018), p. 756.

[27] Nathaniel J. Dominy. "Ferment in the family tree". *Proceedings of the National Academy of Sciences* 112.2 (2015), pp. 308–309.

[28] Frédéric Leroy and Luc De Vuyst. "Lactic acid bacteria as functional starter cultures for the food fermentation industry". *Trends in Food Science & Technology* 15.2 (2004), pp. 67–78.

[29] Tanja M. Gruber and Carol A. Gross. "Multiple sigma subunits and the partitioning of bacterial transcription space". *Annual Reviews in Microbiology* 57.1 (2003), pp. 441–466.

[30] Vladimir Bidnenko, Pierre Nicolas, Aleksandra Grylak-Mielnicka, Olivier Delumeau, Sandrine Auger, Anne Aucouturier, Cyprien Guerin, Francis Repoila, Jacek Bardowski, Stéphane Aymerich, et al. "Termination factor Rho: from the control of pervasive transcription to cell fate determination in *Bacillus subtilis*". *PLoS Genetics* 13.7 (2017), e1006909.

[31] Zachary F. Mandell, Reid T. Oshiro, Alexander V. Yakhnin, Rishi Vishwakarma, Mikhail Kashlev, Daniel B. Kearns, and Paul Babitzke. "NusG is an intrinsic transcription termination factor that stimulates motility and coordinates gene expression with NusA". *Elife* 10 (2021), e61880.

[32] Sujatha Thankeswaran Parvathy, Varatharajalu Udayasuriyan, and Vijaipal Bhadana. "Codon usage bias". *Molecular Biology Reports* 49.1 (2022), pp. 539–565.

[33] Yun Wang, Suzanne E. Kern, and Dianne K. Newman. "Endogenous phenazine antibiotics promote anaerobic survival of *Pseudomonas aeruginosa* via extracellular electron transfer". *Journal of Bacteriology* 192.1 (2010), pp. 365–369.

[34] Linda S. Thomashow and David M. Weller. "Role of a phenazine antibiotic from Pseudomonas fluorescens in biological control of *Gaeumannomyces graminis* var. tritici". *Journal of Bacteriology* 170.8 (1988), pp. 3499–3508.

[35] Dmitri V. Mavrodi, Olga V. Mavrodi, James A. Parejko, Robert F. Bonsall, Youn-Sig Kwak, Timothy C. Paulitz, Linda S. Thomashow, and David M. Weller. "Accumulation of the antibiotic phenazine-1-carboxylic acid in the rhizosphere of dryland cereals". en. *Applied Environmental Microbiology* 78.3 (Feb. 2012), pp. 804–812.

[36] Darcy L. McRose and Dianne K. Newman. "Redox-active antibiotics enhance phosphorus bioavailability". *Science* 371.6533 (2021), pp. 1033–1037.

[37] George O. Poinar JR and Gerard M. Thomas. "A new bacterium, *Achromobacter nematophilus* sp. nov.(Achromobacteriaceae: Eubacteriales) associated with a nematode". *International Journal of Systematic and Evolutionary Microbiology* 15.4 (1965), pp. 249–252.

[38] George O. Poinar Jr and Gerard M. Thomas. "Significance of *Achromobacter nematophilus* Poinar and Thomas (Achromobacteraceae: Eubacteriales) in the development of the nematode, DD-136 (Neoaplectana sp. Steinernematidae)". *Parasitology* 56.2 (1966), pp. 385–390.

[39] Ilker Kepenekci, Selcuk Hazir, Ercin Oksal, and Edwin E. Lewis. "Application methods of *Steinernema feltiae*, *Xenorhabdus bovienii* and *Purpureocillium lilacinum* to control root-knot nematodes in greenhouse tomato systems". *Crop Protection* 108 (2018), pp. 31–38.

[40] S. Manochaya, Shashikant Udikeri, B. S. Srinath, Mantri Sairam, Srinivas V. Bandlamori, and Krishnaveni Ramakrishna. "*In vivo* culturing of entomopathogenic nematodes for biological control of insect pests: A review". *Journal of Natural Pesticide Research* 1 (2022), p. 100005.

[41] Yi-Ming Shi, Merle Hirschmann, Yan-Ni Shi, Shabbir Ahmed, Desalegne Abebew, Nicholas J Tobias, Peter Grün, Jan J. Crames, Laura Pöschel, Wolfgang Kuttenlochner, et al. "Global analysis of biosynthetic gene clusters reveals conserved and unique natural products in entomopathogenic nematode-symbiotic bacteria". *Nature chemistry* 14.6 (2022), pp. 701–712.

[42] S. Patricia Stock. "Partners in crime: symbiont-assisted resource acquisition in *Steinernema* entomopathogenic nematodes". *Current Opinion in Insect Science* 32 (2019), pp. 22–27.

Chapter 2

ENGINEERING *PSEUDOMONAS SYNXANTHA* 2-79 INTO A RATIOMETRIC REPORTER FOR PHOSPHORUS LIMITATION

The contents of this chapter are reproduced from the following published work:

> Elin M. Larsson, Richard M. Murray, and Dianne K. Newman. "Engineering the soil bacterium *Pseudomonas synxantha* 2–79 into a ratiometric bioreporter for phosphorus limitation". *ACS Synthetic Biology* 13.1 (2024), pp. 384–393. DOI: 10.1021/acssynbio.3c00642.

2.1 Introduction

In the past 30 years, whole-cell microbial bioreporters and biosensors have been developed for applications in environmental sustainability and medicine. In the simplest case, they are made up of a promoter that gets activated by a target signal that then drives the expression of genes that result in a measurable output such as luminescence or fluorescence. The simplicity and versatility of this structure has allowed the development of biosensors for heavy metals [1], pathogens [2] and plant nutrients [3].

One advantage of microbial biosensors is that they can detect the target analyte concentrations at microscopic scales in an environment of interest. This makes them promising candidates for future monitoring technologies in medicine and agriculture. An application where they could be useful is in precision agriculture, a farming practice that collects spatial and temporal information about different parameters, such as moisture content and nutrient levels, and uses it to make decisions about where action needs to be taken [4]. In the case of fertilizer application, for this to be effective, the detection of nutrients must target the bioavailable portion that can be utilized by crops. For this reason, detection methods that measure the total nutrient content are not as informative. If high resolution, accurate measurements can be made of bioavailable nutrient concentrations, that information can be used to apply an appropriate amount of fertilizer, reducing the over-application. A good target nutrient for this application is phosphorus, a non-renewable resource commonly added to agricultural fields. When applied to soils it can get bound by minerals, which makes it unavailable for plant uptake [5]. It is

also common for the phosphorus to be flushed away with surface run-off, ending up in water bodies where it causes eutrophication.

A prerequisite for engineering a microbial biosensor for agriculture is the ability of the chassis to stably colonize the soil environment and persist throughout the growing season. For example, *E. coli* K-12 gets outcompeted rapidly, about two weeks after being introduced to soil [6]. Pseudomonads, a class of bacteria that are ubiquitous in soil, have been common target chassis for engineering soil biosensors. Not only are they well-adjusted to the soil environment, they are in many cases known to promote plant-growth and protect against plant pathogens [7, 8]. Although it is not certain that engineered isolates can persist long-term in soil, it has been reporter previously that can persist and retain their engineered function for months in soil [9].

The first engineered bioreporter for phosphorus limitation in a pseudomonad was developed by de Weger et al. [10]: they inserted *lacZ* in random places in the *Pseudomonas putida* WCS358 genome and found colonies that responded to phosphorus limitation with β-galactosidase activity. A similar approach was taken by Kragelund et al. [11] who instead integrated the *lux* operon onto the *Pseudomonas fluorescens* DF57 genome. The first use of an exogenous P limitation promoter in a pseudomonad was done by Dollard et al. [12], who used the *E. coli* P_{phoA} promoter in *Pseudomonas fluorescens* DF57 and showed successful expression of the *lux* operon during P limitation. Native promoters have evolved in the context of maximizing host fitness [13, 14]. Sometimes non-native genetic elements can outperform native ones for engineering applications that instead prioritize sensor performance, for example by maximizing expression levels or by reducing the risk of metabolic cross-talk [15, 16]. However, to our knowledge there has not been a direct comparison between the performance of the *E. coli* P_{phoA} promoter and native *Pseudomonas* promoters for use in P limitation reporters. In addition, none of the described P reporters implement a ratiometric output readout. Ratiometric reporters are advantageous because they control for cellular metabolic activity and permit normalization of the bulk output signal.

In this study, we develop a ratiometric reporter for P limitation in the wheat isolate *Pseudomonas synxantha* 2-79. We selected this strain as our chassis because it is known for its ecological importance in the biocontrol of wheat in the Pacific Northwest Columbia Plateau, and phosphorus content has been mapped in this region using traditional methods [7].

We characterize its performance under environmentally-relevant conditions, including pH and phosphate source, cross-talk with other nutrient limitations, and performance in a soil context. Our work builds upon previous efforts by (1) directly comparing the performance of the exogenous P_{phoA} promoter to native promoters, showing that the P_{phoA} promoter outperforms native promoters and (2) creating a ratiometric sensor.

2.2 Results and Discussion

Selection and characterization of a promoter induced by phosphorous limitation

We first set out to determine whether the exogenous *E. coli* P_{phoA} promoter performs better or worse than native *P. synxantha* promoters as a bioreporter for phosphorous (P) limitation. Specifically, we compared P_{phoA} to five native *P. synxantha* promoters. Three were chosen by performing RNA-sequencing and selecting the three most upregulated genes. Additionally, two promoters that have annotated binding regions in *Pseudomonas fluorescens* Pf1-0 [17] were chosen as promoter candidates for the reporter. We used the intergenic region upstream of the five chosen genes to construct all promoter fusions (Table S1).

These promoters all respond to the PhoB-PhoR two-component system to sense the limitation of phosphate in their surroundings (Figure 2.1A, left). After phosphate has been imported to the periplasm through porins, it passes through the phosphate transporter PstS into the cytosol [19]. When the transporter is saturated, the adjacent histidine kinase PhoR remains inactive, however, when the levels of phosphate reach a critically low level (4 μM in *E. coli*) [20], PhoR is activated and phosphorylates the transcriptional regulator PhoB. The activation of PhoB leads to its binding to DNA regions called PHO-boxes that are found upstream of genes that are part of the Pho-regulon, involved in conservation and scavenging of phosphorus [19] .

We developed reporter constructs for the selected promoters by cloning them upstream of the green fluorescent protein mNeonGreen [21], driven by a strong synthetic ribosome binding sequence [22] (Figure 2.1A, right). Each reporter variant was integrated in single copy on the *P. synxantha* genome using transposon-based integration at the Tn7 site [23]. We then grew these constructs strains under P limited (25-500 μM) and P replete (7 mM) conditions and measured their optical density (OD) and fluorescence. Because *P. synxantha* makes phenazines [24] and pyoverdine [25] that can interfere with the GFP signal, we also grew wild-type

Table S1. Promoter sequences. PHO-boxes are highlighted.

Promoter name	**Sequence**
P_{phoA} (*E. coli*)	ATGAGCTCAAAAGTTAATCTTTTCAACAG**CTGTCAT**AA AG**TTGTCAC**GGCCGAGACTTATAGTCGCTTTGTTTTTA TTTTTTAA
P_{pstS} (RS29030)	GCTAAAGCCAGCCTGATCCACTGTGGCGAGGGAGCTT GCTCCCGCTGGGGCGCGAAGCGGCCCTTAAAGATGG GACTGCTGCGCAGTCCAACGGGAGCAAGCTCCCTCGC CACAATGAAAGTGTTTGTTCGGTGTTTTACCTCGCATA CCTTCGCTTCCCGATAGTGGC**CTTTCAT**CTAA**TTGTCAT** ATTTA**AG**A**CAT**AGAGTGTTCACACGGCCTCCCGATACT TGGCCCCGATCCAATTATCCCTATCTGCTAGGAGCAAG GC
P_{acpA} (RS03720)	TCACCTCGGTGATGTGCATTAGAAACTCAGTCTAGCAG CGCTTACTCTGTGTAGACACGCCCCACCCATCACTTGT GTGTCTTCGTTCCGTCACATTCCATTGCTACCGTCCTGC GAAATATCTTGCAACATCTCGCCAAGGACTCCCCCGCA AT
P_{pstS} (RS14750)	GGCGCTGGCGGATCCGAGCATTTTAGTCGCATTTTGTT ACTAACCAATGCACTAAAAATATAGGGCTGTAGTGGC AAACCGGGACAAAACCCCGGTTTGCCACTCAAT**TTTCA T**AAAAATGTAACAACCCTGCTGCACAGTTCGGGAGCC CGTCACCACAACGAGTTCCTTTTA
P_{phoX} (RS26910) Monds et al [1]	TGGGCGAACGTCTTCAAA**CTGCAA**CAATCTG**GTCA**CA AGTGCTGCTTAAGGTGT**CTGCAA**AAACCGCAGGGAGC CTGAG
P_{phoD} (RS04350) Monds et al [1]	GTGTTGACGGGGTTGGTGTATGCGCTGCTTAAGCGAC CGGAAGCTGTGGAACTGACGGTCACTGCTGCCAAGGG CTGATGGGATTCAAAATGTGGGAGGGGGCTTGCCCCC GATAGCGATGTATCAGTCAGCCTATTTTTAGCTGACAC ACTGCTATCGGGAGCAAGCCCCCTCCCACATTTGGATT TTCATTGGCTGTAAGGGTG**GTGTCA**TCTCTGC**TTCAT**C CCTACGTGCTTAAGTGGCCCTTTTGATACTCAAGAGGG CACCTGC

(WT) cells that did not contain the reporter construct to normalize the output of the reporter cells by the native cell background.

We observed that of the five native promoters tested, P_{pstS} had the strongest signal (Figure 2.2). Three of the promoter fusions had no significant signal compared to WT. The lack of signal from the P_{phoX} and P_{phoD} promoters was surprising, as reporters had previously been constructed in *Pseudomonas fluorescens* with annotated regions of the PHO-box [17]. One potential explanation could be secondary structures forming between the promoter and RBS region, hindering the ribosome from binding. An alternative explanation could be that other growth conditions than the ones tested are necessary for activation in *P. synxantha* 2-79.

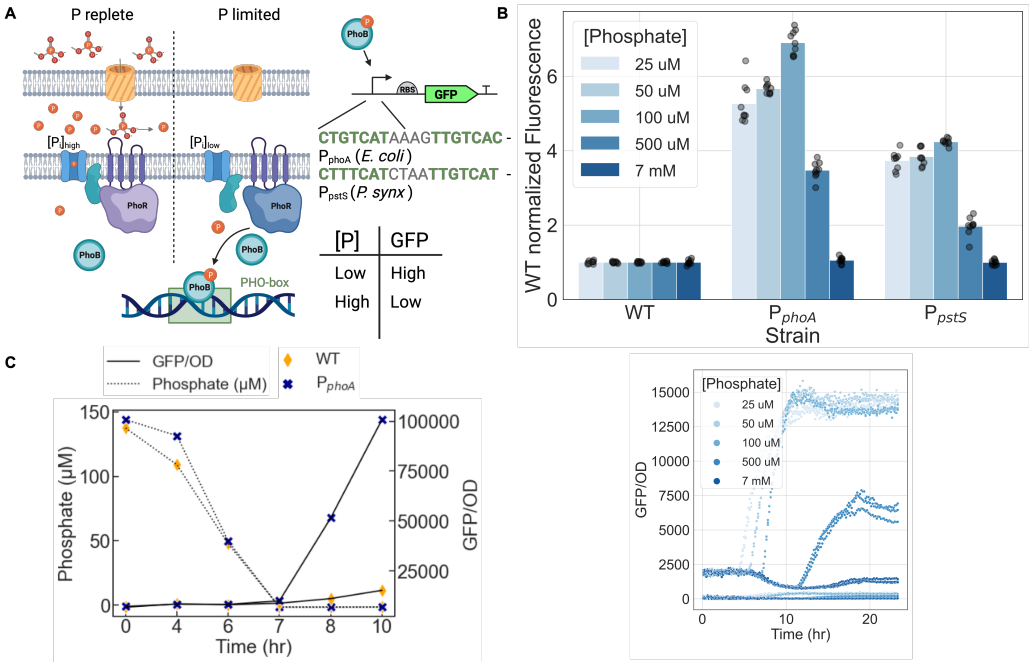

Figure 2.1: (A) Left: Schematic of *E. coli* phosphorus sensing. Right: Construct diagram for the two promoter fusions. The PhoB binding region is annotated in bold. The *E. coli* annotation is from [18]. The annotation for the *P. synxantha* promoter are from *Pseudomonas fluorescens* Pf0-1 in [17]. (B) Upper: Promoter response to different initial phosphate concentrations. The data is normalized by the WT fluorescence at the final timepoint of the experiment (24 hours). Bars show the average fluorescence value, dots show raw data for three biological replicates, with three technical replicates each. Lower: Representative plot for fluorescence/OD for P_{phoA} at different initial phosphate concentrations. The lag-time for the response is longer the more phosphate is provided at the start. (C) One out of three biological replicates showing GFP/OD (line) and phosphate concentrations (dotted line) over 10 hours of growth (the two other biological replicates are found in Figure 2.5). Phosphate is depleted in the culture over time. Once a critically low concentration (below 50 μM) is reached, the GFP signal is turned on at 7-8 hours of growth for the reporter cells (crosses) whereas WT (diamonds) fluorescence increases only by a small amount.

After identifying P_{pstS} as the strongest native promoter, we compared its response to the non-native *E. coli* P_{phoA} promoter at a range of initial P concentrations. We observed that the promoter P_{phoA} had the strongest signal with a fluorescence that was 5.3- to 6.9-fold higher than the WT strain (Figure 2.1B). The native P_{pstS} promoter was 3.7- to 4.2-fold more fluorescent than WT. Both promoters showed similarly minimal levels of leak, with fluorescence signals being comparable to WT levels at replete (7 mM) P concentrations.

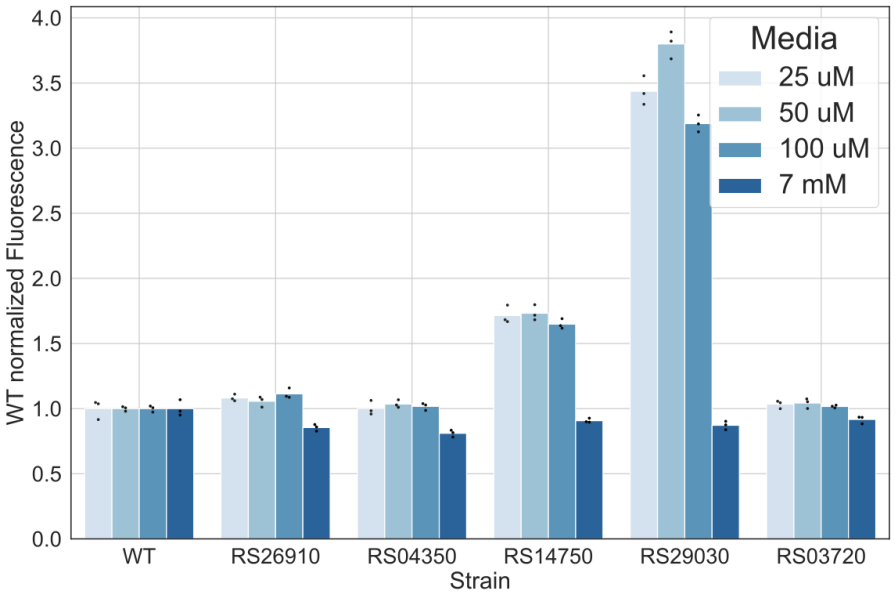

Figure 2.2: Screen of promoter fusions for 5 native *P. synxantha* intergenic regions. Promoter fusion strains were grown in minimal media with different concentrations of phosphorus for 24 hours. End point GFP fluorescence is normalized by the fluorescence of WT cells without any integrated promoter fusion.

For the promoters that responded to P limitation, we observed that increasing P concentrations corresponded to delayed activation of the GFP signal (Figure 2.1B, bottom, Figure 2.3 and 2.4). We hypothesized this delay arises because the cells gradually deplete the phosphorous in their medium and only turn on the GFP signal when the P concentration crosses below a critical threshold. We tested this hypothesis by simultaneously measuring the cellular fluorescence and phosphate concentration from a growing culture of the the P_{phoA} reporter strain (Figure 2.1C, Figure 2.5). As expected, the critical threshold for GFP signal activation was below 50 μM, which is consistent with the range of P concentrations that are limiting for wheat (20-200 μM) [26].

Taken together, these results demonstrate that the exogenous *E. coli* promoter P_{phoA} has a stronger response to P limitation at physiologically relevant concentrations than two native P-responsive promoters in *P. synxantha* 2-79. We therefore chose P_{phoA} as the basis for the continued characterization and development of our bioreporter.

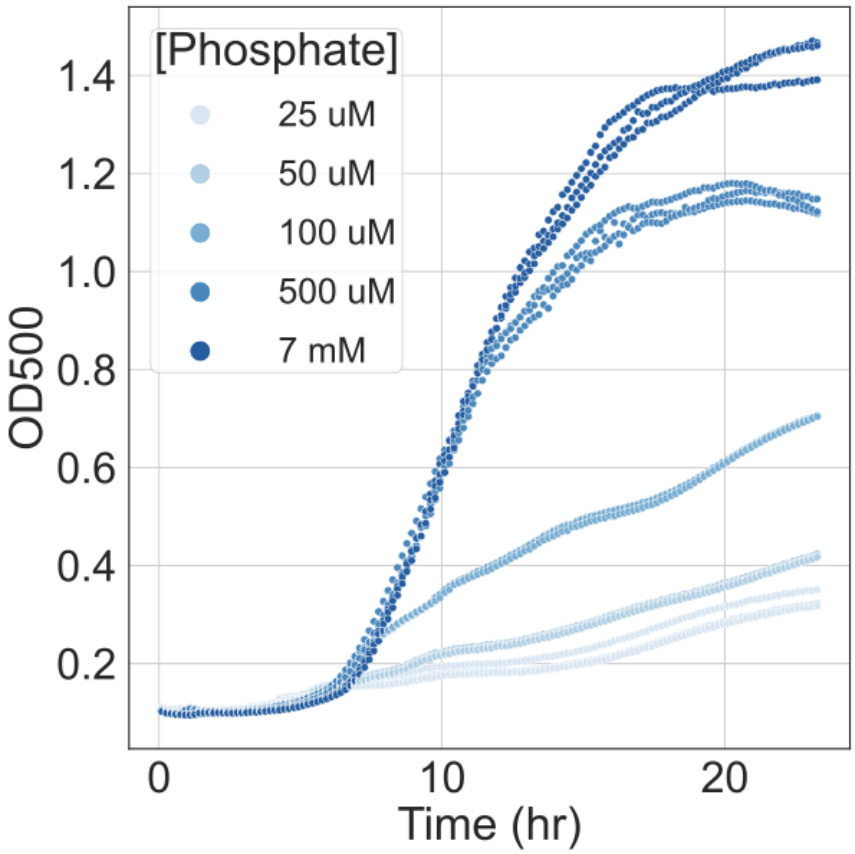

Figure 2.3: OD trace for panel B in Figure 2.1.

The *E. coli* P_{phoA} promoter does not exhibit cross-talk with carbon and nitrogen starvation conditions

Minimizing cross-talk, the activation of the response by unintended signals, is one of the central challenges in engineering bioreporters. There are two major categories of cross-talk: it could arise from the activation of the promoter by other cellular elements responding to the target signal in unpredictable ways (genetic cross-talk), or it could arise from other signals directly activating the promoter (Figure 2.6A). Because we chose to use an exogenous promoter as the basis for our bioreporter, the possibility of genetic cross-talk was particularly important to address.

To test whether the activation of P_{phoA} during P limitation arises exclusively through the PhoB-PhoR pathway, we integrated the P_{phoA} reporter into a Δ*phoB* deletion strain and measured its response to P limitation (Figure 2.6B). We observed that the

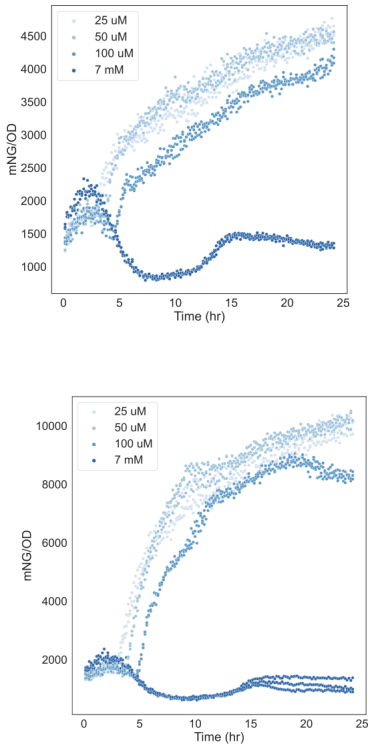

Figure 2.4: GFP fluorescence normalized by OD for 24 hours of growth. Upper: Promoter RS14750. Lower: Promoter RS29030.

reporter in the Δ*phoB* strain does not activate GFP expression during P limitation, indicating that PhoB is indeed necessary for P_{phoA} activation in *P. synxantha* 2-79.

We next sought to determine the extent of signal cross-talk in our system by assessing the reporter's response to other types of nutrient limitation. Metabolic pathways for different nutrients are sometimes regulated by overlapping pathways in bacteria [19, 27, 28], as this can help the cell adapt to various environmental nutrient conditions [29].

We measured the response of the P_{phoA} reporter to limiting concentrations of phosphorous (P), carbon (C), and nitrogen (N), as these are all nutrients that can limit bacterial growth in soils [30]. The reporter had a minimal response to C and N limitation (approximately 1.2-fold average increase in fluorescence over WT) compared to P limitation (approximately 5.3-fold average increase over WT) (Figure 2.6C).

Together, these experiments confirm that the P_{phoA} promoter exhibits minimal genetic cross-talk and signal cross-talk to other relevant limiting nutrients.

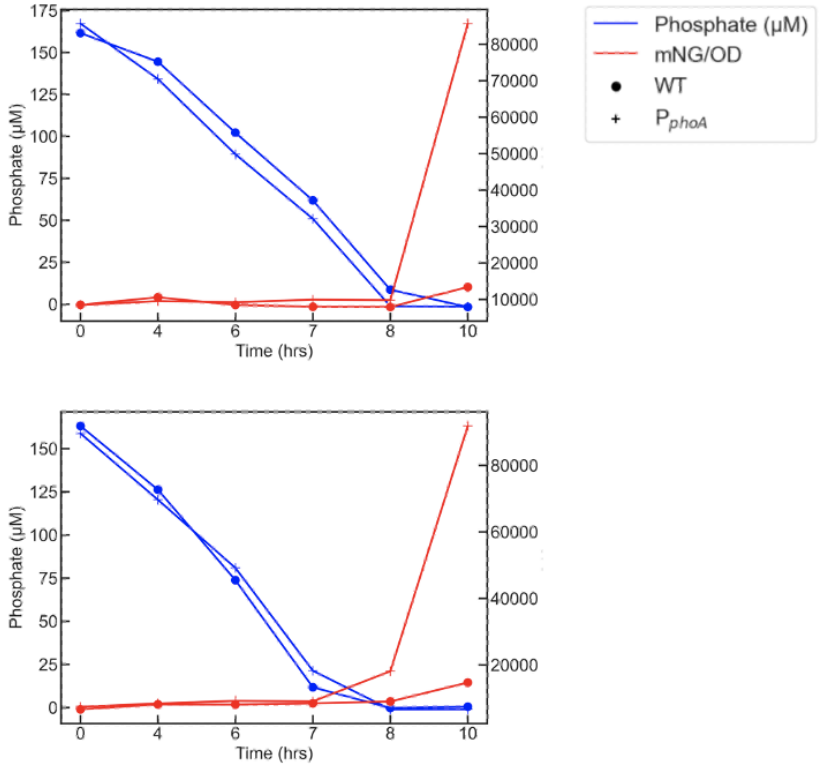

Figure 2.5: Phosphate, OD and fluorescence measurements over 10 hours of growth of WT and P_{phoA} cells. Biological replicates from two separate days.

pH has variable effects on reporter performance

Another challenge associated with engineering microbial bioreporters is that environmental parameters like pH often differ from those of the standard laboratory conditions typically used to prototype the constructs. Furthermore, in natural environments like soils, the values of these parameters can vary over time and across sites [31]. The pH of the Cook Agronomy Farm, from where the *P. synxantha* strain in this study was isolated, has historically been reported to range between acidic and alkaline depending on the sampling location [32–34]. Ideally, a reporter should function robustly across a range of different pH conditions as well as changes in pH caused by biological processes.

To assess the robustness of our reporter to different pH conditions, we measured its response to P limitation under acidic (pH=5.8), neutral (pH=7), and alkaline (pH=8) conditions. We additionally measured the performance of the P_{phoA} reporter in the Δ*phoB* background, as *E. coli* Pho regulon genes have previously been shown to be

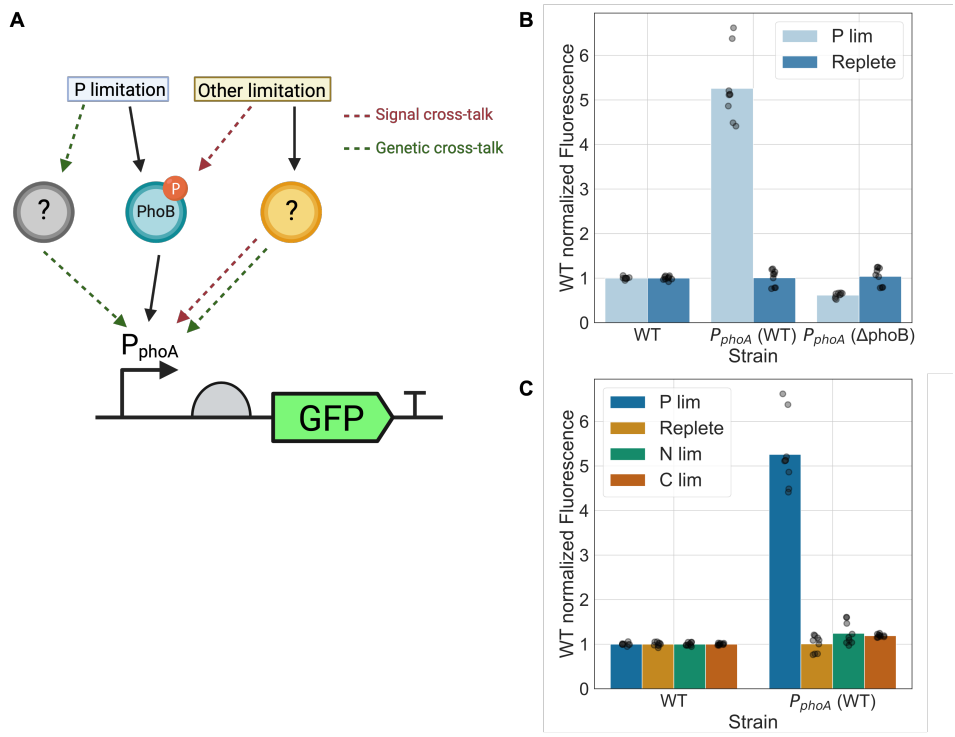

Figure 2.6: (A) Schematic showing potential genetic and signal cross-talk in the system. (B) The reporter fusion was integrated in the ΔphoB background and grown in P limited (50 μM) and P replete (7 mM) media. The fluorescence output is compared to the reporter in the WT background and normalized to WT. (C) P reporter grown in medium limited for carbon, nitrogen or phosphorus compared to growth in nutrient replete medium. WT normalized fluorescence signal is plotted as an endpoint value at 24 hours of growth. Bars show the average fluorescence value, dots show raw data for three biological replicates, with three technical replicates each.

induced by acidic conditions even in PhoB deletion mutants as well as in P replete conditions [35].

We observed that the average fold increase in fluorescence signal for the WT-background reporter strain was 6.1 for acidic pH, 6.6 for neutral pH, and 7.7 for alkaline pH (Figure 2.7A). Optical density measurements also indicate that the cells grew more poorly in the acidic condition compared to the neutral and alkaline conditions (Figure 2.7B), which may have contributed to the lower expression level observed in the acidic condition. The leaky GFP expression from the reporter, however, remained consistently low in replete P across all tested pH conditions. Furthermore, in the Δ*phoB* background, the reporter did not respond to P limitation under any of the tested pH conditions. These results together indicate that *P. synxan-*

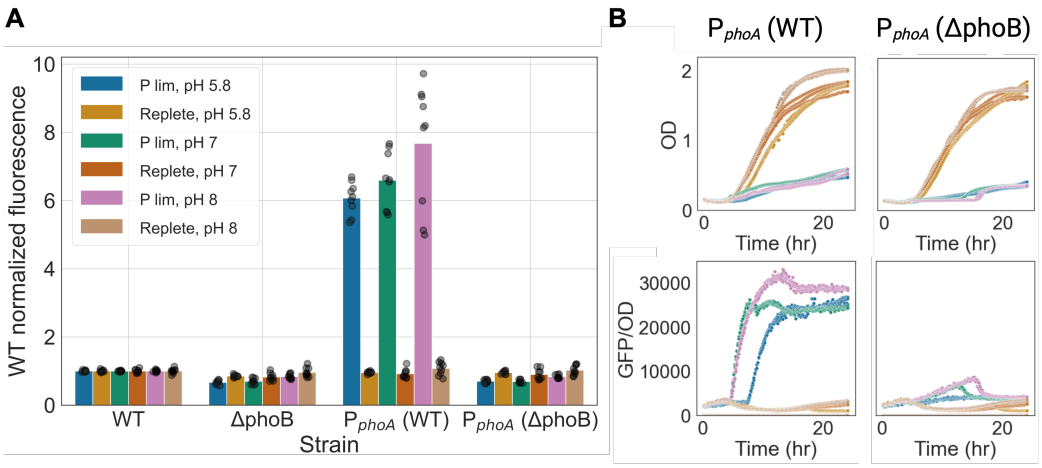

Figure 2.7: The P reporter strain in WT and ΔphoB background was grown in P limited and P replete media at three different pH conditions. A) Barplots of WT normalized fluorescence at 24 hours of growth. Bars show the average fluorescence value, dots show raw data for three biological replicates, with three technical replicates each. B) Representative growth curves and GFP/OD traces for P_{phoA} in the WT and ΔphoB deletion strain.

tha 2-79 does not appear to experience the acidity-induced Pho regulon upregulation that was observed in *E. coli* [35]. However, the fact that the expression level of the ON condition differs across pH highlights the importance of characterizing system performance across different pH values that are relevant to the soil environment.

The reporter response is robust to the presence of organic P compounds

Up until this point, we have characterized the reporter's behavior in low and high concentrations of inorganic P, which is accessible to plants. However, soil environments contain many other organic forms of P that are inaccessible as nutrients to plants but potentially accessible to bacteria [36] (Figure 2.8A). To properly indicate the limitation of bioavailable phosphorous, it is essential that our reporter be insensitive to concentrations of organic phosphorous.

To evaluate the robustness of our reporter's response, we tested if the addition of organic P sources to a medium limited for inorganic P would rescue the reporter from the P limited condition and turn the reporter off. We predicted the output signal would remain on even after organic P is added to the medium if our reporter is insensitive to organic P sources. When we performed this experiment with four

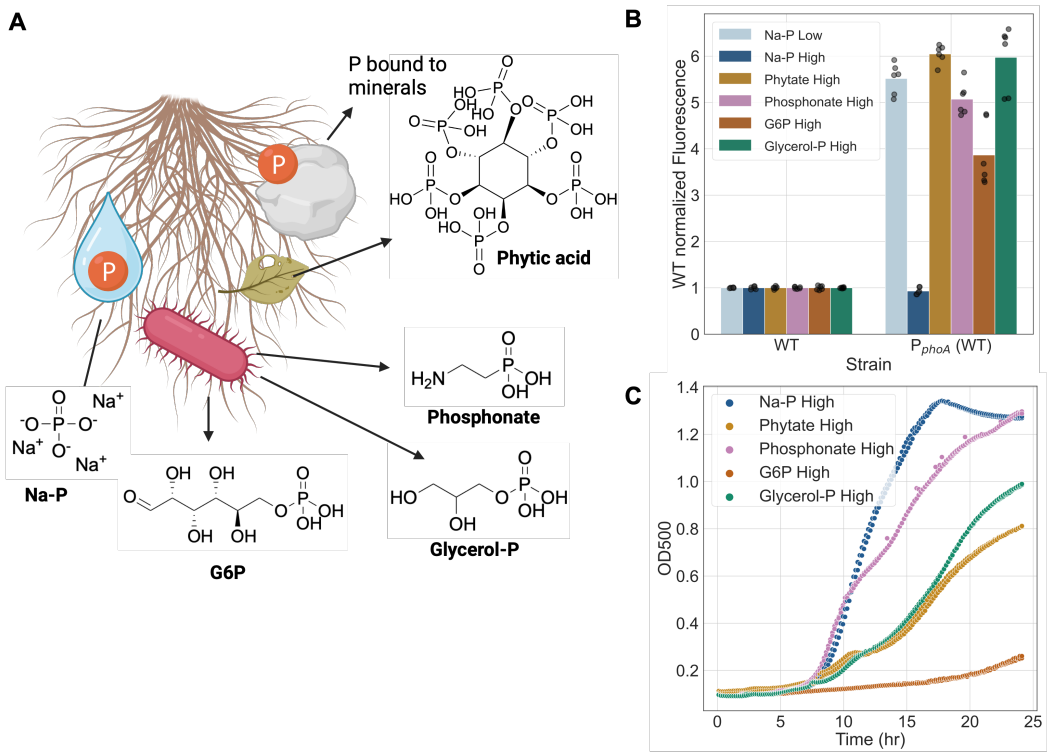

Figure 2.8: (A) Schematic showing examples of P types can be found as in the soil. Inorganic P can be tighly bound to minerals like calcium or iron or soluble in the pore water and available for plant uptake. Organic P in the soil can originate from dead plant material containing the main plant P storage molecule phytate. Organic P can also originate from other dead organisms like bacteria or it can come from anthropogenic sources, e.g., in herbicides. Organic P cannot be utilized by plants for growth. (B) Reporter cells were grown in different P sources (Na-P, phytate, phosphonate, glucose 6-phosphate and glycerol 3-phosphate) at replete conditions (1 mM) or in inorganic P (Na-P) at limited conditions (50 μM). The WT normalized fluorescence is plotted at 24 hours of growth. Bars show the average fluorescence value, dots show raw data for three biological replicates, with two technical replicates each. (C) Representative growth curves for one out of three biological replicates for the P replete condition.

different organic P sources commonly found in soils, we found that none were able to reduce the reporter output down to replete levels (Figure 2.8B, Figure 2.9). When limited for inorganic P (Na-P), the reporter exhibited a 5.5-fold increase in fluorescence over the WT background. When replete concentrations of Na-P (1 mM) were added, the reporter response went down to WT background levels, as expected. However, when the four organic P sources were added to 1 mM concentration, the reporter signal remained between 3.9- and 6-fold above WT levels. These results

indicate that organic P sources are unable to rescue the reporter from its P limited state.

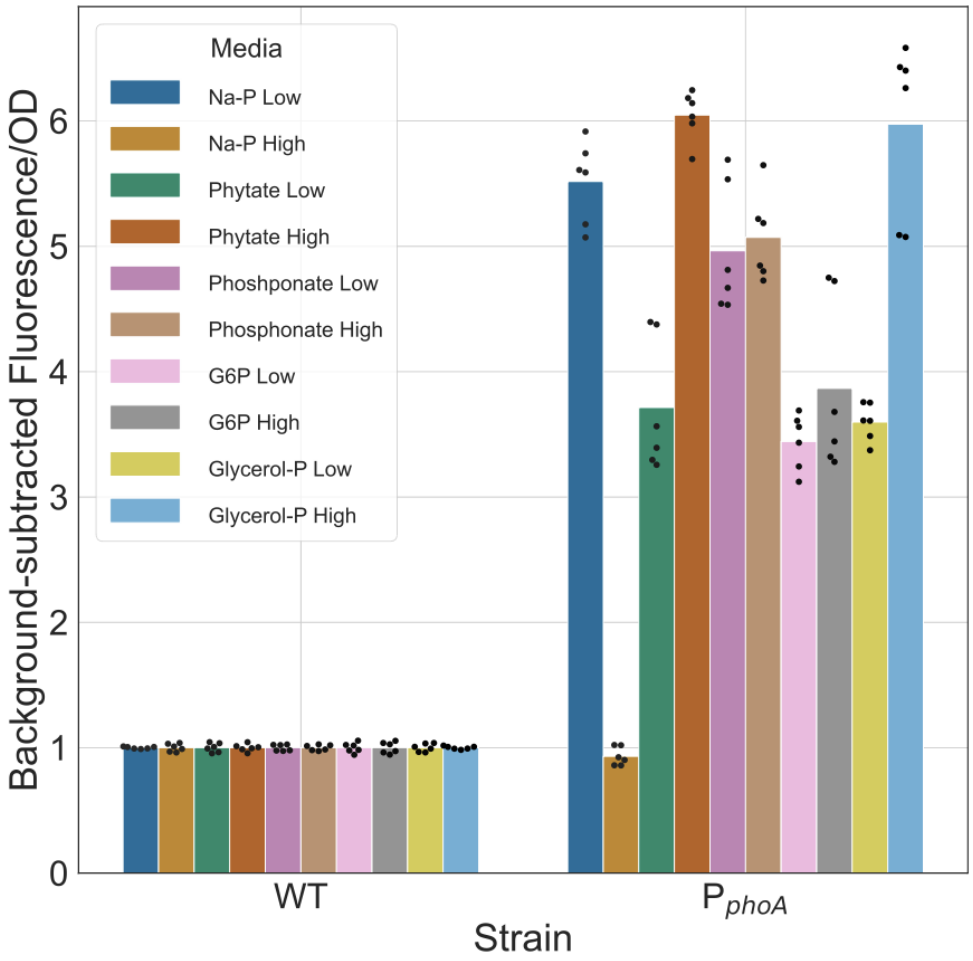

Figure 2.9: End point fluorescence after 24 hours of growth in diffent P sources. Low indicates 50 μM and High indicates 1 mM of added P.

We note that some of the P sources are more difficult for the cells to import or degrade than others, which impacts the cells' growth dynamics (Figure 2.8C). For example, phytic acid readily forms complexes with minerals like calcium that decrease the bioavailability of both calcium and phosphorus [37]. Phosphonate seems to be the most preferred organic P source, while the cells can barely utilize glucose 6-phosphate.

These results show that the P reporter signal is only silenced by inorganic P among the P sources tested in this experiment. This means that in the presence of phosphorus that is not available to plants, the limitation signal is on.

Selection of a constitutive promoter for the ratiometric reporter

Having demonstrated that the P_{phoA} promoter can act as a specific and reliable indicator of inorganic P limitation in *P. synxantha* 2-79, we proceeded to develop our strain into a ratiometric bioreporter by incorporating the constitutive expression of a distinct fluorescent protein. Ratiometric readouts expand the utility of bioreporters by providing a measure of global cellular activity that can be used to calibrate the measured expression level from the inducible promoter. In environments like soils where only a fraction of the population may be active at any given time, such calibrations are essential for properly interpreting the reporter's behavior. The constitutive expression signal can also be used to identify the spatial location of the bioreporters.

We chose to use the bright red fluorescent protein mScarletI [38] (RFP) as the constitutive reporter. In selecting the strength of the RFP output, it is important that it is strong enough to be easily detectable without being so strong that it sequesters cellular resources away from the expression of the output GFP signal [39]. We created three candidate dual reporter constructs where mNeonGreen is driven by P_{phoA} and mScarletI is driven by either the constitutive lac derived promoter Pa10403 [40] or by one of two synthetic Anderson promoters [41] that were previously found to express in *P. synxantha* [42]. We integrated these reporter constructs into the genome and measured the expression strengths of both fluorescent proteins under P limited and P replete conditions.

We observed that all three dual reporters exhibited a lower maximal GFP signal compared to the GFP-only reporter, which had a 5.9-fold increase in fluorescence over WT in the P limited condition (Figure 2.10A). Although the Pa10403 variant reduced this maximal GFP expression to 3.4-fold over WT, the two Anderson variants maintained GFP expression at 5- to 5.1-fold above WT. Interestingly, the RFP signal was higher in the P limited conditions than the P replete conditions for all three constitutive promoters (Figure 2.10B). Consistent with previous reports [42], the J23101 promoter was stronger than the J23116 promoter. We therefore chose to express the RFP from the J23101 promoter in our final dual reporter construct, as it decreased GFP expression to a similar level as J23116 while having a 2.8-fold higher RFP expression level.

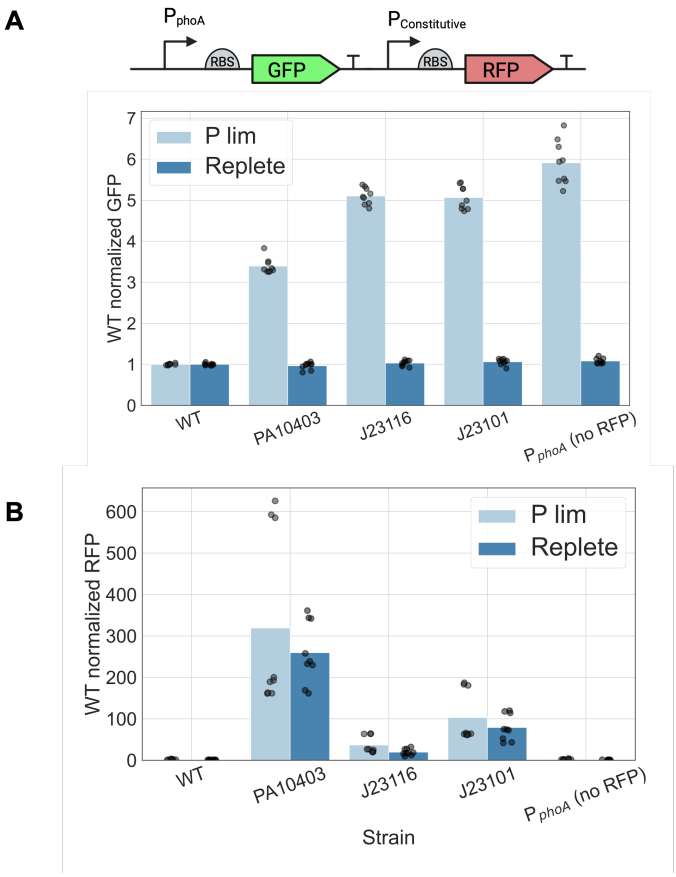

Figure 2.10: Three ratiometric variants were constructed and tested under P limited and replete conditions. (A) Comparison in GFP levels, normalized by WT, with three different constitutive promoters driving expression of mScarletI, compared to no RFP expression. (B) WT normalized RFP expression under three constitutive promoters compared to background fluorescence. Bars show the average fluorescence value, dots show raw data for three biological replicates, with three technical replicates each.

Ratiometric reporter performance in a soil context

To assess the performance of our dual reporter in a soil context, we grew the reporter strain in soil slurries that were generated by mixing soil from the Cook Agronomy Farm (CAF), from which *P. synxantha* 2-79 was isolated [43], with medium that was either limited (50 μM) or replete (7 mM) with P. To verify soil slurries were limited for P, we measured aqueous P in abiotic controls after incubations for 24 hours. There was no detectable P present in these samples, indicating P in the

limited medium had sorbed to the soil (Table 2.1). Similarly, lower soluble P was measured in soil samples that had been mixed with replete P medium.

Sample	**[Soluble P]**
Limited medium (no soil)	35 μM
Limited medium + soil (replicate #1)	Not detectable
Limited medium + soil (replicate #2)	Not detectable
Limited medium + soil (replicate #3)	Not detectable
Replete medium + soil	2300 μM

Table 2.1: Malachite green assay P concentrations after 24 h incubation.

Cells were grown for 24h in the slurry and then extracted for analysis by flow cytometry (Figure 2.11A). As a comparison, we also analyzed the response of the reporter grown in pure growth medium to determine whether it is predictive of the reporter's performance in the soil context.

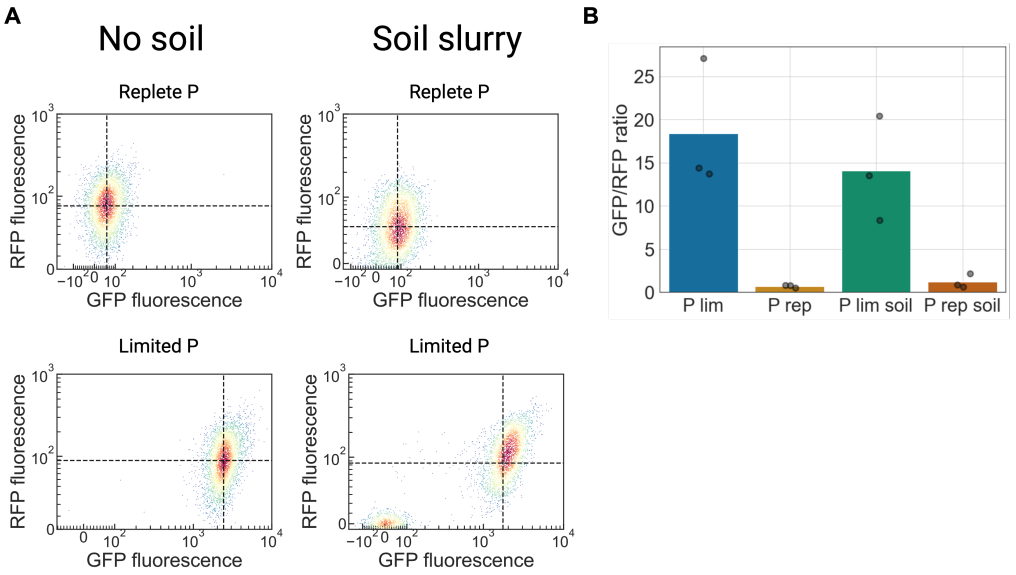

Figure 2.11: Flow cytometry measurement of three biological replicates taken on three different days in liquid cultures and soil slurries.(A) Representative plot of density gated flow cytometry data for one out of three biological replicates. The median intensities of GFP and RFP fluorescence are identified at the intersection of the dashed lines. (B) The median fluorescence intensities for GFP and RFP are divided by each other for each biological replicate. Bars show the average ratio, dots show each ratio for three biological replicates.

The use of calibration beads to measure fluorescent protein expression in absolute fluorescent units enabled us to directly compare the measured values across different conditions. Expression strengths of both GFP and RFP were generally similar between the soil slurry and pure growth medium within a P condition (Figure 2.11A). The major distinction came from the fact that 29-64% of the cells in the P limited soil slurry had minimal expression levels of both GFP and RFP, suggesting that they are metabolically inactive or dead.

We then computed the median GFP and RFP fluorescence values for each condition and divided them to obtain a GFP/RFP ratio that corresponds to the ratiometric readout value for each condition (Fig 2.11B). We can observe that in the soil slurry, the reporter has a slightly higher leak (1.2 compared to 0.7) and lower dynamic range than in the pure growth medium. The underlying reason for this difference is unknown, but may be related to stress imposed on the cell grown in the presence of soil. However, the reporter nonetheless maintains a 12-fold response to the limitation of P in the soil slurry.

Taken together, these results indicate that soil context affects the performance of the reporter in two major ways. First, it creates an inactive fraction of the population. Second, it reduces the dynamic range by both increasing the leaky expression level and decreasing the maximal expression level. However, despite these effects, our ratiometric reporter can still provide a reliable readout for P limitation in the soil slurry with a 12-fold dynamic range. Given that the reporter exhibits a 27-fold dynamic range in pure growth medium, further improvements need to be made to increase performance robustness in the soil environment. Furthermore, different types of soil with varying properties (pH, porosity, composition, texture, etc.) need to be tested as they may have different effects on the reporter performance. Future experiments to better understand the physiological impacts of the soil context will help expand the applicability of the reporter to different types of environmental contexts.

2.3 Conclusion

This study presents a framework for testing environmentally relevant parameters when engineering a bacterial bioreporter in a bacterium isolated from the context of its intended application, in this case, the wheat rhizosphere of the Columbia Plateau. Our work demonstrates the utility of selecting a non-native promoter for synthetic

biology applications in a new chassis organism, and characterizing its response under environmentally relevant conditions (pH, P sources, soil).

Future steps to refine the reporter for rhizosphere applications include further characterization of the ratiometric reporter in conditions more similar to the actual soil environment, for example by reducing the water content or examining its performance in the presence of native soil microbes by not autoclaving the soil prior to the experiments. Another worthwhile pursuit would be to alter the promoter region to achieve stronger GFP expression.

Although long-term *in situ* use of genetically engineered bioreporters is not practical today, work towards understanding what underpins lonegvity and reliable performance over time is necessary for bioreporters to realize their full potential in agricultural applications. The modular structure of many bioreporters can be leveraged both to sense other parameters of interest (e.g., different nutrients, such as ammonium or nitrate) and/or to enable actuation rather than reporting, opening up the possiblity of modulating the soil environment for bioremediation or liberation of nutrients bound to minerals.

2.4 Methods

Construction and genome integration of *P. synxantha* reporters

All cloning to produce *P. synxantha* genomic integration constructs was done using *E. coli* DH10B (Invitrogen) with the backbone pJM220 [44]. For the native promoters the intergenic region upstream of the *pstS* (locus tag C4K02 RS29030) and *phoX* (locus tag C4K02 RS26910) genes were amplified via PCR adding Gibson overhangs for the pJM220 backbone vector. Gibson assembly was then done for each construct and transformed into *E. coli* DH10B competent cells. Plasmids were purified using a QIAprep Spin Miniprep kit (Qiagen).

The constructs were then integrated on the *P. synxantha* chromosome using transposase based insertion at the Tn7 site. The protocol used for making and transforming competent cells was modified from Choi et al. [23].

Briefly, electrocompetent *P. synxantha* cells were electroporated in 1 mm-gap cuvettes (at 1.8 mV, 600 Ω and 10 μF) with the construct plasmid as well as a plasmid containing the transposase and genes required for genome insertion [45]. The cells were then recovered in rich medium (SOC) for 3 hours at 30℃ and plated onto LB agar plates containing gentamicin (20 μg/ml) and incubated for 24 hours before picking colonies for sequence verification.

Plate reader assay for *in vivo* fluorescence

In vivo fluorescence was measured using a Biotek (Synergy H1) plate reader. The experiments ran for 24 hours at 30℃ using continuous orbital shaking starting from an overnight culture diluted to OD 0.1. OD was measured every 10 minutes at 500 nm and fluorescence was measured at 490/520 nm for mNeonGreen and at 569/593 nm for mScarletI. In experiments where phenazine-1-carboxylic acid was assessed, absorbance at 367 nm was measured. The background fluorescence of the wild-type strain was subtracted from the fluorescence values of the reporter strains in Figure 2.6B.

Measurement of phosphate supernatant concentration

Measurements of phosphate concentration in the growth medium supernatant were done using a Malachite green phosphate assay kit (Sigma-Aldrich, Cat. No. MAK307). After collecting the supernatant, the sample was filtered through a 0.22 μm filter and stored at -20°C.

Preparation of cells for flow cytometry

Starting from an individual colony, a culture was grown in LB medium overnight. 1 ml of the culture was pelleted and washed once in minimal P limited medium. The cells were then resuspended in 1 ml minimal P limited medium (30 uM P). For the no soil condition, 3 ml of minimal medium (P limited or replete) was inoculated with the washed overnight culture (at OD 0.15). For the soil condition, tubes filled with 4 g of autoclaved soil were filled with 4 ml medium (P limited or replete). The tubes were then vortexed to mix the soil and liquid to yield a slurry. The tubes were then inoculated at the same cell density as the no soil cultures. All cultures were grown for 24 hours at 30℃ and 220 rpm shaking. The soil in the tubes was then separated from the bacteria following the protocol in Chemla et al. [9]. The soil slurries were centrifuged at 1000 xg for 2 minutes in room temperature. The supernatant containing bacteria was then removed from the tubes. All supernatants were then diluted 1:100 and filtered through a 10 μm filter before proceeding to flow cytometry measurements.

Flow cytometry and data analysis

The flow cytometry measurements were performed on a CytoFLEX S flow cytometer using the 610 Yellow and 525 Blue lasers. Approximately 10000 events were collected for each sample. In each experiment, the fluorescence of calibration beads

(Spherotech) was measured to enable convertion of the arbitrary fluorescence units (AFU) to molecules of equivalent fluorophore (MEF) using the pipeline developed by Castillo-Hair et al. [46].

The analysis followed the Castillo-Hair et al. protocol [46]. First, the calibration bead data was used to convert the arbitrary units on the machine to MEF. Then, background noise that was not single cells was gated out and 40 percent of the events in the densest region were kept for further analysis. From the remaining events, the median fluorescence was calculated for both flourescent proteins. The GFP values were then divided by the RFP values for each experimental condition.

RNA sequencing (sample collection, RNA extraction, data preprocessing)

Cells (wild-type and the ΔphoB mutant) were grown from a single colony in minimal medium overnight. The cells were then washed three times and diluted to OD 0.05 into P limited medium at 35 μM P and grown to an OD of 0.3. The cells were then separated into two 15 ml tubes at a volume of 6 ml each and P was added to one of the tubes to reach a P concentration of 5 mM and incubated at 30 °C for 5 minutes. The cell cultures were then centrifuged at 6200 xg and the supernatant was decanted, and cell pellets were immediately flash frozen by submerging the tubes into liquid nitrogen. Cell pellets were stored at -80 °C until performing RNA extractions. A Qiagen RNeasy kit was used for the RNA extractions and RNA concentrations were determined using a Nanodrop. RNA sequencing was done at the Millard and Muriel Jacobs Genetics and Genomics Laboratory at Caltech. The raw data was pre-processed using STARaligner, featureCounts and DESeq. Sorting on lowest p-value, the three most upregulated genes, that were not also upregulated in the ΔphoB mutant, were selected as candidates for P reporter constructs.

Media recipes

For routine growth we used LB and LB agar. For limitation assays, the cells were grown in minimal media containing 0.41 mM MgSO4, 0.68 mM CaCl2 and 25 mM MOPS (or 12.5 mM MES for low pH medium). Aquil trace metals [47] were added containing 10 μM Fe and 100 μM EDTA. The limited media were designed according to the Redfield ratio with guidance from D. McRose [48]. For P limited medium, the final concentration of potassium phosphate was 20, 30, 50 or 100 μM. For N limited medium, the final concentration of ammonium chloride was 1 mM. For C limited medium the final concentration of glucose was 6.625 mM.

In the P source experiment, the concentration of P source (sodium phosphate, 2-aminoethyl phosponic acid, phytic acid, glucose 6-phosphate or glycerol 3-phosphate) in the replete condition was 1 mM and the limited condition was 50 μM. The concentration of added KCl was 1 mM in both limited and replete media.

Acknowledgements

We thank R. Alcalde for insightful discussions regarding project conceptualization and for creating the P_{phoA}-mNeonGreen strain. We thank I. Antoshechkin at the Millard and Muriel Jacobs Genetics and Genomics Laboratory at Caltech for assistance in pre-processing the RNA sequencing raw data and Jamie. We also thank D. McRose for sharing the initial Δ*phoB* strain, and thank J. Marken, D. Mavrodi, O. Mavrodi, G. Squyres, L. Tsypin, and S. Wilbert for fruitful discussions that helped move this work forward. All figures were created using BioRender.com. This work was supported by the Institute for Collaborative Biotechnologies through contract W911NF-19-D-0001 from the U.S. Army Research Office and Caltech's Resnick Sustainability Institute. The content of the information in this chapter does not necessarily reflect the position or the policy of the Government, and no official endorsement should be inferred.

Supporting information references

[1] Russell D. Monds, Peter D. Newell, Julia A. Schwartzman, and George A. O'Toole, "Conservation of the pho regulon in *Pseudomonas fluorescens* Pf0-1," Applied Environmental Microbiology, vol. 72, pp. 1910–1924, Mar. 2006.

References

[1] Aziz Babapoor, Reza Hajimohammadi, Seyyed Mohammad Jokar, and Meysam Paar. "Biosensor design for detection of mercury in contaminated soil using rhamnolipid biosurfactant and luminescent bacteria". *Journal of Chemistry* 2020 (2020), pp. 1–8.

[2] Ying Wu, Chien-Wei Wang, Dong Wang, and Na Wei. "A whole-cell biosensor for point-of-care detection of waterborne bacterial pathogens". *ACS Synthetic Biology* 10.2 (2021), pp. 333–344.

[3] Kristen M. DeAngelis, Pingsheng Ji, Mary K. Firestone, and Steven E. Lindow. "Two novel bacterial biosensors for detection of nitrate availability in the rhizosphere". *Applied and Environmental Microbiology* 71.12 (2005), pp. 8537–8547.

[4] Robin Gebbers and Viacheslav I. Adamchuk. "Precision agriculture and food security". *Science* 327.5967 (2010), pp. 828–831.

[5] David L. Jones and Eva Oburger. "Solubilization of phosphorus by soil microorganisms". *Phosphorus in action: biological processes in soil phosphorus cycling* (2011), pp. 169–198.

[6] Ghislaine Recorbet, Christine Picard, Philippe Normand, and Pascal Simonet. "Kinetics of the persistence of chromosomal DNA from genetically engineered *Escherichia coli* introduced into soil". *Applied and Environmental Microbiology* 59.12 (1993), pp. 4289–4294.

[7] Linda S. Thomashow and David M. Weller. "Role of a phenazine antibiotic from Pseudomonas fluorescens in biological control of *Gaeumannomyces graminis* var. tritici". *Journal of Bacteriology* 170.8 (1988), pp. 3499–3508.

[8] Yawen Chen, Xuemei Shen, Huasong Peng, Hongbo Hu, Wei Wang, and Xuehong Zhang. "Comparative genomic analysis and phenazine production of *Pseudomonas chlororaphis*, a plant growth-promoting rhizobacterium". en. *Genom Data* 4 (June 2015), pp. 33–42.

[9] Yonatan Chemla, Yuval Dorfan, Adi Yannai, Dechuan Meng, Paul Cao, Sarah Glaven, D. Benjamin Gordon, Johann Elbaz, and Christopher A. Voigt. "Parallel engineering of environmental bacteria and performance over years under jungle-simulated conditions". *PloS One* 17.12 (2022), e0278471.

[10] Letty A. De Weger, Linda C. Dekkers, Arjan J. Van Der Bij, and Ben J. J. Lugtenberg. "Use of phosphate-reporter bacteria to study phosphate limitation in the rhizosphere and in bulk soil". *Molecular Plant-Microbe Interactions* 7.1 (1994), pp. 32–38.

[11] Lene Kragelund, Carsten Hosbond, and Ole Nybroe. "Distribution of metabolic activity and phosphate starvation response of lux-tagged *Pseudomonas fluorescens* reporter bacteria in the barley rhizosphere". *Applied and Environmental microbiology* 63.12 (1997), pp. 4920–4928.

[12] Marie Andrée Dollard and Patrick Billard. “Whole-cell bacterial sensors for the monitoring of phosphate bioavailability”. en. *Journal of Microbiological Methods* 55.1 (Oct. 2003), pp. 221–229.

[13] Erez Dekel and Uri Alon. “Optimality and evolutionary tuning of the expression level of a protein”. *Nature* 436.7050 (2005), pp. 588–592.

[14] Luis López-Maury, Samuel Marguerat, and Jürg Bähler. “Tuning gene expression to changing environments: from rapid responses to evolutionary adaptation”. *Nature Reviews Genetics* 9.8 (2008), pp. 583–593.

[15] Weston R. Whitaker, Elizabeth Stanley Shepherd, and Justin L. Sonnenburg. “Tunable expression tools enable single-cell strain distinction in the gut microbiome”. *Cell* 169.3 (2017), pp. 538–546.

[16] Karsten Temme, Rena Hill, Thomas H. Segall-Shapiro, Felix Moser, and Christopher A. Voigt. “Modular control of multiple pathways using engineered orthogonal T7 polymerases”. *Nucleic Acids Research* 40.17 (2012), pp. 8773–8781.

[17] Russell D. Monds, Peter D. Newell, Julia A. Schwartzman, and George A. O’Toole. “Conservation of the Pho regulon in *Pseudomonas fluorescens* Pf0-1”. en. *Applied Environmental Microbiology* 72.3 (Mar. 2006), pp. 1910–1924.

[18] Stewart G. Gardner and William R. McCleary. “Control of the phoBR Regulon in *Escherichia coli*”. *EcoSal Plus* 8.2 (2019), pp. 10–1128.

[19] Fernando Santos-Beneit. “The Pho regulon: a huge regulatory network in bacteria”. en. *Frontiers in Microbiology* 0 (2015).

[20] Barry L. Wanner. “Gene regulation by phosphate in enteric bacteria”. *Journal of Cellular Biochemistry* 51.1 (1993), pp. 47–54.

[21] Nathan C. Shaner, Gerard G. Lambert, Andrew Chammas, Yuhui Ni, Paula J. Cranfill, Michelle A. Baird, Brittney R. Sell, John R. Allen, Richard N. Day, Maria Israelsson, et al. “A bright monomeric green fluorescent protein derived from Branchiostoma lanceolatum”. *Nature methods* 10.5 (2013), pp. 407–409.

[22] Michael B. Elowitz and Stanislas Leibler. “A synthetic oscillatory network of transcriptional regulators”. *Nature* 403.6767 (2000), pp. 335–338.

[23] Kyoung-Hee Choi and Herbert P. Schweizer. “mini-Tn7 insertion in bacteria with single att Tn7 sites: example *Pseudomonas aeruginosa*”. *Nature Protocols* 1.1 (2006), pp. 153–161.

[24] Dmitri V. Mavrodi, Vladimir N. Ksenzenko, Robert F. Bonsall, R. James Cook, Alexander M. Boronin, and Linda S. Thomashow. “A seven-gene locus for synthesis of phenazine-1-carboxylic acid by *Pseudomonas fluorescens* 2-79”. *Journal of Bacteriology* 180.9 (1998), pp. 2541–2548.

[25] William S. Kisaalita, Patricia J. Slininger, and Rodney J. Bothast. “Defined media for optimal pyoverdine production by *Pseudomonas fluorescens* 2-79”. *Applied Microbiology and Biotechnology* 39 (1993), pp. 750–755.

[26] Hafiz Muhammad Bilal, Tariq Aziz, Muhammad Aamer Maqsood, Muhammad Farooq, and Guijun Yan. “Categorization of wheat genotypes for phosphorus efficiency”. *PloS One* 13.10 (2018), e0205471.

[27] Ankita Puri-Taneja, Salbi Paul, Yinghua Chen, and F Marion Hulett. *CcpA Causes Repression of the phoPR Promoter through a Novel Transcription Start Site, P* $_{A6}$. 2006.

[28] Juan F. Martín, Alberto Sola-Landa, Fernando Santos-Beneit, Lorena T. Fernández-Martínez, Carlos Prieto, and Antonio Rodríguez-García. “Cross-talk of global nutritional regulators in the control of primary and secondary metabolism in Streptomyces”. *Microbial Biotechnology* 4.2 (2011), pp. 165–174.

[29] Piotr Bielecki, Vanessa Jensen, Wiebke Schulze, Julia Gödeke, Janine Strehmel, Denitsa Eckweiler, Tanja Nicolai, Agata Bielecka, Thorsten Wille, Roman G. Gerlach, et al. “Cross talk between the response regulators PhoB and TctD allows for the integration of diverse environmental signals in *Pseudomonas aeruginosa*”. *Nucleic Acids Research* 43.13 (2015), pp. 6413–6425.

[30] Fredrik Demoling, Daniela Figueroa, and Erland Bååth. “Comparison of factors limiting bacterial growth in different soils”. *Soil Biology and Biochemistry* 39.10 (2007), pp. 2485–2495.

[31] Stefanie Heinze, Joachim Raupp, and Rainer Georg Joergensen. “Effects of fertilizer and spatial heterogeneity in soil pH on microbial biomass indices in a long-term field trial of organic agriculture”. *Plant and Soil* 328 (2010), pp. 203–215.

[32] Richard W. Smiley and R. James Cook. “Relationship between Take-all of wheat and rhizosphere pH”. *Phytopathology* 63 (1973), pp. 882–890.

[33] Richard W. Smiley. “Rhizosphere pH as influenced by plants, soils, and nitrogen fertilizers”. *Soil Science Society of America Journal* 38.5 (1974), pp. 795–799.

[34] Aline Ortega-Pieck, Jessica Norby, Erin S. Brooks, Daniel Strawn, Alex R. Crump, and David R. Huggins. *Sources and subsurface transport of dissolved reactive phosphorus in a semiarid, no-till catchment with complex topography*. Tech. rep. doi:10.1002/jeq2.20114. Wiley Online Library, 2020.

[35] Lolo Wal Marzan and Kazuyuki Shimizu. “Metabolic regulation of *Escherichia coli* and its *phoB* and *phoR* genes knockout mutants under phosphate and nitrogen limitations as well as at acidic condition”. en. *Microbial Cell Factories* 10 (May 2011), p. 39.

[36] Hans Lambers. “Phosphorus acquisition and utilization in plants”. *Annual Review of Plant Biology* 73 (2022), pp. 17–42.

[37] Frida Grynspan and Munir Cheryan. “Calcium phytate: effect of pH and molar ratio on *in vitro* solubility”. *Journal of the American Oil Chemists' Society* 60.10 (1983), pp. 1761–1764.

[38] Daphne S. Bindels, Lindsay Haarbosch, Laura Van Weeren, Marten Postma, Katrin E. Wiese, Marieke Mastop, Sylvain Aumonier, Guillaume Gotthard, Antoine Royant, Mark A. Hink, et al. “mScarlet: a bright monomeric red fluorescent protein for cellular imaging”. *Nature Methods* 14.1 (2017), pp. 53–56.

[39] Cameron D. McBride, Theodore W. Grunberg, and Domitilla Del Vecchio. “Design of genetic circuits that are robust to resource competition”. *Current Opinion in Systems Biology* 28 (2021), p. 100357.

[40] Michael Lanzer and Hermann Bujard. “Promoters largely determine the efficiency of repressor action.” *Proceedings of the National Academy of Sciences* 85.23 (1988), pp. 8973–8977.

[41] *Promoters/Catalog/Anderson - parts.igem.org — parts.igem.org*. `http://parts.igem.org/Promoters/Catalog/Anderson`. [Accessed 05-09-2023].

[42] Joseph T. Meyerowitz, Elin M. Larsson, and Richard M. Murray. “Development of cell-free transcription–translation systems in three soil Pseudomonads”. *ACS Synthetic Biology* 13.2 (2024), pp. 530–537.

[43] David M. Weller, R. James Cook, et al. “Suppression of take-all of wheat by seed treatments with fluorescent pseudomonads”. *Phytopathology* 73.3 (1983), pp. 463–469.

[44] Jeffrey Meisner and Joanna B. Goldberg. “The *Escherichia coli* rhaSR-PrhaBAD inducible promoter system allows tightly controlled gene expression over a wide range in *Pseudomonas aeruginosa*”. *Applied and environmental microbiology* 82.22 (2016), pp. 6715–6727.

[45] Kyoung-Hee Choi, Jared B Gaynor, Kimberly G White, Carolina Lopez, Catharine M Bosio, RoxAnn R Karkhoff-Schweizer, and Herbert P Schweizer. “A Tn 7-based broad-range bacterial cloning and expression system”. *Nature Methods* 2.6 (2005), pp. 443–448.

[46] Sebastian M. Castillo-Hair, John T. Sexton, Brian P. Landry, Evan J. Olson, Oleg A. Igoshin, and Jeffrey J. Tabor. “FlowCal: A user-friendly, open source software tool for automatically converting flow cytometry data from arbitrary to calibrated units”. *ACS Synthetic Biology* 5.7 (2016), pp. 774–780.

[47] Robert A. Andersen. *Algal culturing techniques*. Elsevier, 2005.

[48] Darcy L. McRose and Dianne K. Newman. “Redox-active antibiotics enhance phosphorus bioavailability”. en. *Science* 371.6533 (Mar. 2021), pp. 1033–1037.

Chapter 3

IN VITRO TRANSCRIPTION TRANSLATION (TX-TL) IN CELL-EXTRACTS FROM NON-MODEL SOIL ORGANISMS

The work described in this chapter is a modification of the following publication:

> Joseph T. Meyerowitz*, Elin M. Larsson*, and Richard M. Murray. "Development of cell-free transcription–translation Systems in three soil pseudomonads". *ACS Synthetic Biology* 13.2 (2024), pp. 530–537. DOI: 10.1021/acssynbio.3c00468.

All experiments in this chapter that involve TX-TL made from pseudomonads were done by J. Meyerowitz and all experiments that involve engineered living cells were done by E. Larsson as described in the Author Contribution section below.

3.1 Introduction

The field of synthetic biology has advanced considerably over the past years. From scar-free DNA assembly [1] to CRISPR-mediated genome editing [2], new technologies have made it possible to tackle increasingly complex tasks in the engineering and control of biological systems. Synthetic biology has advanced to a point where we can reliably engineer bacteria to perform varying and complex tasks including synthesis of precious chemicals [3, 4], performance of logical operations [5, 6] and sensing [7]. Substantial challenges still remain with the use of synthetic biology tools. While the cost of DNA sequencing and DNA synthesis continues to decline [8, 9], and databases of genetic information [10], protein structure [11], and characterized genetic parts [12–14] continue to expand, composing these separate advances into engineered biological systems is complicated and incompletely systematized. Because of this difficulty, new techniques in the field are often implemented only in well-understood model organisms like *Escherichia coli*, *Bacillus subtilis*, *Pseudomonas putida* and *Saccharomyces cerevisiae*. To expand the range of projects possible with synthetic biology, developing tools for use with non-model organisms is essential. Environmental bacteria often have desirable traits unavailable in model organisms, such as the ability to perform specific types of metabolism [15], tolerate certain stresses and inhibitors [16] and colonize different environments [17–19]. Making non-model organisms tractable for engineering also

enables targeted experiments to reveal the roles these organisms play in their natural niches.

While some advances have been made in engineering non-model organisms [20–22], "domesticating" a non-model organism remains challenging. For a new organism of interest, the first steps for engineering are to find methods for cultivation and transformation. A later step is to characterize genetic parts from which new circuits can be built. One reason why working with non-model organisms is challenging comes from the variation in each species' underlying biology, requiring species-by-species tailoring of every protocol. An example of this variation can be seen in the mechanism for ribosomal initiation, which can have dramatic differences from commonly used organisms such as *E. coli* which use Shine-Delgarno led initiation and other bacteria such as *Deinococcus deserti* or *Mycobacterium tuberculosis* which frequently use leaderless mRNA sequences without a Shine-Delgarno sequence [23].

One approach used to accelerate engineering of non-model organisms is *in vitro* transcription-translation (TX-TL), or "cell-free protein synthesis". TX-TL reactions re-comprise the machinery necessary for RNA transcription and protein translation. By removing soluble internal components from a species of interest and producing a clarified lysate, this process results in a non-living, simplified system that can be used to prototype genetic parts and enzymes [24]. TX-TL is particularly useful for the study of non-model organisms that may be difficult to genetically transform or grow under certain conditions [25]. Instead of cloning and re-isolating the correct transformed cells, plasmid DNA or PCR products containing the circuit can be added to a mixture of the lysate and other components needed such as amino acids and salts. This procedure allows characterization of the test parts within hours. Genetic manipulation of some non-model organisms can take days or weeks to complete.

Creating TX-TL reactions using extracts from non-model organisms can be challenging, as the activity depends on factors such as growth phase during harvest. Some species have long doubling times which makes the process of reaching high cell densities time consuming and contamination-prone. Because of the extensive knowledge about the *E. coli* genome, certain genetic alterations have been shown to increase *in vitro* activity by removing DNA and amino acid degrading enzymes [26]. Such a strategy cannot be applied generally with non-model organisms, as the identify of similar genes may not be known. Despite these challenges, TX-TL has been successfully created from non-model organisms including *Bacillus megaterium* [25] and several Streptomycetes [27] .

In this study, we demonstrate the production and characterization of TX-TL systems from three soil-derived wild-type Pseudomonads. Soil provides a high-lignin environment where bacteria may have evolved tolerance to certain stresses ill-tolerated by the gastrointestinal dweller *Escherichia coli* [28]. To find potential new chassis for engineering with the desired stress tolerances, three bacteria, *Pseudomonas synxantha* 2-79 ("PSX"), *Pseudomonas chlororaphis* PCL1391 ("PCL"), and *Pseudomonas aureofaciens* 30-84 ("PAU"), were chosen for testing.

P. aureofaciens 30-84 is also called *P. chlororaphis subvar. aureofaciens* 30-84, and is closely related to *P. chlororaphis* PCL1391. PSX is more distantly related, with a similar distance between its genome, *E. coli*, PCL, and PAU as measured by digital DNA-DNA hybridization [29]. The phylogenetic relationships between the three target bacteria and other bacteria used for TX-TL are described in Figure 3.1 and Figure 3.2 . All three of the Pseudomonads are wild-type isolates without many of the common mutations such as restriction system knockouts seen in more domesticated strains [30].

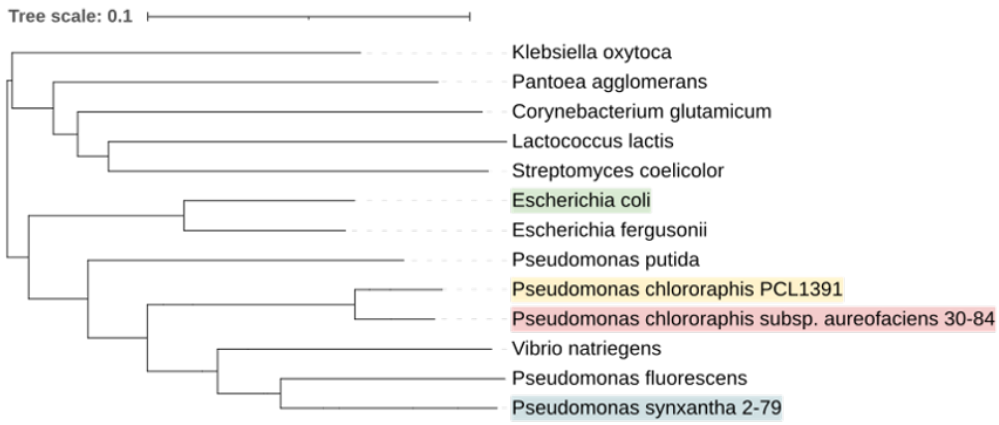

Figure 3.1: Phylogenetic tree of bacteria used for in vitro transcription-translation (TX-TL), including the three in this study (highlighted).

This class of organisms is important because of their ecological ubiquity, and these specific *Pseudomonas* species have been studied separately and together as symbionts of plant roots. They produce anti-microbial phenazines [31–33], promoting plant growth [34, 35]. The phenazines from these bacteria are known to control take-all, a disease in wheat plant roots, and damping-off disease, a multi-pathogen constellation of seed and seedling injuries across different plant species

dDDH d4 in % [C.I.] (G+C difference)	*Pseudomonas synxantha* 2-79	*Pseudomonas chlororaphis* PCL1391	*Pseudomonas aureofaciens* 30-84	*Escherichia coli*
Pseudomonas synxantha 2-79		25.4 [23.0 - 27.8] (2.9%)	25.6 [23.3 - 28.1] (3.17%)	22.8 [20.5 - 25.2] (9.14%)
Pseudomonas chlororaphis PCL1391	25.4 [23.0 - 27.8] (2.9%)		58.3 [55.5 - 61.0] (0.27%)	21.7 [19.5 - 24.1] (12.18%)
Pseudomonas aureofaciens 30-84	25.6 [23.3 - 28.1] (3.17%)	58.3 [55.5 - 61.0] (0.27%)		21.8 [19.6 - 24.3] (12.31%)
Escherichia coli	22.8 [20.5 - 25.2] (9.14%)	21.7 [19.5 - 24.1] (12.18%)	21.8 [19.6 - 24.3] (12.31%)	

Figure 3.2: Genome-to-genome distances determined by digital DNA-DNA hybridiszation (dDDH) with the genome-length independent d4 measure, confidence intervals [low-high] brackets and (G+C content difference) in parenthesis. Higher dDDH d4 values indicate closer genomic distances.

[36]. It has also been suggested that these molecules may play a role in nutrient cycling in the soil [37].

Pseudomonads also demonstrate an innate tolerance to certain growth inhibitory compounds in the environment and in industrial fermentation settings. Their ability to tolerate solvents and certain growth inhibitors found in low-cost industrial feedstock make them good candidates for commercial applications [38]. These bacteria can sometimes metabolize lignocellulosic growth inhibitors as well, showcasing their evolutionary adaptation to environments abundant in plant material [39, 40]. Root-living bacteria typically also evolve tolerance to anti-microbial compounds, such as penicillins, produced by other bacteria competing to inhabit the same ecological niche [41]. The creation of these three TX-TL systems from wild-type strains expand the toolkit for engineering these and other environmental bacteria.

3.2 Results and Discussion

In vitro transcription-translation systems are possible with three new wild-type Pseudomonads

We conducted *in vivo* experiments exploring the phenotypic differences between the Pseudomonads and *E. coli*, showing different growth inhibitors have varied degrees of effect on each species (Figure 3.3,3.4,3.5 and 3.6). With this validation

showing meaningful new capabilities in these Pseudomonad chassis, we attempted to produce functional Pseudomonad *in vitro* transcription-translation systems for use in prototyping similar to how *E. coli* cell-free systems have been used previously.

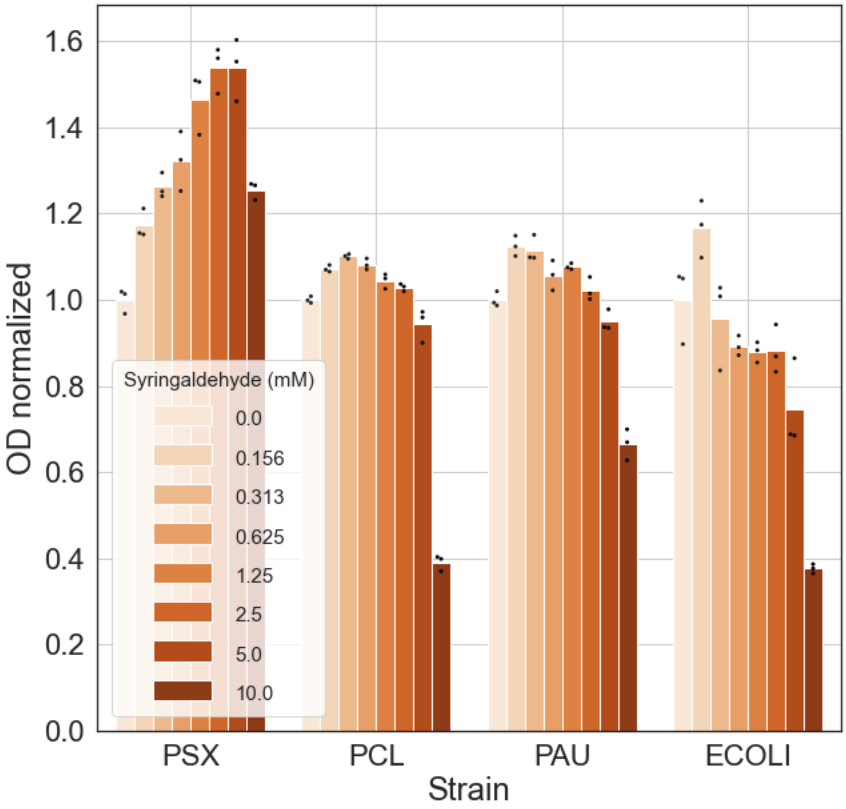

Figure 3.3: Differences in growth when exposed to syringaldehyde. Barplots are showing one biological replicate of the final optical density (OD) after 24 hours of growth normalized to the OD of cells grown without any growth inhibitor.

We tested the growth rates of each Pseudomonad at 50 mL scale in 250 mL baffled flasks of each species with inoculum sizes of 1:100 and 1:1000 from overnight 5 mL cultures in 2xYTPG. Growth was sufficient to support production of cell pellets for TX-TL use, shown in Supplementary Section C, and identified likely time and OD600 ranges for early exponential phase harvest.

Scale-up continued to 660 mL scale in 2.8L baffled flasks. Cultures were harvested at OD 3.0 ±10% for all three *Pseudomonas* species to begin with; initial testing showed *P. chlororaphis* lysate required an earlier harvest, chosen to be at OD 1.5

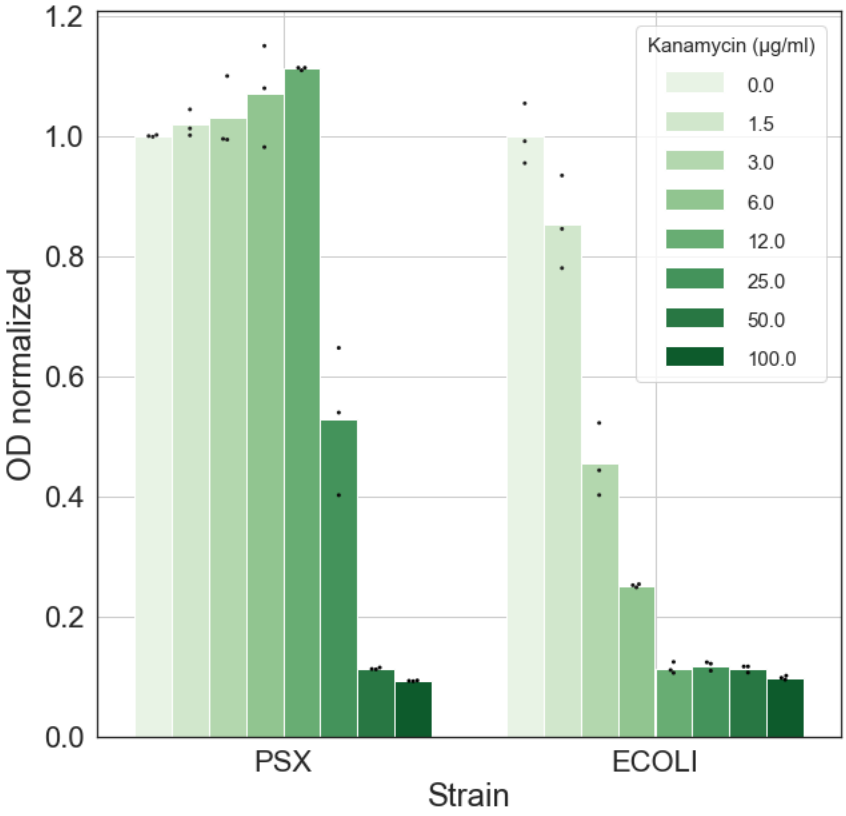

Figure 3.4: Differences in growth when exposed to kanamycin. Barplots are showing one biological replicate of the final optical density (OD) after 24 hours of growth normalized to the OD of cells grown without any growth inhibitor.

±10% (data not shown). Each replicate for each species was grown on a different day in 3x 660 mL volume, harvested, washed, split into two 50 mL tubes, and flash frozen as a set of two pellets for later processing into clarified lysate. The total wet cell weight of the combined pair of pellets from each growth was 14.2g ±0.6g (s.d.) for PSX, 8.6g ±0.1g (s.d.) for PCL, and 15.4g ±1.4g (s.d.) for PAU.

The first lysates were produced using one of the two frozen pellets with varying process conditions. In previous work, two of the most important parameters to optimize after harvest time have been lysis and runoff [42]. Here we try three different sonication amplitudes and three different runoff times, and test each combination across six different reaction conditions (Figure 3.7A). These varied protocol parameters show different protein yields across lysates from all three species

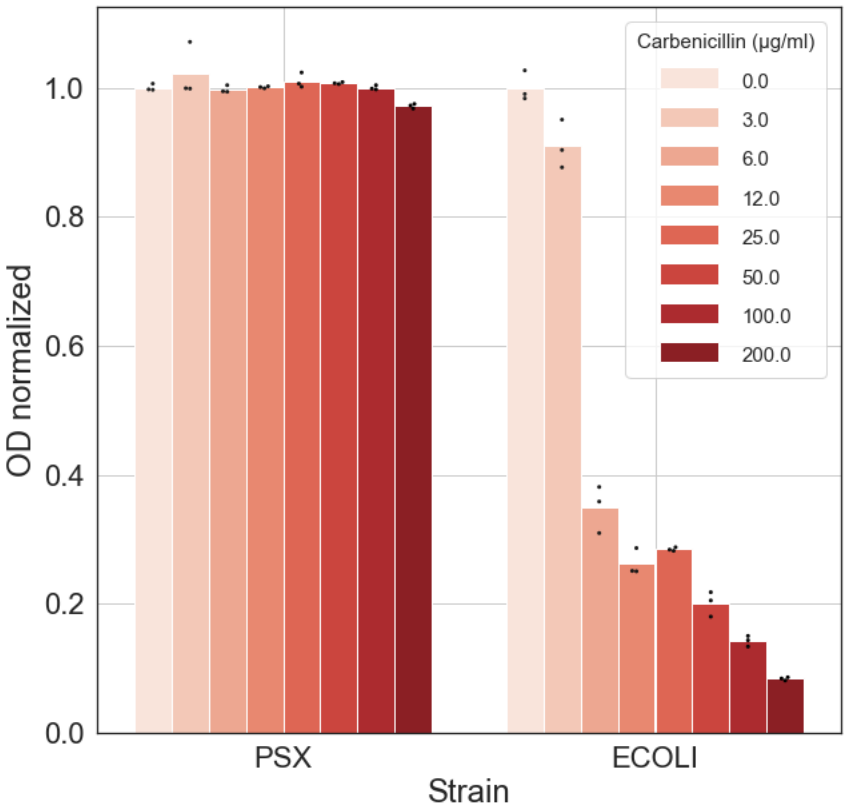

Figure 3.5: Differences in growth when exposed to streptomycin. Barplots are showing one biological replicate of the final optical density (OD) after 24 hours of growth normalized to the OD of cells grown without any growth inhibitor.

(Figure 3.7B). The protein concentrations of the lysates used were similar across all conditions
(Figure 3.8). Negative controls with no DNA template showed little change in fluorescence over time.

One important note is that these reaction conditions were prepared by creating a single mix of energy solution, amino acid mix, and PEG, then adding it to 384 well plates with the different salts. The pattern of increased and decreased yield is unlikely to be the result of differences in the preparation of the reaction buffer, as all of the data here come from the preparation of a single mixture of the common reaction components. Any variation between reactions here would be due to differences between the Pseudomonads and their lysates as prepared here.

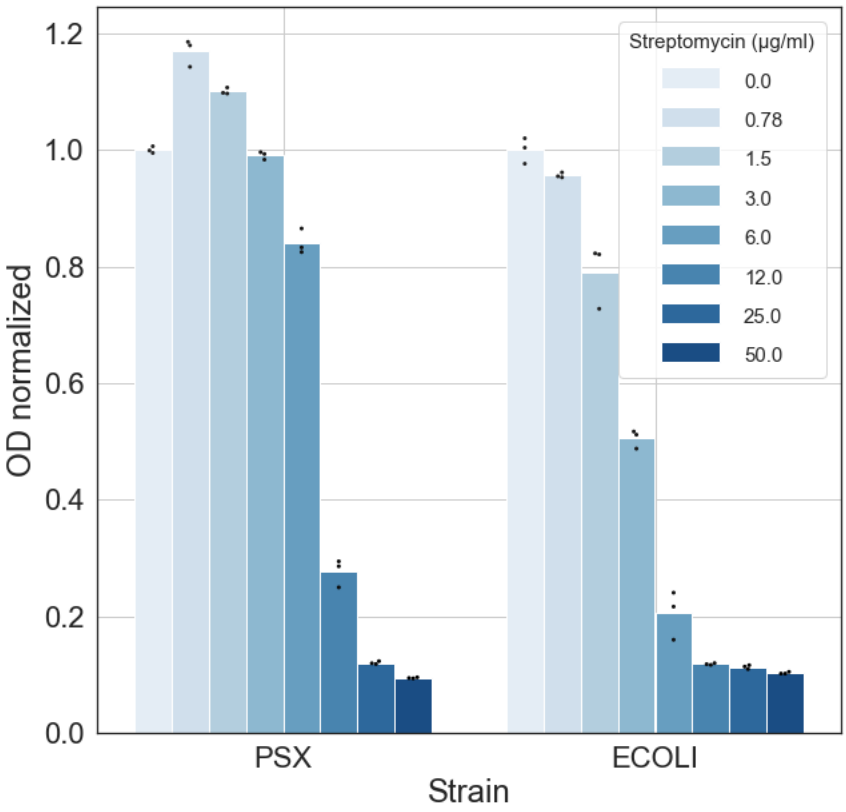

Figure 3.6: Differences in growth when exposed to carbenicillin. Barplots are showing one biological replicate of the final optical density (OD) after 24 hours of growth normalized to the OD of cells grown without any growth inhibitor.

Batch-to-batch variability is a known issue for cell-free studies, and differences are expected between each batch of lysate grown and processed on different days [43]. The results here show a range of viable conditions for productive lysates and similar trends across the process conditions for all three species. This wide range of usable variations with this protocol demonstrate a degree of robustness to variation in lysate processing and reaction preparation.

Repeating lysis production at larger scale improved yield and consistency of *P. synxantha* TX-TL

Next, three new batches of PSX lysate were produced on separate days at a single sonication amplitude (‘50’) and a single runoff time (60 minutes), affording more

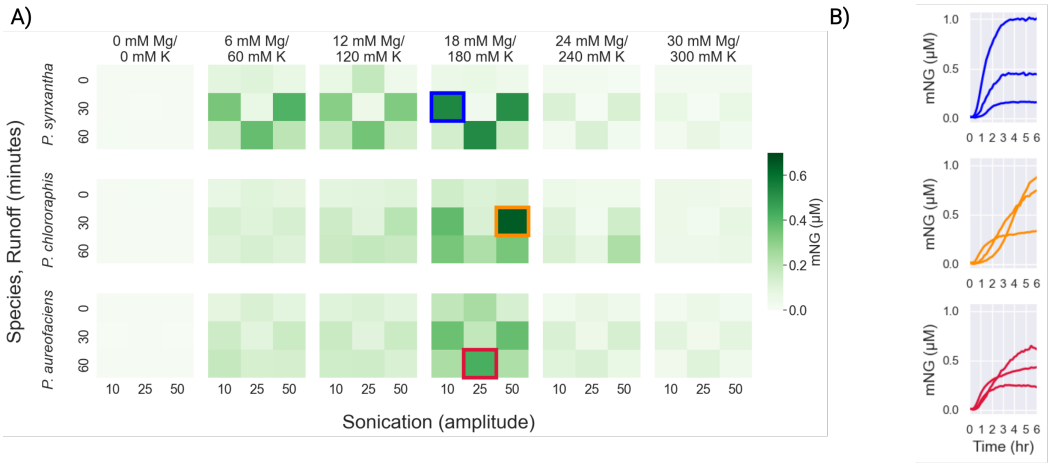

Figure 3.7: All three species show productive TX-TL systems across a range of lysate preparation and reaction parameters. (a) Mean protein yield across biological replicates, different sonication amplitudes, runoff times, salt concentrations, and species, shown after 6 hours of TX-TL reaction time. (b) Individual traces showing the increase in fluorescence over time from each species across biological replicates (PSX in blue, PCL in orange, PAU in red).

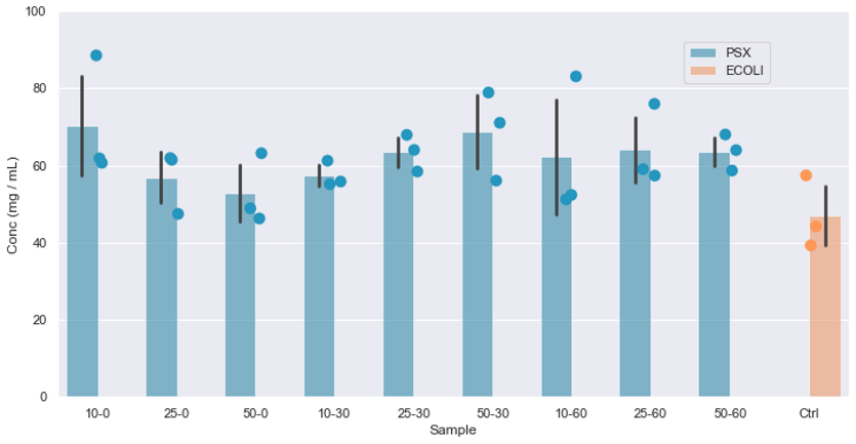

Figure 3.8: Protein concentrations of different *P. synxantha* lysates as determined by Bradford assay. The sample labels at the bottom indicate "sonication amplitude" (left, arbitrary units) and "runoff time" (right, minutes). Bar heights are averages, error bars are standard deviation, and the dots are the individual measurements.

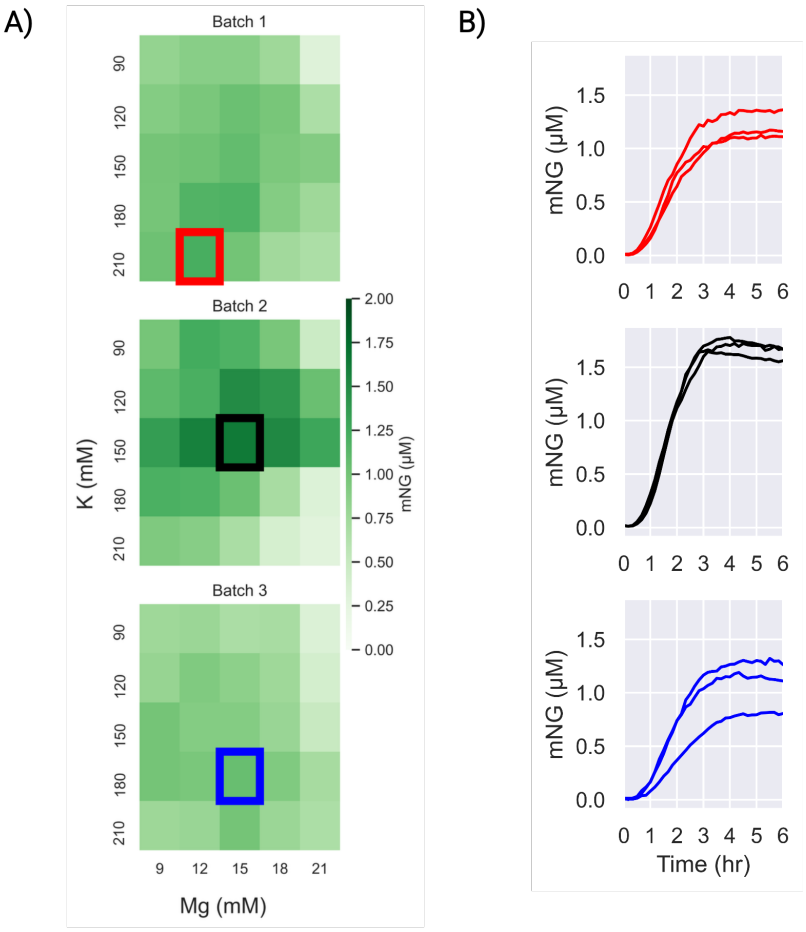

Figure 3.9: Salt panel for the follow-on batches of PSX lysate. (a) Variations in reaction salt optima across three batches of *P. synxantha* lysate shown after 6 hours of TX-TL reaction time. (b) Individual time traces from each batch, each chart showing technical replicates.

lysate for detailed testing. These conditions were within the range of process parameters that produced productive extract, and were not at any specific optimum shown across the biological triplicates above. These new batches used the second of the two frozen pellets from the triplicate growths described above. Batch 1 was made from the same harvested culture as the first PSX replicate in Figure 1, Batch 2 and Batch 3 correspond to the second and third cultures used as well.

These follow-on lysates show an approximately doubled protein yield and increased consistency between biological replicates compared to the reactions in Figure 1 and were produced from the same cultures. There were improvements in speed of processing time due to the simpler procedure with one sonication energy and one runoff time, and additional improvements in speed due to increased experience with processing the pellets into lysates. The causes of the improvements in these follow-on lysates were not explored in greater depth.

Potassium and magnesium salts were tested with more detail across a narrower range of concentrations (Figure 3.9A). The test conditions show a clear fluorescent signal accumulating over the first 4-5 hours of the reaction for all three of the new batches (Figure 3.9B). The yields and optimum salt concentrations vary across the different batches to a degree similar to past *E. coli* TX-TL reactions. These results demonstrate the extract making process was repeatable, and illustrate the degree of variation batch-to-batch.

Increases in DNA template produce higher protein yields

Next, using these three "big batches" of extract with their respective salt optimization values, we tested a varying amount of DNA template added to the reaction (Figure 3.10A-B). Each batch of extract produced a similar amount of the fluorescent reporter for a given template concentration. Across the tested template concentrations, more template always results in more protein. Doubling the amount of template doubles the amount of fluorescent reporter made within some of the tested range.

Qualitatively all of the extracts stop producing mNeonGreen at around 4 hours regardless of the amount of template that is added. Reactions producing protein at a high rate might exhaust some key resource faster compared to reactions with lower protein production rates. However, here the data show no change in the duration of protein synthesis across a wide range of protein production rates.

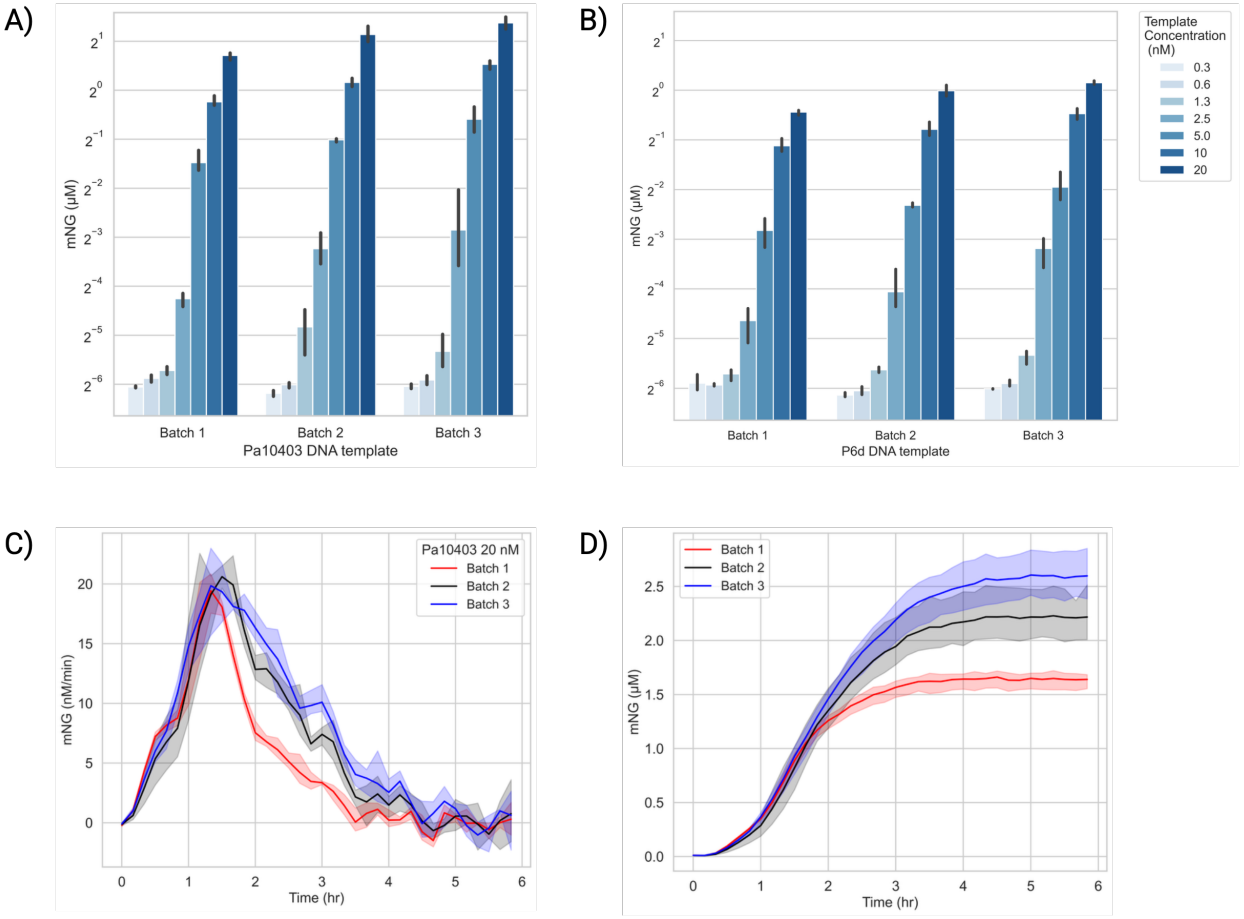

Figure 3.10: Fluorescence measurements at different DNA template concentrations. (a and b) Endpoint protein yield across the three *P. synxantha* extract batches with varied DNA template concentration and two different templates. (c and d) Protein synthesis rates and cumulative protein yield across the same three batches with Pa10403 template at 20.0 nM. Error bands show standard deviation across technical replicates.

The 20 nM Pa10403 condition using the third extract batch reached the highest concentration of mNeonGreen among all of the PSX experiments here at approximately 2.5 μM with a peak synthesis rate of 20 nM/min (Figure 3.10C-D). Over the course of the reaction this protein yield is equal to 125 proteins produced per DNA template.

Protein synthesis rates are similar across all three batches in the early part of the reaction through the peak. The differences in protein yield between the batches are attributable to different rates of the reaction slowing post-peak.

Promoters tested *in vivo* and *in vitro* show similar strengths

To evaluate whether we could use the *P. synxantha* extract for prototyping of genetic elements as seen in previous studies of *E. coli* [44] and *B. megaterium* [25], we compared protein synthesis levels for 11 different constitutive promoters from *E. coli* and *P. putida* driving expression of a genomically integrated fusion with the green fluorescent protein mNeonGreen (Figure 3.11).

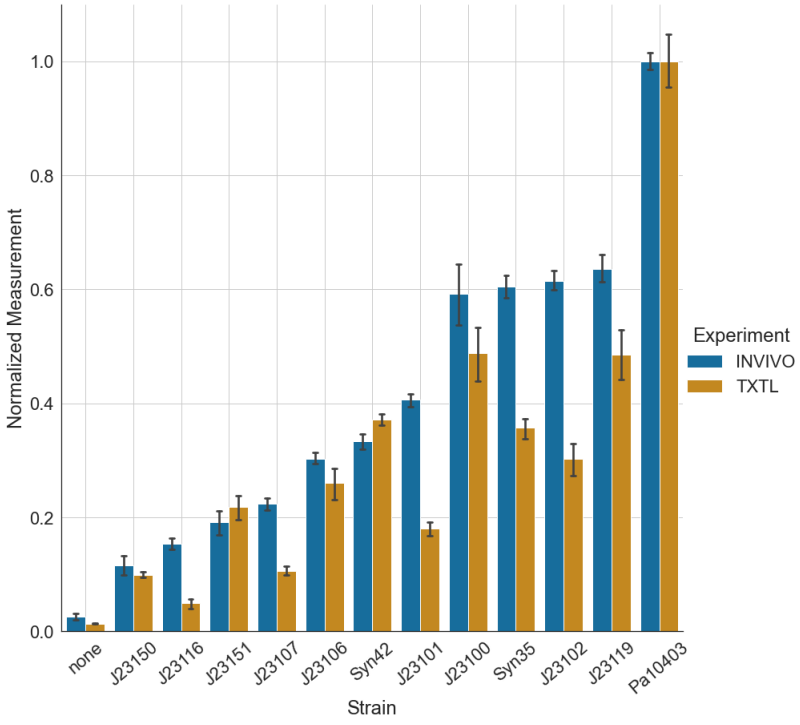

Figure 3.11: Constitutive promoters driving the expression of mNeonGreen were compared *in vivo* in *P. synxantha* living cells and *in vitro* in the *P. synxantha* TX-TL systems produced here. All expression levels are normalized to the expression level of the strongest promoter fusion using the Pa10403 promoter.

The fluorescence below is normalized by optical density at 500 nm at 24 hours of growth. To compare the results from the *in vitro* TX-TL reactions, we take the fluorescence from a time course at 6 hours into the reaction. We then normalize all fluorescence values to the largest fluorescence value of the strongest promoter Pa10403 [45]. The reactions *in vitro*, regardless of promoter strength, all stop producing protein at approximately the same time.

We can distinguish between strong and weak constitutive promoters using cell-free prototyping, but we cannot always accurately predict the rank of strength within these groups, as seen in previous work [25]. The normalized fluorescence in the TX-TL reactions is consistently lower than the corresponding *in vivo* values. Even though the *in vivo* to TX-TL comparison is not perfectly matched, the number of genetic elements that need to be tested *in vivo* can be reduced by first prototyping them using the TX-TL system. This also highlights the limitation of using TX-TL as a prototyping tool for *in vivo* expression. Some of this variation between contexts may be due to expression from a plasmid *in vitro* and the genome *in vivo*.

3.3 Conclusion

Together these experiments show that our target *Pseudomonas* spp. have pre-existing tolerance to some growth inhibitors that reduce the growth capacity of *E. coli*, and these species are tractable for further engineering work. The TX-TL measurements of the promoter panel match the *in vivo* measurements of the same promoters. This shows the TX-TL system can be used for characterizing parts for later use *in vivo*. The ability to perform TX-TL reactions with these species is a key component of engineering and rapid prototyping with new non-model organisms. A working TX-TL system can enable a faster design-build-test cycle, and make characterization of new parts practical.

3.4 Methods

Bacterial strains and growth conditions

Pseudomonas synxantha 2-79, *Pseudomonas chlororaphis* PCL1391, and *Pseudomonas aureofaciens* 30-84 were obtained from the Newman lab at Caltech. Cells were grown by streaking onto 2xYTPG (16 g/L tryptone, 10 g/L yeast extract, 5 g/L NaCl, 40 mM potassium phosphate dibasic, 22 mM potassium phosphate monobasic, 2% glucose) agar or LB (10 g/L tryptone, 5 g/L yeast extract, 5 g/L NaCl) agar without antibiotics and incubating for 18-36 hours at 30°C. Individual colonies were picked and grown in 5 mL of 2xYTPG with shaking at 200-220 rpm

at 30°C overnight. As needed, 50 mL of 2xYTPG in a 250 mL baffled flask or 660 mL of 2xYTPG in a 2.8L baffled flask with an adhesive AirOTop sterile seal would be inoculated 1:1000 the next day. Cell growth was monitored by optical density at 500 or 600 nm, with 1:1, 1:4, 1:16, 1:64, and 1:256 dilutions of culture samples prepared in fresh 2xYTPG media to stay in the Biotek H1MF plate reader linear range for absorption measurements (OD 0.005 to 0.5).

In vivo growth inhibition tests

Cells were grown with continuous shaking in a Biotek H1MF plate reader for 24 hours. The cells were grown in LB medium with added growth inhibitor in serial dilutions with a starting concentration of 10 mM syringaldehyde, 50 μg/ml streptomycin, 100 μg/ml kanamycin and 200 μg/ml carbenicillin. *P. synxantha* was grown at 30°C and *E. coli* was grown at 37°C.

Construction of DNA templates

DNA parts including promoters, ribosome binding sites, reporters, terminators, and backbones with antibiotic resistance were amplified by PCR in NEB Q5 2x Master Mix, purified by gel extraction and QIAGEN MinElute spin columns, and assembled using NEB Hifi 2x Master Mix.

Measurement of protein concentration

For each extract produced for the sonication, runoff, and salt panels, protein concentration was measured using a Bradford assay. In brief, a 1:50 dilution of lysate was prepared in Tris-buffered saline. A bovine serum albumin standard was used to prepare 8 different concentrations for a standard curve. Standard curves were prepared in triplicate on every 96-well plate used for protein measurement, and samples were also prepared in triplicate.

Production of *Pseudomonas* cell-free extracts

The protocol from Sun et al [42] and the protocol from Kwon et al [46] for *E. coli* TX-TL were repurposed for the *Pseudomonas* TX-TL protocol with minor modifications.

Briefly, in the top row step 1, cells are grown on 2xYTPG agar. After 18-36 hours of growth at 30°C, the plates are stored at 4°C for up to a month. In step 2, individual colonies are picked and used to grow 5 mL overnight cultures in 14 mL tubes. In step 3, 2.8 L baffled shake flasks with 660 mL of 2xYTPG are inoculated 1:1000 the

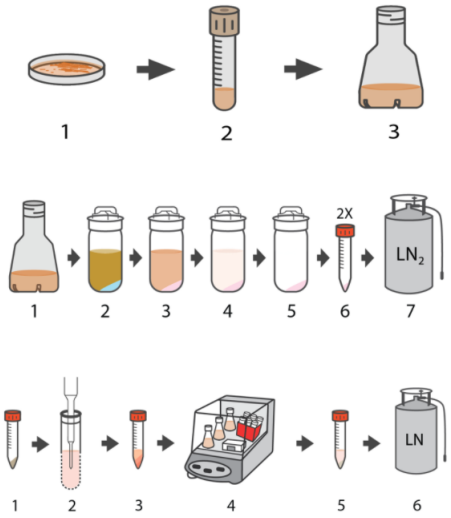

Figure 3.12: Graphical illustration of the growth, harvest, extract production, and reaction set-up steps used in this study.

next day and grown for 8-12 hours. Note that unlike previous protocols, the final culture is inoculated directly from a 5 mL overnight, without an intermediate 50 mL culture.

In the middle row step 1, cells are grown to the harvest optical density (absorption at 600 nm per cm, or "OD"), with monitoring of OD performed every 60 minutes until the last doubling of the growth, then monitoring increases to once per 20 minutes. Dilutions of 1:4, 1:16, 1:64, or 1:256 in fresh 2xYTPG media are used to produce a sample with an optical density within the specific plate reader's linear range (here determined to be under OD 0.5). In step 2 200 mL of Buffer A (1.8 g/L Tris-acetate, 3 g/L Mg-acetate, and 12.2 g/L K-glutamate, adjusted to pH 8.2 with 2M Tris and autoclaved, then 1 mL / L of 1M DTT is added) is frozen in 1L centrifuge bottles stored at -20°C at an angle for 1-2 hours. Do not freeze buffer in fully upright centrifuge bottles, as the expansion of the freezing liquid may exert pressure and deform the bottle. This step is an addition to the previous protocols.

At harvest time, the cell culture is decanted into the 1L centrifuge bottles over the wedge of buffer ice. This brings the culture temperature down from 30°C to 10°C within a few minutes. In step 3, the cell culture is centrifuged at 4800g for 12 minutes at 4°C. The supernatant is decanted, and the bottles are partially submerged in wet water ice. The cell pellet otherwise follows the protocol in [42] with Buffer A, passing through two wash steps in 1L bottles, followed by transfer into two weighed

50 mL tubes and a final wash step. The supernatant is removed, each 50 mL tube is re-weighed, and the pellet is flash frozen in liquid nitrogen and stored at -80°C.

At a later time, the cell pellet is removed from the freezer and placed on wet water ice to thaw. In the bottom row step 1, 1 mL / g of Buffer A is used to re-suspend the pellet, then equal volumes of re-suspended cell pellet are added to each 14 mL Falcon tube (3-5 mL). In step 2, each tube is sonicated for 120s, 5s on, 10s off, with an amplitude of 10, 25, or 50 on a Qsonica Q700. In step 3, the tubes are centrifuged at 12,000g for 10 minutes at 4°C. In step 4, the supernatant is transferred to new 1.4 mL or 14 mL tubes and incubated in a "runoff" step with open lids shaking at 220 rpm at 30°C for 0-60 minutes. These tubes are centrifuged again at 12,000g for 10 minutes at 4°C, then the supernatant is transferred to a new tube. Aliquots of this final clarified lysate are made for freezing in LN2 and storage at -80°C.

TX-TL reaction conditions

Reaction conditions also follow the *E. coli* protocol in Sun et. al. [42], including the composition of the energy solution and amino acid mix. In brief, each 10 microliter reaction in a 384 well plate contains 29% buffer, 13% potassium and magnesium glutamate salts, 25% DNA template solution, and 33% processed lysate. The buffer consists of 26% energy solution, 57% amino acid mix (6 mM of each amino acid, 1.5 mM in the final reaction), and 17% of 40% PEG-8000 in water. These are mixed on ice and hand-pipetted carefully to avoid introducing bubbles. Individual reactions are prepared in glass-bottomed 384 well plates sealed with an oxygen-permeable Breathe-Easy seal. The plate is centrifuged for 2 minutes to mix the reagents and reduce bubbles in the wells, then read at 30°C in the plate reader.

Preparation of DNA template for TX-TL reactions

E. coli JM109 or DH10B cells with DNA constructs were grown to 100 mL (midiprep) or 400 mL (maxiprep) scale. Pellets were processed using Macherey-Nagel midiprep or maxiprep kits to produce 100s to 1000s of micrograms of purified DNA, including a "finalizer" step to re-purify and concentrate the eluate from the kit. When reactions are prepared, a stock solution of purified DNA template is diluted as necessary and added to produce a final DNA concentration of 10 nM in the TX-TL reaction in all experiments except those shown in Figure 3, where the concentration was varied.

Measurement of *in vitro* fluorescence

Biotek H1M and H1MF plate readers were used to measure fluorescence of mNeonGreen (excitation 490 nm, emission 520 nm) and optical density (500 nm and 600 nm). mNeonGreen protein was produced in *E. coli*, purified using a his-tag and NiNTA columns, and UV absorption was used to quantify the amount of purified protein. Triplicate dilutions at 8 concentrations from 20 nM to 0 nM in 1x phosphate-buffered saline pH 7.4 were measured five times in all plate readers, and separate standard curves were created for each plate reader. Dilutions were incubated at 30°C during fluorescence measurements. Due to the amount of protein needed for calibration for this study, there was no attempt to synthesize the protein used for calibration with an *in vitro* TX-TL system, and it was assumed the *in vivo* produced protein would have comparable fluorescence properties to the *in vitro* produced protein.

Construction of constitutively fluorescent *P. synxantha*

All cloning to produce *P. synxantha* genomic integration constructs was done using *E. coli* DH10B with the backbone pJM220 [47]. Constitutive promoters from *E. coli* (http://parts.igem.org/Promoters/Catalog/Anderson) and *P. putida* [48] were fused to the fluorescent protein mNeonGreen. The constructs were then integrated on the *P. synxantha* chromosome using transposase based insertion at the Tn7 site. The protocol used for making and transforming competent cells was modified from Choi et al [49].

Briefly, electrocompetent *P. synxantha* cells were electroporated in 1 mm-gap cuvettes (at 1.8 mV, 600 Ω and 10 μF) with the construct plasmid as well as a plasmid containing the transposase and genes required for genome insertion [50]. The cells were then recovered in rich medium (SOC) for 3 hours at 30°C and plated onto LB agar plates containing gentamicin (20 μg/ml) and incubated for 24 hours before picking colonies for sequence verification.

Plate reader assay for *in vivo* fluorescence

In vivo fluorescence was measured using a Biotek (Synergy H1) plate reader. The experiments ran for 24 hours at 30°C using continuous orbital shaking starting from an overnight culture diluted to approximately OD 0.1 into LB medium. OD was measured every 10 minutes at 500 nm and fluorescence was measured at 490/520 nm.

Author Contribution

JTM, EML and RMM conceptualized the project. JTM and EML designed the experiments and analyzed the data. JTM performed TX-TL experiments. EML performed *in vivo* experiments, with the exception of the syringaldehyde experiment which was performed by JTM. EML did the plasmid construction and integration. JTM and EML wrote the manuscript with input from RMM.

Acknowledgements

With thanks to M. Prator for performing the Bradford assays of the lysates, to Z. Jurado for purifying the mNeonGreen fluorescence standard, to Prof. Dianne Newman for the *Pseudomonas* strains and R. Alcalde for the Pa10403-mNeonGreen plasmid and *P. synxantha* strain, to Dr. R. Sidney Cox III for assistance with data visualization, to Dr. A. Pandey for assistance with data processing, and to Dr. Dmitri Mavrodi for assistance with the genomic integration protocol for *P. synxantha*. This research is supported by the Institute for Collaborative Biotechnologies through contract W911NF-19-D-0001, cooperative agreement W911NF-19-2-0026, and grant W911NF-09-0001 from the U.S. Army Research Office, the National Science Foundation through grant CBET-1903477, and the International Human Frontiers Science Program. The content of this chapter does not necessarily reflect the position or the policy of the U.S. Government, and no official endorsement should be inferred.

References

[1] Daniel G. Gibson, Lei Young, Ray-Yuan Chuang, J. Craig Venter, Clyde A. Hutchison III, and Hamilton O. Smith. “Enzymatic assembly of DNA molecules up to several hundred kilobases”. *Nature Methods* 6.5 (2009), pp. 343–345.

[2] Rodolphe Barrangou and Jennifer A. Doudna. “Applications of CRISPR technologies in research and beyond”. *Nature Biotechnology* 34.9 (2016), pp. 933–941.

[3] Dae-Kyun Ro, Eric M. Paradise, Mario Ouellet, Karl J. Fisher, Karyn L. Newman, John M. Ndungu, Kimberly A. Ho, Rachel A. Eachus, Timothy S. Ham, James Kirby, et al. “Production of the antimalarial drug precursor artemisinic acid in engineered yeast”. *Nature* 440.7086 (2006), pp. 940–943.

[4] Jie Zhang, Lea G. Hansen, Olga Gudich, Konrad Viehrig, Lærke MM Lassen, Lars Schrübbers, Khem B. Adhikari, Paulina Rubaszka, Elena Carrasquer-Alvarez, Ling Chen, et al. “A microbial supply chain for production of the anti-cancer drug vinblastine”. *Nature* 609.7926 (2022), pp. 341–347.

[5] Baojun Wang, Richard I. Kitney, Nicolas Joly, and Martin Buck. "Engineering modular and orthogonal genetic logic gates for robust digital-like synthetic biology". *Nature Communications* 2.1 (2011), p. 508.

[6] Victoria Hsiao, Yutaka Hori, Paul W. K. Rothemund, and Richard M. Murray. "A population-based temporal logic gate for timing and recording chemical events". *Molecular Systems Biology* 12.5 (2016), p. 869.

[7] Maggie Hicks, Till T. Bachmann, and Baojun Wang. "Synthetic biology enables programmable cell-based biosensors". *ChemPhysChem* 21.2 (2020), pp. 132–144.

[8] Kris A. Wetterstrand. "DNA Sequencing Costs: Data from the NHGRI Genome Sequencing Program (GSP) Available at: www. genome. gov/sequencingcostsdata". *Accessed August* (2019).

[9] Randall A. Hughes and Andrew D. Ellington. "Synthetic DNA synthesis and assembly: putting the synthetic in synthetic biology". *Cold Spring Harbor Perspectives in Biology* 9.1 (2017), a023812.

[10] Eric W. Sayers, Mark Cavanaugh, Karen Clark, Kim D. Pruitt, Conrad L. Schoch, Stephen T. Sherry, and Ilene Karsch-Mizrachi. "GenBank". *Nucleic Acids Research* 50.D1 (2022), p. D161.

[11] John Jumper, Richard Evans, Alexander Pritzel, Tim Green, Michael Figurnov, Olaf Ronneberger, Kathryn Tunyasuvunakool, Russ Bates, Augustin Žídek, Anna Potapenko, et al. "Highly accurate protein structure prediction with AlphaFold". *Nature* 596.7873 (2021), pp. 583–589.

[12] Alec A. K. Nielsen, Bryan S. Der, Jonghyeon Shin, Prashant Vaidyanathan, Vanya Paralanov, Elizabeth A. Strychalski, David Ross, Douglas Densmore, and Christopher A. Voigt. "Genetic circuit design automation". *Science* 352.6281 (2016), aac7341.

[13] Adam J. Meyer, Thomas H Segall-Shapiro, Emerson Glassey, Jing Zhang, and Christopher A. Voigt. "*Escherichia coli* "Marionette" strains with 12 highly optimized small-molecule sensors". *Nature Chemical Biology* 15.2 (2019), pp. 196–204.

[14] Barry Canton, Anna Labno, and Drew Endy. "Refinement and standardization of synthetic biological parts and devices". *Nature Biotechnology* 26.7 (2008), pp. 787–793.

[15] Claudia Knief, André Lipski, and Peter F Dunfield. "Diversity and activity of methanotrophic bacteria in different upland soils". *Applied and Environmental Microbiology* 69.11 (2003), pp. 6703–6714.

[16] Juan-Luis Ramos, Maria Sol Cuenca, Carlos Molina-Santiago, Ana Segura, Estrella Duque, María R Gómez-García, Zulema Udaondo, and Amalia Roca. "Mechanisms of solvent resistance mediated by interplay of cellular factors

in *Pseudomonas putida*". *FEMS Microbiology Reviews* 39.4 (2015), pp. 555–566.

[17] Hayley E. Knights, Beatriz Jorrin, Timothy L. Haskett, and Philip S. Poole. "Deciphering bacterial mechanisms of root colonization". *Environmental Microbiology Reports* 13.4 (2021), pp. 428–444.

[18] Thomas Bjarnsholt, Peter Østrup Jensen, Mark J. Fiandaca, Jette Pedersen, Christine Rønne Hansen, Claus Bøgelund Andersen, Tacjana Pressler, Michael Givskov, and Niels Høiby. "*Pseudomonas aeruginosa* biofilms in the respiratory tract of cystic fibrosis patients". *Pediatric Pulmonology* 44.6 (2009), pp. 547–558.

[19] Spencer V. Nyholm and Margaret J. McFall-Ngai. "A lasting symbiosis: how the Hawaiian bobtail squid finds and keeps its bioluminescent bacterial partner". *Nature Reviews Microbiology* 19.10 (2021), pp. 666–679.

[20] Bradley W. Biggs, Stacy R. Bedore, Erika Arvay, Shu Huang, Harshith Subramanian, Emily A. McIntyre, Chantel V. Duscent-Maitland, Ellen L. Neidle, and Keith E. J. Tyo. "Development of a genetic toolset for the highly engineerable and metabolically versatile *Acinetobacter baylyi* ADP1". *Nucleic Acids Research* 48.9 (2020), pp. 5169–5182.

[21] Mao Taketani, Jianbo Zhang, Shuyi Zhang, Alexander J. Triassi, Yu-Ja Huang, Linda G. Griffith, and Christopher A. Voigt. "Genetic circuit design automation for the gut resident species *Bacteroides thetaiotaomicron*". *Nature Biotechnology* 38.8 (2020), pp. 962–969.

[22] Weston R. Whitaker, Elizabeth Stanley Shepherd, and Justin L. Sonnenburg. "Tunable expression tools enable single-cell strain distinction in the gut microbiome". *Cell* 169.3 (2017), pp. 538–546.

[23] Lorenzo Eugenio Leiva and Assaf Katz. "Regulation of leaderless mRNA Translation in Bacteria". en. *Microorganisms* 10.4 (Mar. 2022).

[24] Khushal Khambhati, Gargi Bhattacharjee, Nisarg Gohil, Darren Braddick, Vishwesh Kulkarni, and Vijai Singh. "Exploring the potential of cell-free protein synthesis for extending the abilities of biological Systems". en. *Frontiers in Bioengineering and Biotechnology* 7 (Oct. 2019), p. 248.

[25] Simon J. Moore, James T. MacDonald, Sarah Wienecke, Alka Ishwarbhai, Argyro Tsipa, Rochelle Aw, Nicolas Kylilis, David J. Bell, David W. McClymont, Kirsten Jensen, Karen M. Polizzi, Rebekka Biedendieck, and Paul S. Freemont. "Rapid acquisition and model-based analysis of cell-free transcription-translation reactions from nonmodel bacteria". en. *Proceedings of the National Academy of Sciences U. S. A.* 115.19 (May 2018), E4340–E4349.

[26] Stephanie D. Cole, Aleksandr E. Miklos, Abel C. Chiao, Zachary Z. Sun, and Matthew W. Lux. "Methodologies for preparation of prokaryotic extracts for cell-free expression systems". *Synthetic and Systems Biotechnology* 5.4 (2020), pp. 252–267.

[27] Simon J. Moore, Hung-En Lai, Jian Li, and Paul S. Freemont. "*Streptomyces* cell-free systems for natural product discovery and engineering". *Natural Product Reports* (2023).

[28] Rahul Datta, Aditi Kelkar, Divyashri Baraniya, Ali Molaei, Amitava Moulick, Ram Swaroop Meena, and Pavel Formanek. "Enzymatic degradation of lignin in soil: A review". *Sustainability* 9.7 (2017), p. 1163.

[29] Jan P. Meier-Kolthoff and Markus Göker. "TYGS is an automated high-throughput platform for state-of-the-art genome-based taxonomy". *Nature Communications* 10.1 (2019), p. 2182.

[30] Pablo I. Nikel, Esteban Martínez-García, and Víctor de Lorenzo. "Biotechnological domestication of pseudomonads using synthetic biology". en. *Nature Reviews Microbiology* 12.5 (May 2014), pp. 368–379.

[31] Muhammad Bilal, Shuqi Guo, Hafiz M. N. Iqbal, Hongbo Hu, Wei Wang, and Xuehong Zhang. "Engineering *Pseudomonas* for phenazine biosynthesis, regulation, and biotechnological applications: a review". *World Journal of Microbiology and Biotechnology* 33 (2017), pp. 1–11.

[32] Dieter Haas and Geneviève Défago. "Biological control of soil-borne pathogens by fluorescent pseudomonads". en. *Nature Reviews Microbiology* 3.4 (Apr. 2005), pp. 307–319.

[33] Kai Nesemann, Susanna A. Braus-Stromeyer, Andrea Thuermer, Rolf Daniel, Dmitri V. Mavrodi, Linda S. Thomashow, David M. Weller, and Gerhard H. Braus. "Draft Genome Sequence of the Phenazine-Producing Pseudomonas fluorescens Strain 2-79". en. *Genome Announcements* 3.2 (Mar. 2015).

[34] Linda S. Thomashow and David M. Weller. "Role of a phenazine antibiotic from Pseudomonas fluorescens in biological control of *Gaeumannomyces graminis* var. tritici". *Journal of Bacteriology* 170.8 (1988), pp. 3499–3508.

[35] Dieter Haas and Geneviève Défago. "Biological control of soil-borne pathogens by fluorescent pseudomonads". *Nature Reviews Microbiology* 3.4 (2005), pp. 307–319.

[36] T. M. Timms-Wilson, R. J. Ellis, A. Renwick, DJ Rhodes, D. V. Mavrodi, David M. Weller, Linda S. Thomashow, and M. J. Bailey. "Chromosomal insertion of phenazine-1-carboxylic acid biosynthetic pathway enhances efficacy of damping-off disease control by Pseudomonas fluorescens". *Molecular Plant-Microbe Interactions* 13.12 (2000), pp. 1293–1300.

[37] Darcy L. McRose and Dianne K. Newman. "Redox-active antibiotics enhance phosphorus bioavailability". *Science* 371.6533 (2021), pp. 1033–1037.

[38] Helene Bendstrup Klinke, A. B. Thomsen, and Birgitte Kiær Ahring. "Inhibition of ethanol-producing yeast and bacteria by degradation products produced during pre-treatment of biomass". *Applied Microbiology and Biotechnology* 66 (2004), pp. 10–26.

[39] Jun Hirose, Akari Nagayoshi, Naoya Yamanaka, Yuji Araki, and Haruhiko Yokoi. "Isolation and characterization of bacteria capable of metabolizing lignin-derived low molecular weight compounds". *Biotechnology and Bioprocess Engineering* 18 (2013), pp. 736–741.

[40] Thomas Kuhnigk and Helmut König. "Degradation of dimeric lignin model compounds by aerobic bacteria isolated from the hindgut of xylophagous termites". *Journal of Basic Microbiology* 37.3 (1997), pp. 205–211.

[41] Ismail Mahdi, Nidal Fahsi, Mohamed Hijri, and Mansour Sobeh. "Antibiotic resistance in plant growth promoting bacteria: A comprehensive review and future perspectives to mitigate potential gene invasion risks". *Frontiers in Microbiology* 13 (2022).

[42] Zachary Z. Sun, Clarmyra A. Hayes, Jonghyeon Shin, Filippo Caschera, Richard M. Murray, and Vincent Noireaux. "Protocols for implementing an *Escherichia coli* based TX-TL cell-free expression system for synthetic biology". en. *The Journal of Visualized Experiments* 79 (Sept. 2013), e50762.

[43] Katherine A Rhea, Nathan D McDonald, Stephanie D Cole, Vincent Noireaux, Matthew W Lux, and Patricia E Buckley. "Variability in cell-free expression reactions can impact qualitative genetic circuit characterization". en. *Synthetic Biology* 7.1 (Aug. 2022), ysac011.

[44] Zachary Z. Sun, Enoch Yeung, Clarmyra A. Hayes, Vincent Noireaux, and Richard M. Murray. "Linear DNA for rapid prototyping of synthetic biological circuits in an Escherichia coli based TX-TL cell-free system". *ACS Synthetic Biology* 3.6 (2014), pp. 387–397.

[45] Michael Lanzer and Hermann Bujard. "Promoters largely determine the efficiency of repressor action." *Proceedings of the National Academy of Sciences* 85.23 (1988), pp. 8973–8977.

[46] Yong-Chan Kwon and Michael C. Jewett. "High-throughput preparation methods of crude extract for robust cell-free protein synthesis". *Scientific Reports* 5.1 (2015), p. 8663.

[47] Jeffrey Meisner and Joanna B. Goldberg. "The *Escherichia coli* rhaSR-PrhaBAD inducible promoter system allows tightly controlled gene expression over a wide range in *Pseudomonas aeruginosa*". *Applied and environmental microbiology* 82.22 (2016), pp. 6715–6727.

[48] Sebastian Zobel, Ilaria Benedetti, Lara Eisenbach, Victor de Lorenzo, Nick Wierckx, and Lars M. Blank. "Tn7-based device for calibrated heterologous gene expression in *Pseudomonas putida*". *ACS Synthetic Biology* 4.12 (2015), pp. 1341–1351.

[49] Kyoung-Hee Choi and Herbert P. Schweizer. “mini-Tn7 insertion in bacteria with single att Tn7 sites: example *Pseudomonas aeruginosa*”. *Nature Protocols* 1.1 (2006), pp. 153–161.

[50] Kyoung-Hee Choi, Jared B. Gaynor, Kimberly G. White, Carolina Lopez, Catharine M. Bosio, RoxAnn R. Karkhoff-Schweizer, and Herbert P. Schweizer. “A Tn 7-based broad-range bacterial cloning and expression system”. *Nature Methods* 2.6 (2005), pp. 443–448.

Chapter 4

A DNA PART LIBRARY FOR RELIABLE ENGINEERING OF THE EMERGING MODEL NEMATODE SYMBIOTIC BACTERIUM *XENORHABDUS GRIFFINIAE*

The work described in this chapter is unpublished and was done by:
Elin M. Larsson and Olivia Y. Wang
Contributions: EML conceived the idea; EML and OYW designed and performed the experiments, analyzed and visualized the data, and wrote the text. Axenic nematodes used in this chapter were rendered by Carly Myers in the Cao lab at Carnegie Institution for Science.

4.1 Introduction

Nematodes are gaining increasing interest as simple models for studying gut microbiome interactions within a host [1–4]. The entomopathogenic nematodes of genus *Steinernema* are emerging as a model system because they often exhibit highly species-specific associations with a single bacterial strain of *Xenorhabdus* spp. to constitute its core microbiome. The emerging nematode model *Steinernema hermaphroditum* (PS9179), and its symbiotic bacterium *X. griffiniae* HGB2511, are of particular interest due to the nematode being consistently hermaphroditic and both partners being genetically tractable [5, 6]. The symbiotic bacteria are important for the development of the nematodes by providing nutrients [7] as well as a crucial part of their insect-killing life style. The bacteria make a cocktail of insect immunosuppressants, toxins and antibiotics to aid in killing the larvae and protecting the cadaver from the surrounding soil microbiome [8]. Their ability to kill insect larvae together has shed light on them as potential bioalternatives supplementing chemical pesticides in combating crop pests in agriculture.

There are many open questions about how this mutualistic relationship emerges and is maintained. Many of these knowledge gaps persist because of a lack of a genetic toolkit to develop synthetic genetic circuits such as biosensors and actuators within *Xenorhabdus*, to enable sensing and modulation of the nematode gut environment. Well-characterized libraries of genetic parts with different gene expression properties are an essential component of such genetic toolkits [9, 10].

Unlike model organisms like *E. coli*, the number of available well-characterized DNA parts for engineering *X. griffiniae* is small. To our knowledge, there are only two fluorescent proteins, one ribosome binding site (RBS) and one constitutive promoter described in *X. griffiniae* [6]. Here, we build and characterize a genetic part library consisting of constitutive promoters, RBS and coding sequences for *Xenorhabdus griffiniae*, the symbiotic partner of the emerging nematode model *Steinernema hermaphroditum*. The *in vitro* characterization of the parts translates to relative performance in the *in vivo* context and allow predictable construction of IPTG inducible constructs in *X. griffiniae* for the first time.

The donor strains have been submitted to Addgene (plasmid ID 238378-238408) and can be used to integrate these constructs in other *Xenorhabdus* species or to make the vector needed to construct new genetic circuits using the parts characterized in this work.

Results

Characterization of DNA libraries in *Xenorhabdus griffiniae*

To enable rapid cloning followed by conjugation into *Xenorhabdus*, we modified an existing Tn7-based conjugation plasmid (HGB1262) [6] by adding UNS sequences flanking the insert region of the plasmid. By doing this, the plasmid backbone can be used for 3G cloning [11] with the CIDAR MoClo kit [12] and the CIDAR MoClo extension kit [13]. Using this plasmid, genetic constructs can be integrated at a single locus on the *X. griffiniae* chromosome, thereby avoiding variability in plasmid copy number.

We choose to focus on promoters and RBS because they allow tuning of the expression of fluorescent proteins that are already known to express well in *X. griffiniae*. We built promoter and RBS constructs by varying only the promoter or RBS and fixing the RBS or promoter, respectively (Figure 4.2A). After building the promoter and RBS libraries, we characterized their relative strengths by measuring the fluorescence output normalized by optical density after 24 hours of growth. We can see that the strongest promoter is P5d (J23102), which is consistent with the strength in *E. coli* [12] (Figure 4.2B). The strongest RBS is U25m (Figure 4.2C). The U25m RBS sequence is a variant of U4m that includes the genetic insulator RiboJ upstream. Previous work in *E. coli* has shown that RiboJ increases the expression of downstream genes by between 2-fold and 10-fold [14]. Here, we see that RiboJ

increases the expression of TurboRFP driven by U4m by nearly 7-fold, which is consistent with the *E. coli* data.

For both promoters and RBS we see an increase in fluorescence early in the time trace (Figure 4.2B-C). This is caused by fluorescent protein already being present in the cells from the overnight growth, that then gets normalized by the low OD from diluting the cells. When growing cells overnight carrying an inducible TurboRFP construct, this increase is not seen (Figure 4.4C), since there is no TurboRFP present when the inducer is not added.

In addition to promoter and RBS sequences, we also tested the ability of various coding sequences to express within *X. griffiniae*. For this we tested the expression of sfGFP, sfYFP, mScarlet3 and the *luxCDABE* operon. Except for mScarlet3, these express well in *Xenorhabdus* (Figure 4.2panel) and offer an alternative readout to the fluorescent proteins that were already known to work well. Although mScarlet3 has a 3-fold increase in fluorescence compared to wildtype bacteria, the level of fluorescence is low compared to expression of TurboRFP under the same promoter which has a signal more than 30-fold stronger than the wildtype background (Figure 4.1).

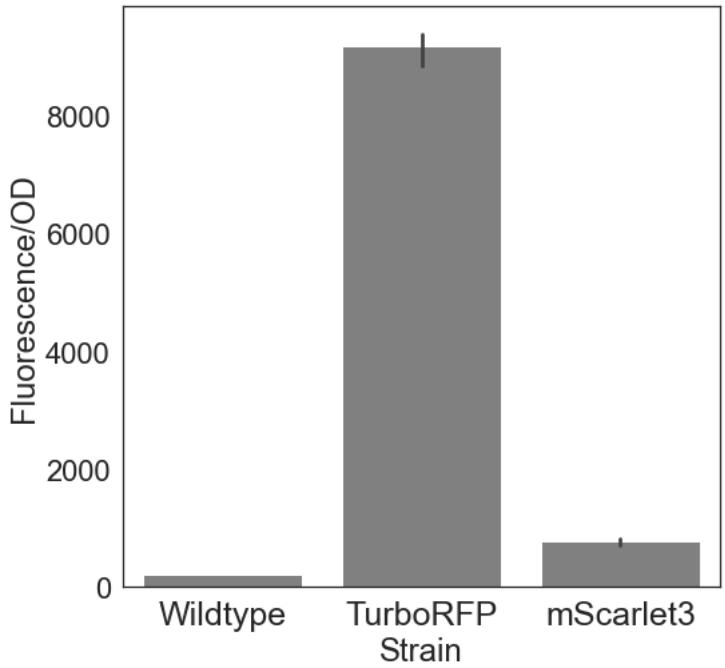

Figure 4.1: Endpoint RFP fluorescence for WT, TurboRFP and mScarlet3 driven by the same promoter.

After characterizing the parts in liquid culture, we chose three strains with different levels of TurboRFP expression to colonize nematodes and measure the fluorescence *in vivo* (Figure 4.2D). We can see the difference between a strong and weak promoter *in vivo* by imaging the whole nematode and comparing the fluorescence signal (Figure 4.2D). As predicted, P2m-U25m is stronger than P1m-U3d, but less so than in the liquid culture experiment, probably because the fluorescence signal in the microscopy experiment is saturated for P2m-U25m, or because *in vivo* expression is weaker than *in vitro* expression. The area of each colonization event is similar for all three strains (Figure 4.3).

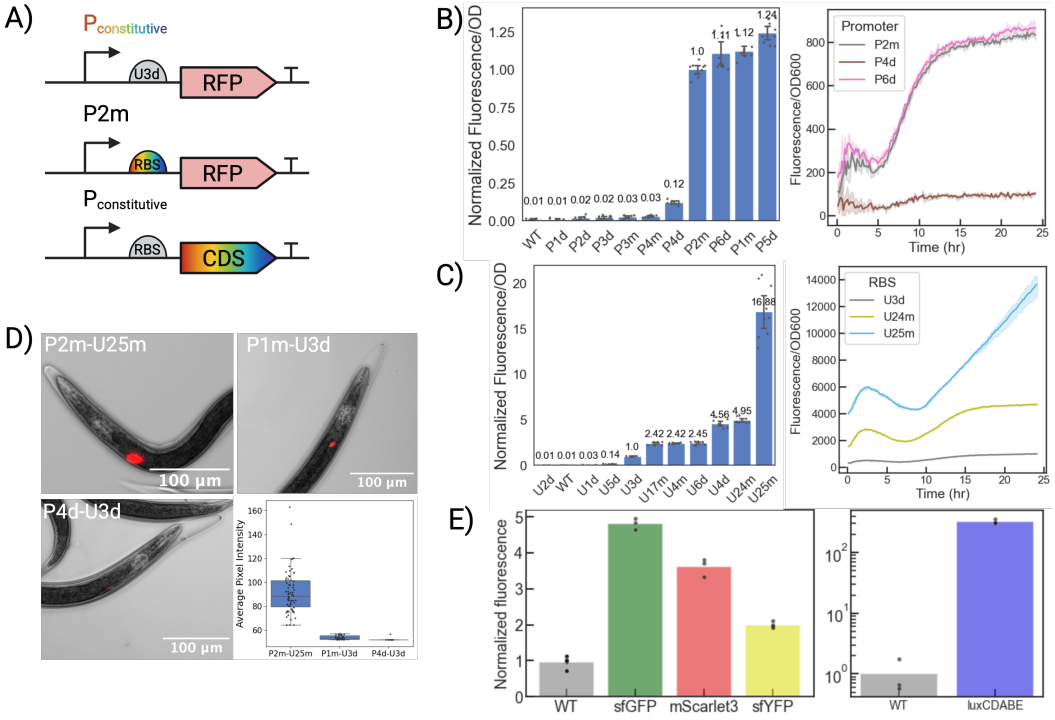

Figure 4.2: (A) Circuit diagrams for part library. (B) Left: Promoter strength order at the end of 24 hours of growth. Three technical replicates each for three biological replicates are plotted. Right: representative time trace for a subset of the strains. (C) Left: RBS strength order at the end of 24 hours of growth. Three technical replicates each for three biological replicates are plotted. Right: representative time trace for a subset of the strains. (D) Upper left and right, lower left: Representative microscopy images of nematodes with intensity values close to the average intensity. Lower right: Average pixel intensity for nematodes colonized by three different bacterial strains. Each dot represents one nematode colonized by bacteria at a detectable level. (E) Left: Normalized fluorescence for strains expressing sfGFP, mScarlet3 and sfYFP. Right: Normalized luminescence for the strain expressing the *luxCDABE* operon. Triplicates from one biological replicate are plotted.

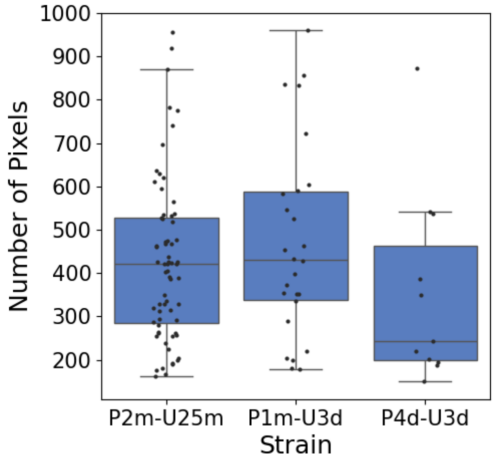

Figure 4.3: Area (pixels) for each colonization event, one dot is one colonized nematode.

Predictive design of an IPTG inducible construct

In order to determine whether the characterization data for the constitutive promoters and RBS sequences lead to more predictable performance of a larger genetic circuit, we built a simple IPTG inducible construct (Figure 4.4A) where we varied the promoters driving expression of *lacI* and the RBS upstream of *lacI* or TurboRFP. All three variants show low leak, meaning that there is enough *lacI* to suppress TurboRFP expression at the non-induced condition. For variant 2 and 3, a weaker promoter, P4d, was chosen to drive expression of *lacI*, leading to increased TurboRFP expression (Figure 4.4B). The highest TurboRFP expression was achieved for variant 3 that also had a weak RBS, U1d, upstream of *lacI*, resulting in even less *lacI* expression.

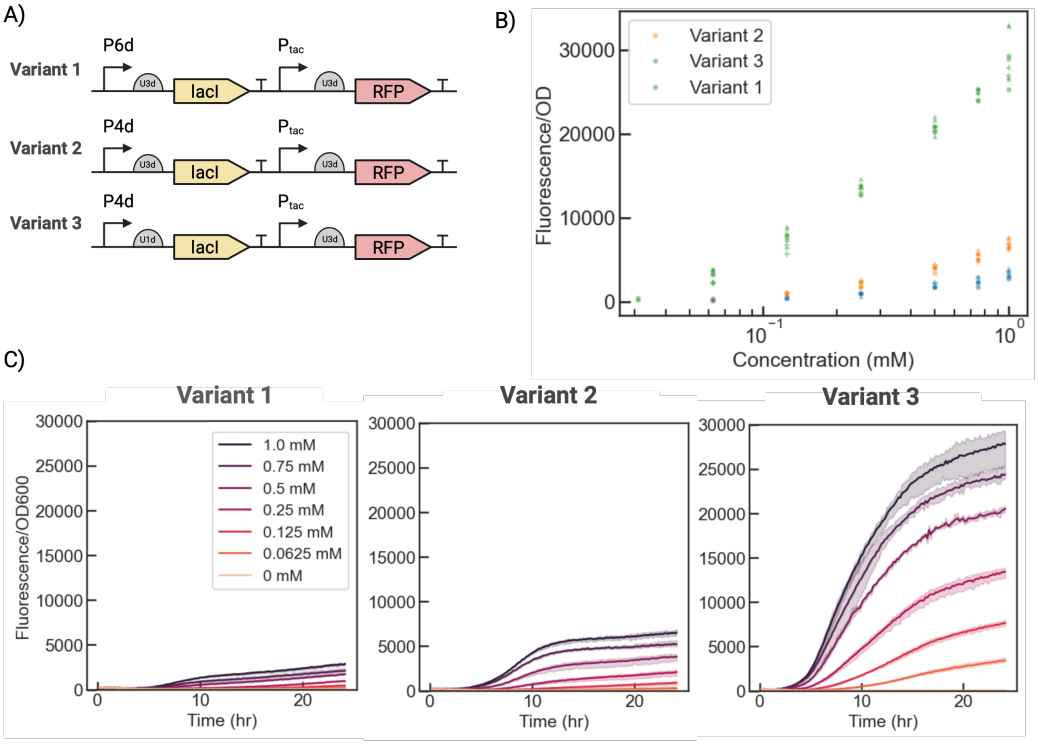

Figure 4.4: (A) Diagrams for three variants of IPTG inducible constructs. (B) IPTG induction curve for all three strains. Three technical replicates per biological replicate (n=3) are plotted. Each biological replicate is represented by a different symbol: cross, triangle and circle. (C) Time traces for one of the biological replicates for all three strains.

Materials and Methods

Cloning

The part library DNA constructs were constructed using the Golden Gate-Gibson (3G) assembly method [11]. Using Golden Gate assembly, the constructs were assembled and and PCR amplified as linear DNA constructs. The linear constructs were inserted into the EML002 backbone a modified plasmid made from of HGB1262 plasmid [6], by Gibson assembly. The Gibson product was then transformed into pir+ competent *E. coli* cells. The transformants were plated on selective (carbenicillin, 100 μg/ml or kanamycin, 50 μg/ml) plates. The chosen colonies were sequence verified by colony PCR. Plasmids were isolated using a Qiagen Miniprep kit. The purified plasmid was then transformed into a diaminopimelic acid (DAP) deficient pir+ *E. coli* strain. The transformants were plated on selective plates with added DAP (0.3 mM).

Conjugation

The protocol used for conjugation was modified from Alani et al. [15]. Conjugation included three strains: donor *E. coli* strain with the designed DNA construct, helper *E. coli* strain, and receiver *X. griffiniae* strain. The helper *X. griffiniae* strain carries the pUX-BF13 plasmid [16], with tns genes. Then, the constructs from the *E. coli* donor strain were integrated as a single copy into the *X. griffiniae* at the Tn7 site downstream of the *glmS* gene. First, the colonies were picked from the DAP deficient donor and helper *X. griffiniae* strains and the *X. griffiniae* strain and were grown in liquid overnights with appropriate antibiotics and DAP added. WT *X. griffiniae* was grown without antibiotics. The next day, the optical density (OD) of the liquid cultures were measured so the correct volumes could be pipetted to have an OD of 3. Then, the liquid cultures were washed twice to get rid of remaining antibiotics. Next, the three strains were mixed together and plated onto a filter on LB+DAP agar plates and incubated overnight at 30°C. The next day, the bacteria were resuspended by vigorously vortexing the filter in a falcon tube filled with 5 ml LB. The conjugation mixture was then plated on kanamycin plates. After a day of growth, *X. griffiniae* colonies were picked and grown in 30 μL LB overnight. The following day, 4 μl of overnight culture was diluted into 46 μl of nuclease free water and boiled for 10 minutes at 100°C. The boiled culture was then incubated at 4°C for 10 minutes and centrifuged using a table top centrifuge for two minutes. Then, the colonies were sequence verified using colony PCR (primer sequences in SI).

Plate reader operations

Starting from an single colony, strains were grown overnight at 30°C in LB. The overnight cultures were diluted with M9 to OD of 0.05. The fluorescence and optical density (600 nm) was measured using a BioTek Synergy H1F Multi-Mode Microplate Reader for 24 hours. TurboRFP fluorescence was measured at an excitation of 550 nm and an emission of 580 nm with a gain of 61 and 100 for the promoter screen and gain of 61 and 80 for the RBS screen and inducible constructs. The cultures were grown in 30°C and shaken linearly continuously at a frequency of 567 cpm.

Preparation of liver-kidney plates

This recipe is a modification of protocol described by Sicard et al. [7].
For 500 ml agar:

- 50 g beef kidney
- 50 g beef liver
- 2.5 g NaCl
- 7.5 agar
- Water to 500 ml

Use a blender to grind the liver and kidney. Add 250 ml of water and the remaining ingredients to the blender. Blend until almost smooth, but still containing some chunks. Pour into a 1 L flask. Use the remaining water to rinse the blender and pour into the flask to a total final volume of 500 ml. Autoclave the agar for 45 minutes and cool in 55°C for 30 minutes. Add kanamycin (50 μg/ml). When pouring the plates, swirl the flask in between plates to prevent the chunks from sinking to the bottom.

Nematode colonization

The nematode colonization protocol was modified from St. Thomas et al. [6]. 700 μL of the bacterial overnight *X. griffiniae* culture was added to a liver-kidney (LK) agar plate. Then, 1 mL of axenic *S. hermaphroditum* nematodes was added to each 1.5 mL Eppendorf tube. Axenic nematodes were rendered as described by Cao et al. [5], with the modification of using beef instead of pork liver and kidney. The nematodes were centrifuged for 30 s at 6.0 rcf. Then, 900 μL of the supernatant was discarded and 900 μL of 1% bleach solution was added. The tube was inverted for 1:30 min to kill bacteria on the nematodes' surface. The nematodes were

then washed with water three times to remove residual bleach. Using a dissecting microscope, the number of nematodes in 2 μl droplets was counted to determine the concentration of nematodes in the solution. The appropriate volume of nematodes was then added to each LK plate such that there were approximately 200 nematodes per plate. After one week, the nematodes were trapped in water by placing the LK plate in a larger petri dish where the bottom was covered in autoclaved water. After another week, nematodes were collected from the water traps.

In vivo imaging of nematodes

Before imaging, the nematodes were paralyzed with levamisole (200 μM). The colonized nematodes were imaged using a Nikon Ti2 fluorescence microscope using phase contrast and the RFP fluorescence channel at 10x magnification. The RFP channel images went through the same enhancing, denoising, and normalization to adjust the pixel to a range of 1 to 255 (supp #). Clusters of at least 150 pixels and a threshold of intensity 40 were identified as colonized regions and cross-referenced with the corresponding phase contrast worm images. The average pixel intensities for each colony was calculated by averaging the selected pixels in the determined regions. The percent of detected events was calculated by dividing the number of detected events by the total number of worms imaged for each strain.

Acknowledgements

We thank Dr. David Garcia for help with writing the code for the image analysis. We thank Carly Myers and Dr. Mengyi Cao for teaching us techniques used to colonize nematodes with bacteria. We thank Carly Myers for rendering the axenic nematodes used in the nematode colonization experiment. We thank Dr. Mengyi Cao for use of a Cao lab dissecting microscope. We thank Prof. Dianne Newman for use of the Newman lab fluorescence microscope. All figures were created using BioRender.com. This work was supported by Caltech's Resnick Sustainability Institute, DaRin Butz Foundation, and Caltech Summer Undergraduate Research Fellowships (SURF) program.

References

[1] Philipp Dirksen, Sarah Arnaud Marsh, Ines Braker, Nele Heitland, Sophia Wagner, Rania Nakad, Sebastian Mader, Carola Petersen, Vienna Kowallik, Philip Rosenstiel, et al. "The native microbiome of the nematode *Caenorhabditis elegans*: gateway to a new host-microbiome model". *BMC Biology* 14 (2016), pp. 1–16.

[2] In Young Hwang, Elvin Koh, Adison Wong, John C March, William E Bentley, Yung Seng Lee, and Matthew Wook Chang. "Engineered probiotic *Escherichia coli* can eliminate and prevent *Pseudomonas aeruginosa* gut infection in animal models". *Nature Communications* 8.1 (2017), p. 15028.

[3] Timothy A. Scott, Leonor M. Quintaneiro, Povilas Norvaisas, Prudence P. Lui, Matthew P. Wilson, Kit-Yi Leung, Lucia Herrera-Dominguez, Sonia Sudiwala, Alberto Pessia, Peter T. Clayton, et al. "Host-microbe co-metabolism dictates cancer drug efficacy in *C. elegans*". *Cell* 169.3 (2017), pp. 442–456.

[4] Fan Zhang, Maureen Berg, Katja Dierking, Marie-Anne Félix, Michael Shapira, Buck S Samuel, and Hinrich Schulenburg. "*Caenorhabditis elegans* as a model for microbiome research". *Frontiers in Microbiology* 8 (2017), p. 485.

[5] Mengyi Cao, Hillel T. Schwartz, Chieh-Hsiang Tan, and Paul W. Sternberg. "The entomopathogenic nematode *Steinernema hermaphroditum* is a self-fertilizing hermaphrodite and a genetically tractable system for the study of parasitic and mutualistic symbiosis". *Genetics* 220.1 (2022), iyab170.

[6] Nadia M. St Thomas, Tyler G. Myers, Omar S. Alani, Heidi Goodrich-Blair, and Jennifer K. Heppert. "Green and red fluorescent strains of *Xenorhabdus griffiniae* HGB2511, the bacterial symbiont of the nematode *Steinernema hermaphroditum* (India)". *microPublication Biology* 2024 (2024), pp. 10–17912.

[7] Mathieu Sicard, Nathalie Le Brun, Sylvie Pages, Bernard Godelle, Noël Boemare, and Catherine Moulia. "Effect of native *Xenorhabdus* on the fitness of their *Steinernema* hosts: contrasting types of interaction". *Parasitology Research* 91 (2003), pp. 520–524.

[8] S. Patricia Stock. "Partners in crime: symbiont-assisted resource acquisition in *Steinernema* entomopathogenic nematodes". *Current Opinion in Insect Science* 32 (2019), pp. 22–27.

[9] Jennifer A. N. Brophy and Christopher A. Voigt. "Principles of genetic circuit design". *Nature Methods* 11.5 (2014), pp. 508–520.

[10] Felipe Buson, Yuanli Gao, and Baojun Wang. "Genetic parts and enabling tools for biocircuit design". *ACS Synthetic Biology* 13.3 (2024), pp. 697–713.

[11] Andrew D. Halleran, Anandh Swaminathan, and Richard M. Murray. "Single day construction of multigene circuits with 3G assembly". *ACS Synthetic Biology* 7.5 (2018), pp. 1477–1480.

[12] Sonya V. Iverson, Traci L. Haddock, Jacob Beal, and Douglas M. Densmore. "CIDAR MoClo: improved MoClo assembly standard and new *E. coli* part library enable rapid combinatorial design for synthetic and traditional biology". *ACS Synthetic Biology* 5.1 (2016), pp. 99–103.

[13] Samuel Clamons, Leopold Green, Andrew Halleran, Zoila Jurado, John Marken, Reed McCardell, John McManus, James Parkin, Mark Prator, Andrey Shur, et al. “CIDAR MoClo extension part kit, volume 2” (2019).

[14] Kalen P. Clifton, Ethan M. Jones, Sudip Paudel, John P. Marken, Callan E. Monette, Andrew D. Halleran, Lidia Epp, and Margaret S. Saha. “The genetic insulator RiboJ increases expression of insulated genes”. *Journal of Biological Engineering* 12 (2018), pp. 1–6.

[15] Omar S. Alani, Mengyi Cao, Heidi Goodrich-Blair, and Jennifer K. Heppert. “Conjugation and transposon mutagenesis of *Xenorhabdus griffiniae* HGB2511, the bacterial symbiont of the nematode Steinernema hermaphroditum (India)”. *MicroPublication Biology* 2023 (2023), pp. 10–17912.

[16] Ying Bao, Douglas P. Lies, Haian Fu, and Gary P. Roberts. “An improved Tn7-based system for the single-copy insertion of cloned genes into chromosomes of gram-negative bacteria”. *Gene* 109.1 (1991), pp. 167–168.

Chapter 5

THE NEMATODE SYMBIOTIC BACTERIUM *XENORHABDUS GRIFFINIAE* CAN SENSE AND RESPOND TO THE PRESENCE OF ITS HOST, *STEINERNEMA HERMAPHRODITUM*

The work described in this chapter is unpublished and was done by:
Elin M. Larsson, Carly R. Myers, and Mengyi Cao.
Contributions: EML conceived the project idea; EML, CRM, and MC did the experiments; EML analyzed and visualized the data, and wrote the text.

5.1 Introduction

Nematodes are the most ubiquitous metazoans on earth and play key roles in diverse ecosystems, through nutrient cycling, predation, pathogenesis and parasitism with other types of organisms [1–4]. Nematodes' ability to sense and be sensed by other organisms enable many of these ecosystem interactions. Some examples include the ability of *Caenorhabditis elegans* to sense and respond to its bacterial prey [5] and bacterial pathogens [6, 7] and the ability of plants to trigger an immune response in the presence of plant-pathogenic nematodes [8].

Many of these ecosystem interactions occur between nematodes and bacteria. Although the ability of nematodes to sense bacteria is well documented [5–7], much less is understood about how bacteria sense the presence of nematodes (Figure 5.1). To our knowledge, the only documented example of bacterial sensing of a nematode is for the nematode-predatory bacterium *Bacillus nematocida*. This bacterium initiates production of volatile attractants and sporulation upon sensing the *C. elegans*-made gas morpholine in order to germinate and feed on the nematode from within, after surviving engulfment [9]. It is therefore an open question whether bacteria can sense nematodes in non-predation contexts, such as mutualistic relationships.

Entomopathogenic nematodes such as *Steinernema* and *Heterorhabditis* spp. are distinguished by having a microbiome made up of a single bacterial species, with strong specificity between each nematode species and its preferred symbiotic bacterial partner [10, 11]. The bacterium spends most of its life cycle inside the receptacle, a pocket in the nematode intestine, and plays a major role in nematode development

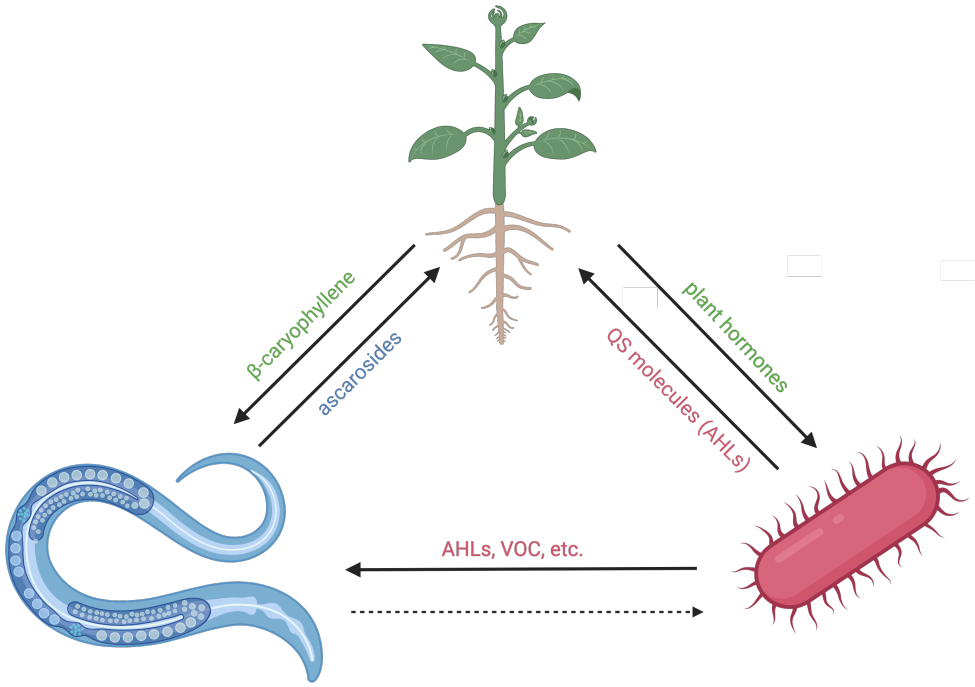

Figure 5.1: Little is known about how bacteria sense the presence of nematodes.

[12–14] and insect killing, digestion and preservation [15–17]. The ability for entomopathogenic nematodes recognize their bacterial symbiotic partners, through the bacterial expression of the *nilABC* genes, has been described [18], but to our knowledge there has been no investigation of whether these bacterial symbionts can sense and respond to the presence of their nematode hosts.

In this work, we leverage the model entomopathogenic nematode-symbiont pair *Steinernema hermaphroditum* and *Xenorhabdus griffiniae* HGB2511 to determine whether *X. griffiniae* can sense and respond to the presence of its nematode host. We show that *X. griffiniae* changes its gene expression profile in a small number of genes in the presence of axenic nematodes, but not in the presence of nematodes that are already colonized by *X. griffiniae*. We select one of these differently regulated genes for further investigation, *ymdA*, and show that it plays a role in biofilm formation and affects host colonization efficiency. This work advances our understanding of bacterial sensing of nematodes and motivates future research in deepening our understanding of this underexplored ecological interaction.

5.2 Results

Xenorhabdus griffiniae exhibits a transcriptional response to axenic *Steinernema hermaphroditum* infective juveniles

In order to assess whether *X. griffiniae* can sense its nematode host, we first considered when in the natural life cycle the two organisms might most need to engage in sensing each other. The bacterial symbiont does not have a free-living stage, but is outside of the nematode during two parts of the life cycle: the insect colonization and nutrient depletion phases (Figure 5.2A). Successful colonization of the nematode during these phases allows the bacterium to disperse out into the wider soil environment. In this part of the life cycle the nematodes are in the infective juvenile (IJ) stage. Therefore, we decided that in order to test whether *X. griffiniae* can sense *Steinernema hermaphroditum*, we needed to test whether *X. griffiniae* can specifically sense *Steinernema hermaphroditum* in the IJ stage.

We then developed a trans-well assay where the nematodes are separated from the bacteria by a membrane, preventing engulfment, that allows diffusion of potential chemical signals involved in sensing (Figure 5.2B). We compared pure cultures of *X. griffiniae* against co-cultures with colonized or axenic *Steinernema hermaphroditum*, in two genetic backgrounds for the nematode (wildtype and *daf-22* deficient [19]). This mutant was included because the *daf-22* gene is involved in the biosynthetic pathway for ascarosides, which are signaling molecules made by nematodes that are known to be metabolized by some bacteria and plants [20]. We therefore hypothesized that this class of molecules could potentially be sensed by bacteria and that including a nematode lacking the natural ascaroside composition might provide additional information about whether this class of molecules was sensed by *X. griffiniae*.

After co-culturing the bacteria and nematodes, we sequenced the bacterial RNA to determine whether the presence of the nematodes altered the transcriptome of the bacteria. We found that *X. griffiniae* only shifted its gene expression profile in response to axenic nematodes and not to colonized nematodes (Figure 5.2C, Figure 5.3 and Figure 5.2). Furthermore, only a small number of genes were differentially expressed in the presence of the axenic wildtype nematodes (Figure 5.2D-E, Table 3 for axenic *daf-22* dataset). These results suggest that *X. griffiniae* can indeed sense the presence of its nematode host *Steinernema hermaphroditum*, but it can only do so when the host is not colonized.

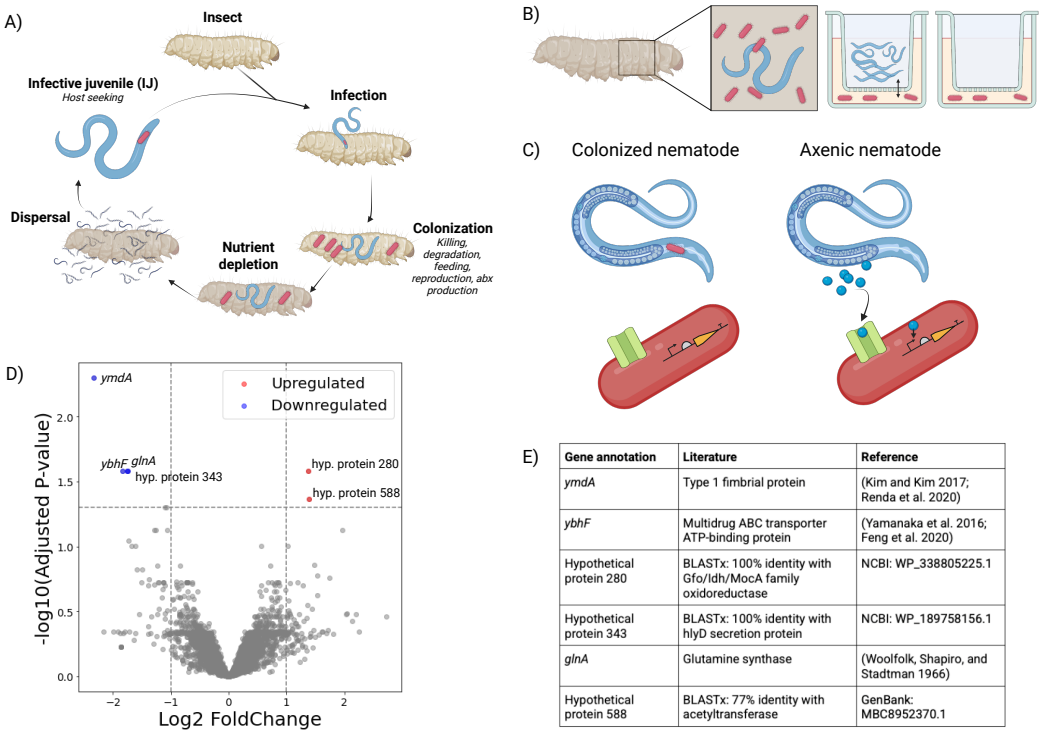

Gene annotation	Literature	Reference
ymdA	Type 1 fimbrial protein	(Kim and Kim 2017; Renda et al. 2020)
ybhF	Multidrug ABC transporter ATP-binding protein	(Yamanaka et al. 2016; Feng et al. 2020)
Hypothetical protein 280	BLASTx: 100% identity with Gfo/Idh/MocA family oxidoreductase	NCBI: WP_338805225.1
Hypothetical protein 343	BLASTx: 100% identity with hlyD secretion protein	NCBI: WP_189758156.1
glnA	Glutamine synthase	(Woolfolk, Shapiro, and Stadtman 1966)
Hypothetical protein 588	BLASTx: 77% identity with acetyltransferase	GenBank: MBC8952370.1

Figure 5.2: (A) *Steinernema-Xenorhabdus* life-cycle overview. (B) The trans-well experiment co-cultures *X. griffiniae* with IJ-stage *S. hermaphroditum*. (C) Schematic of proposed model for signal secretion and sensing. In this model, only axenic nematodes secrete signaling molecules that can be sensed by bacteria. (D) Volcano plot of differential expression in *Xenorhabdus* co-cultured with axenic wildtype *S. hermaphroditum*. (E) Table listing differentially expressed genes in *X. griffiniae* with axenic WT nematodes.

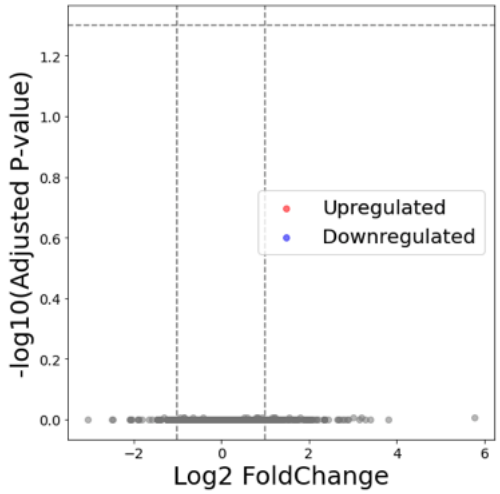

Figure 5.3: Volcano plot for colonized WT nematodes.

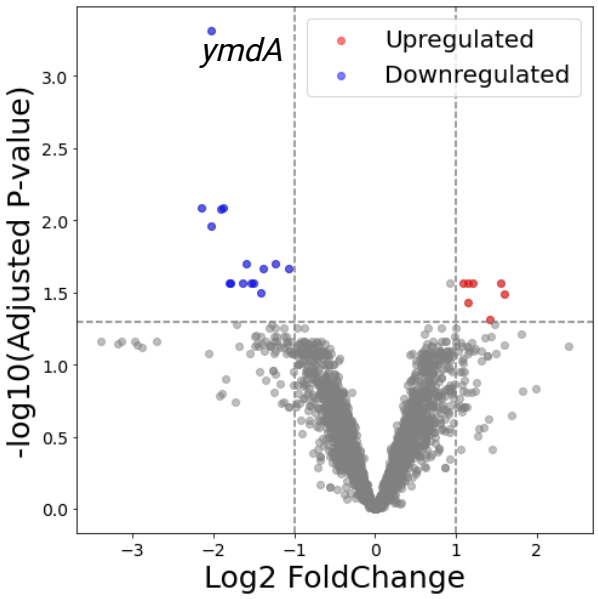

Figure 5.4: Volcano plot for axenic *daf-22* nematodes.

Table 3: Genes differentially expressed for bacteria grown +/- axenic *daf-22* nematodes

Gene annotation	Literature	Reference
ymdA	Type 1 fimbrial protein	(Kim and Kim 2017; Renda et al. 2020)
ybhF	Multidrug ABC transporter ATP-binding protein	(Yamanaka et al. 2016; Feng et al. 2020)
Hypothetical protein 343	BLASTx: 100% identity with hlyD secretion protein	NCBI: WP_189758156.1
cecR	Regulator for chloramphenicol sensitivity in *E. coli*	(Yamanaka et al. 2016)
dps	DNA protection	(Nair et al. 2004)
moeZ	Molybdopterin-synthase adenylyltransferase	
cheW	Chemotaxis	(Liu et al. 1989)
glnA	Glutamine synthase	(Woolfolk, Shapiro, and Stadtman 1966)
tag	DNA-3-methyladenine glycosylase 1	
amtB	Ammonium transporter	(Soupene et al. 1998)
motA	Motility	(Dean et al. 1984)

Overexpressing *ymdA* leads to a biofilm defect *in vitro*

In order to better understand the nature of *X. griffiniae*'s response to the presence of *Steinernema hermaphroditum*, we chose the most significantly differentially

expressed gene from our dataset, a putative homologue of *ymdA*, for further characterization (Figure 5.2D-E). This gene is downregulated in the presence of the nematodes.

In *Escherichia coli*, *ymdA* is a type 1 fimbrial protein that is known to be involved in biofilm formation [21, 22], but its role in *X. griffiniae* has not been studied. To determine if *ymdA* similarly plays a role in biofilm formation in *X. griffiniae*, we performed an *in vitro* biofilm formation experiment on WT, *ymdA* deletion, and *ymdA* overexpression strains. Quantification of crystal violet staining of the biofilm shows that deleting *ymdA* does not significantly affect biofilm formation *in vitro*, but overexpressing *ymdA* significantly reduces the cells' ability to form stable biofilms (Figure 5.5A-B). This effect is likely not due to growth burden associated with *ymdA* overexpression, as growth curves indicate that the *ymdA* overexpression strain grows to a similar density in static liquid cultures (Figure 5.5C).

The *ymdA* overexpression strain forms large microcolonies in early attachment

Several studies show that an increase in fimbrial expression leads to enhanced biofilm formation [23–26]. However, for *ymdA* specifically, two studies show that overexpression leads to a biofilm defect in *E. coli* [21, 22]. The crystal violet experiment suggests that *ymdA* functions similarly in *X. griffiniae* as in *E. coli*. Deficiencies in biofilm formation could occur via a number of mechanisms, such as inhibiting early attachment or inhibiting rigidity required for stable macroscale biofilm growth. To further investigate the role of *ymdA*, we performed a microscopy assay to assess *X. griffiniae*'s ability to form microcolonies, an early attachment stage in biofilm formation.

Interestingly, the *ymdA* overexpression strain formed larger and more clustered microcolonies than WT and *ymdA* deletion strains (Figure 5.6), suggesting that *ymdA* expression can indeed promote cell-cell adherence similarly to bacteria increasing expression of other fimbrial proteins. WT and the deletion mutant microcolony patterns are similar, which might mean that *ymdA* is not required for microcolony formation, or that other fimbrial proteins annotated on the *X. griffiniae* genome (*mrpA*, *yfcS*, *yfcP*, *lpfB*, *lpfA*1/2 and *mrkD*) might be expressed to compensate for the lack of *ymdA* in the deletion strain. These results together suggest that in *X. griffiniae*, high levels of *ymdA* promote cell-cell adherence early at the microcolony scale, but inhibit macroscale biofilm formation that occurs over several days.

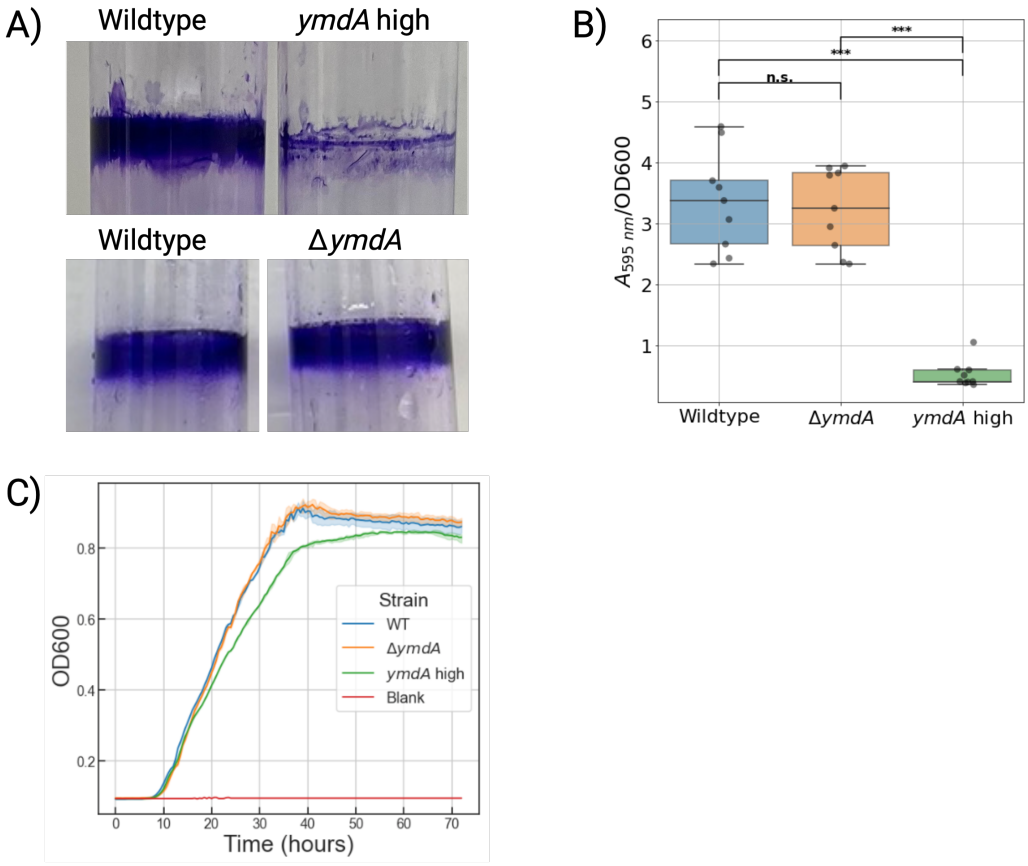

Figure 5.5: (A) Representative image of crystal violet stained biofilms stained after 3 days of static incubation (upper left: WT, upper right: *ymdA* overexpression strain, lower left WT, lower right Δ*ymdA*. (B) Destained biofilms are quantified by measuring crystal violet absorbance at 595 nm normalized by measured optical density. Technical triplicates from three biological replicates are plotted. Welch t-test p-value not significant between WT and Δ*ymdA* and <0.001 for WT and *ymdA* overexpression. (C) Growth curves for static growth in LB.

ymdA overexpression results in a disadvantage in competitive nematode colonization

To determine the consequences of *ymdA* on host colonization we performed a competitive colonization where the WT bacteria were mixed at equal cell density with the *ymdA* overexpression strain (Figure 5.9A). The reasoning for doing a competitive colonization instead of comparing individual colonization efficiency is that the competitive set-up better mimics the setting in the nutrient depleted insect cadaver, because only a fraction of the bacteria in the cadaver will be able to re-colonize the nematode host. The question at hand is what bacteria in a large

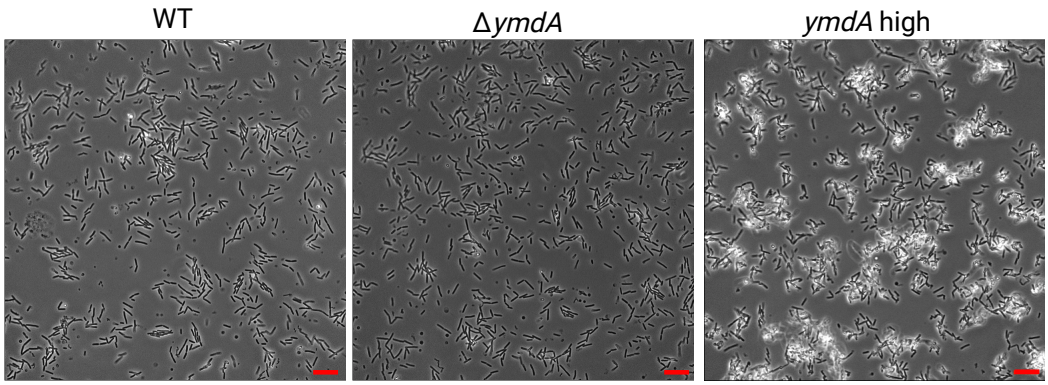

Figure 5.6: Representative images of WT, deletion mutant and overexpression strain cells at 20 hours of growth. Scale bar 5 μm.

population of bacteria are able to most efficiently and robustly colonize the nematode. A small-scale experiment shows that the colonization frequency between WT and the overexpression strain is similar when there is no competition (Figure 5.7)

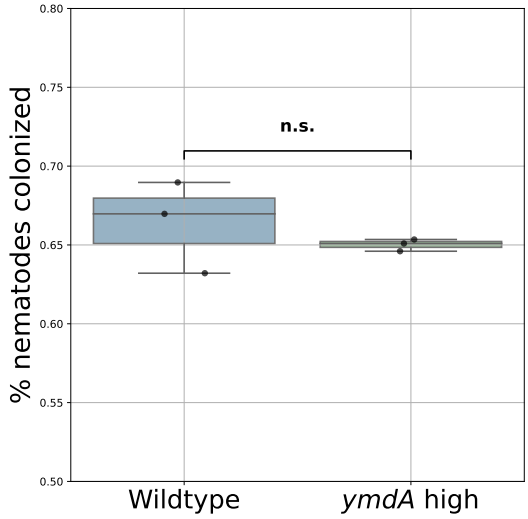

Figure 5.7: Colonization frequency in non-competitive conditions.

Strains overexpressing *ymdA* were significantly inhibited in their ability to colonize the nematode compared to WT, as indicated by both microscopy of whole animals (Figure 5.9B) and CFU counts of ground up nematodes (Figure 5.9C) where WT bacteria on average colonize more than 80% of the colonized nematodes. We chose to focus on competition between these strains since we did not see any significant difference in biofilm or microcolony formation between WT and the deletion mutant in the *in vitro* experiments, and because the lack of fimbriae in *Xenorhabdus* has

been shown to not affect colonization ability in previous studies [27]. A small scale experiment with ten replicates where the deletion mutant was competing against WT showed no significant difference in colonization efficiency between the two strains (Figure 5.8).

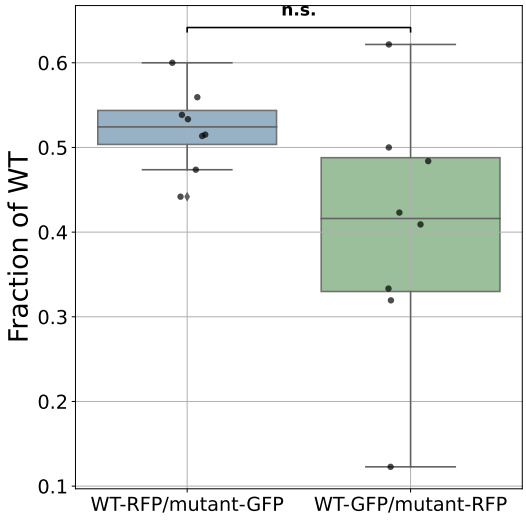

Figure 5.8: Colonization when WT and the deletion strain colonize axenic nematodes competitively (by CFU counts).

These results show that high levels of *ymdA* negatively impacts the ability of *X. griffiniae* to colonize *Steinernema hermaphroditum*. The downregulation of *ymdA* in *X. griffiniae* when co-cultured with *S. hermaphroditum* might therefore be a response made to actively facilitate successful colonization of the nematode.

5.3 Discussion

Our results suggest that the establishment of the host-symbiont pairing between *Steinernema hermaphroditum* and *X. griffiniae* may not purely be a one-sided interaction where the nematode senses and seeks out its symbiont. Instead, it is possible that what we are observing is a two-way interaction where both partners sense and respond to the presence of the other in a way that promotes successful colonization and establishment of the symbiosis. However, the molecular mechanism underlying the ability of *X. griffiniae* to sense its host still needs to be elucidated. The fact that *X. griffiniae* only exhibited a transcriptional response to axenic nematodes indicates that the nematode's secretome may differ between axenic and colonized individuals, as seen in previous studies [28]. These results further suggest the possibility that

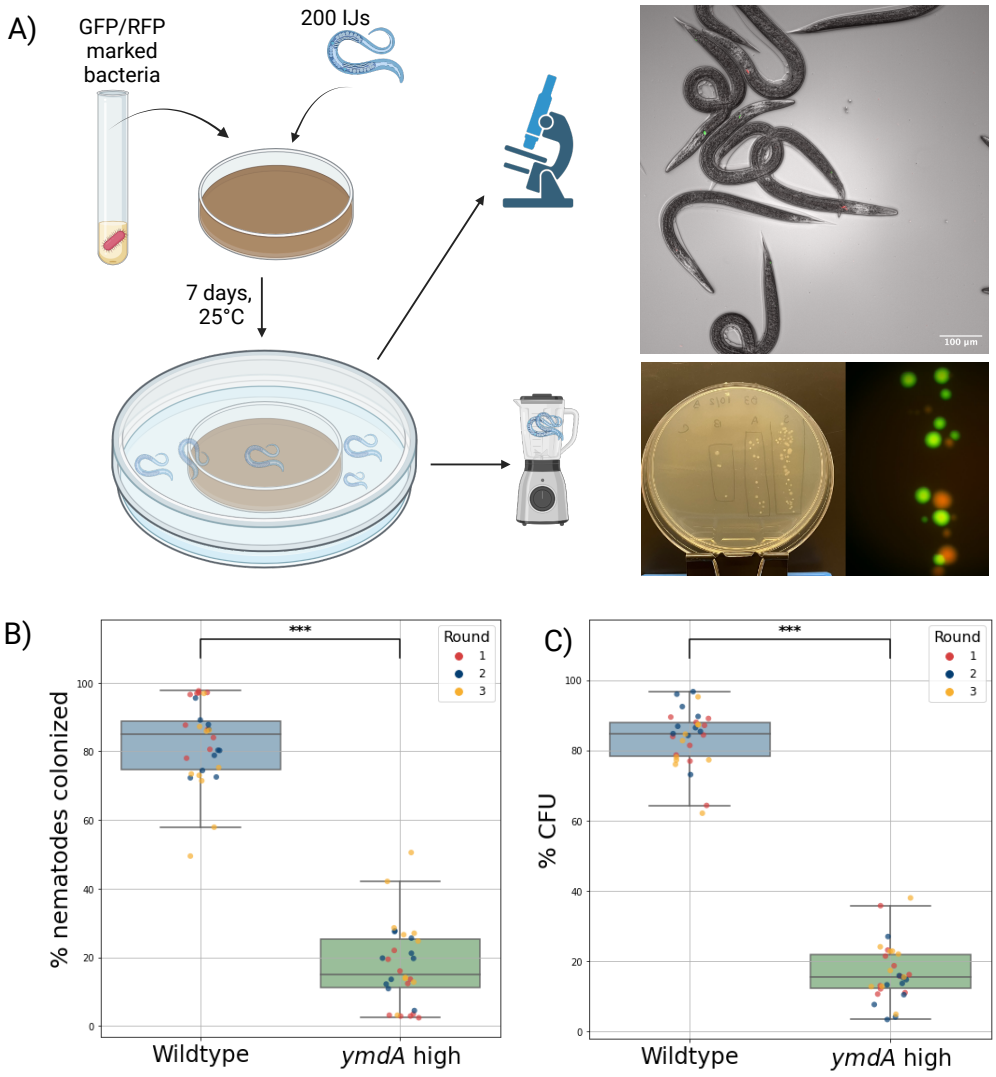

Figure 5.9: (A) Schematic of the experimental procedure for the colonization experiments and representative images of microscopy and colony imaging. (B) Percentages of nematodes colonized by WT and ymdA overexpression strain bacteria. Ten replicates per biological replicate (n=3) are plotted. (C) Percentages of CFUs from WT and ymdA overexpression strain bacteria. Ten replicates per biological replicate (n=3) are plotted. P-values from Welch t-test <0.001.

axenic *Steinernema hermaphroditum* may even actively release chemical cues to signal to *X. griffiniae* that a colonizable host is nearby.

This study also elucidates the role of the fimbrial protein *ymdA* in the colonization process of *Steinernema hermaphroditum*. *ymdA* had opposing impacts on cell-cell interactions at different scales: at the macroscale, increased *ymdA* inhibited biofilm formation, while at the microscale, increased *ymdA* promoted microcolony

clustering and size. One important difference between the two experiments testing biofilm formation is the oxygen concentration which may play a role in the adherence ability. There is also a possibility that cis-interactions with other fimbriae reduce trans-interactions with surfaces and fimbriae on other bacteria. A likely possibility is that there is an optimal intermediate level of fimbriae that maximize robust cell-cell adherence, where cell refers both to other bacterial cells, but also epithelial cells in the nematode receptacle. Future work characterizing other differentially expressed genes may shed more light on this hypothesis. More broadly, deeper understanding of how bacteria sense nematodes can fill in gaps in questions regarding signaling and interactions in different ecosystems.

Furthermore, understanding nematode sensing in bacteria is the first step in enabling several biotechnology applications. One challenge in agriculture is the widespread infections by root-knot nematodes that cause crop yield losses worth over $80 billion per year [29]. In addition to current methods for detection such as soil collection followed by direct counts or qPCR [30], the construction of whole-cell biosensors for certain species could become an important tool for early detection of outbreaks.

Another challenge in agriculture is the infections caused by insect pests. *Steinernema* and *Heterorhabditis* along with their bacterial symbionts have been suggested as potential replacements or supplements to chemical pesticides in agriculture due to their ability to kill insect larvae [31, 32]. Even though it has been known for decades that these organisms have this capability, we are not near widespread use of them in agriculture. This can be due to regulation, scale-up difficulties etc, but could also be due to them not being efficient enough for this application. Deeper understanding into the establishment of the symbiotic relationship and their insect virulence, might allow us to engineer them for improved efficiency.

5.4 Materials and Methods

Preparation of nematodes for trans-well experiment

Production, processing, and optimization of IJs for the trans-well experiment was done by the Cao lab. Briefly, conventional infective juveniles (IJs) were made as described in Cao et al. [33]. Axenic IJs were produced by modifying a previous protocol [34] using beef kidney and liver. Before starting the experiment, the newly emerged IJ nematodes were surface sterilized with 0.5% bleach for 90 seconds to remove the chitinous outer cuticle, followed by three washes with water, and stored at 5 IJs per μL overnight at room temperature. The nematodes were then centrifuged to

produce high density pellets, washed with water and M9 media supplemented with cholesterol (final concentration of 0.1%) to remove the existing excreted molecules, and loaded to trans-wells. The number and viability of the IJs were monitored before and after the trans-well experiment to ensure nearly 100% IJ survival during the time course of the experiment.

Trans-well experiment

Starting from a three individual colonies, three bacterial overnight cultures were inoculated into 5 ml of LB pyruvate medium and grown at 30°C. The following morning, the cultures were washed twice in M9 medium with glucose (Teknova) supplemented with cholesterol (final concentration of 0.1%). The cultures were then diluted to a final OD of 0.05 in a volume of 1.2 ml and transferred to a 24 well plate. A 0.4 μm membrane insert was added to each well and 50 μl of dense nematode pellet was added to each membrane insert, as well as 50 μl of M9 cholesterol medium. In the "no worm condition" the membrane inserts were left empty. The bacterial cultures were grown shaking at 100 rpm for 24 hours. The bacteria were then pelleted at 8000 rpm and flash frozen using liquid nitrogen and stored at -80°C. Bacterial pellets were sent to the microbial sequencing and analysis center at the University of Pittsburgh for RNA extraction and sequencing.

Data analysis and selection of target genes

The abundance quantification of the transcripts was done using kallisto [35], with the default settings except for the boot strap samples that were set to 100. To identify differentially expressed genes, DESeq2 was used [36], using the default settings for calculating the adjusted p-values. We chose a cutoff at an adjusted p-value of 0.05 and fold change of 2.

Construction of deletion mutants, overexpression, and fluorescently labelled strains

Deletion strains were constructed using the pKR100 plasmid as a backbone, using 1500 base pairs upstream and downstream of the gene to be deleted. A kanamycin cassette was placed in between the homology sequences and inserted into the genome, replacing the deleted gene. To make genetic constructs for insertion, 3G cloning was used [37] as described in Chapter 4.

Both deletions and insertion plasmids were transferred to *X. griffiniae* by conjugation. Starting from a single colony, *Xenorhabdus griffiniae*, *E. coli* helper and

E. coli donor were grown overnight in 5 ml LB broth (with added antibiotics and diaminopimelic acid, DAP (0.3 mM), as needed). The ODs of each strain was measured. The volume to obtain OD 3 for each strain was calculated and pelleted. The pellets were then washed twice with LB to remove residual antibiotics. The pellets were combined by sequentially resuspending them in 100 ul of LB until all pellets were mixed. The cells were then pipetted onto a filter membrane on an agar plate and incubated in 30°C overnight. The following day, the filter was transferred to 5 ml of LB in a Falcon tube and vortexed until the bacteria on the filter paper were resuspended in the liquid. The liquid was then plated in serial dilutions onto LB + kanamycin agar plates and incubated in 30°C overnight. Colonies were picked and verified by colony PCR and sequencing.

Crystal violet biofilm assay

The crytal violet assay is modified from a microtiter biofilm protocol [38]. Starting from an overnight LB culture, bacterial strains were diluted in LB to OD 0.003. 1 ml of diluted culture was added to a glass tube and incubated statically in room temperature for 4 days. The cultures were then decanted and the optical density of the liquid was measured. The tubes were then washed twice by submerging them in MilliQ water and tapped on a paper towel to remove most of the residual water. After washing, 1.2 ml of crystal violet (0.1% w/v) was added to each tube. The tubes were incubated for 15 minutes in room temperature and rolled gently at a slight angle twice during the incubation. The crystal violet was then removed by decanting and and the tubes were again washed twice by submerging in MilliQ water. The tubes were then tapped against a paper towel and dried for 24 hours in room temperature. After drying, 1.2 ml of acetic acid (30% v/v) was added to each tube. The tubes were incubated for 10 minutes in room temperature with gentle rolling of the tubes twice during this time. After incubation, the dissolved crystal violet/acetic acid mixture was measured using a Biotek plate reader at 595 nm.

Attachment assay — microcolony formation

An overnight LB culture of WT, Δ*ymdA* and the *ymdA* overexpression strain was diluted to OD 0.01 into M9 medium. 400 μl culture was transferred to a 8 well glass bottom plate and incubated at room temperature for 20 hours. The bottom of each well was then imaged using a Nikon Ti2 microscope at 40x magnification.

Nematode colonization

Preparation of bacteria: Bacterial strains for the colonization experiment were streaked from glycerol stocks onto agar plates containing appropriate antibiotics. The following day, a colony was picked into 5 ml of LB with added antibiotics and grown for 16 hours. The optical density of the cultures was then measured. The competing strains in each condition were mixed at a 1:1 ratio to end up with equal ODs for each strain. 700 μl of the strain mix was added to a liver-kidney plate with added kanamycin. The plates were then incubated at 30°C overnight.

Counting of nematodes: 2 μl of surface sterilized nematodes were added to a microscope slide in triplicate. The number of nematodes was then counted and the concentration (nematode/μl) in the stock solution was calculated.

Nematode colonization and collection: A volume corresponding to 200 IJs was added to each LK plate. The Plates were then incubated in 25°C for 7 days. The nematodes were then water trapped by placing the LK plates in a larger petri dish where the bottom was covered in autoclaved water. After 7 additional days, nematodes trapped in the water could be collected for further experiments.

CFU plating from nematode grounds

After surface sterilizing 200 IJs, the nematodes were ground up in a total volume of 200 μl of LB by bead beating for 6 minutes at 50 s^{-1} amplitude. The grounds were then serially diluted and plated on selective agar plates and incubated in room temperature for two days before colony counting.

Fluorescence microscopy of whole nematodes

Nematodes were collected from the water traps, then they were concentrated to a volume of 300 μl. To this, 5 μl of levamisole (200 uM) was added to the nematodes to paralyze them. The nematodes were then imaged using a Nikon Ti2 microscope at 10x magnification, using the brightfield, GFP and RFP channels. At least 100 nematodes were imaged per condition and replicate (5 technical replicates per biological replicate, where each technical replicate is a nematode population from a separate LK agar plate).

Acknowledgements

We thank Dr. Jennifer Heppert and Prof. Heidi Goodrich-Blair for sending us the donor vectors used in this study. We thank Dr. Lydia Varesio for helping with the development of the crystal violet assay. We thank Dr. Georgia Squyres for helpful

suggestions about image analysis. We thank Dr. Nate Glasser for input on the RNA-sequencing analysis. We thank Prof. Ned Ruby for helpful discussions on biofilm formation and competition. All figures were created using BioRender.com. This work was supported by Caltech's Resnick Sustainability Institute.

References

[1] Mesfin T. Gebremikael, Hanne Steel, David Buchan, Wim Bert, and Stefaan De Neve. "Nematodes enhance plant growth and nutrient uptake under C and N-rich conditions". *Scientific Reports* 6.1 (2016), p. 32862.

[2] Gregor W. Yeates, Tom Bongers, Ron G. M. De Goede, Diana W. Freckman, and SS2619405 Georgieva. "Feeding habits in soil nematode families and genera—an outline for soil ecologists". *Journal of Nematology* 25.3 (1993), p. 315.

[3] Eric Kenney and Ioannis Eleftherianos. "Entomopathogenic and plant pathogenic nematodes as opposing forces in agriculture". en. *International Journal for Parasitology* 46.1 (Jan. 2016), pp. 13–19. ISSN: 00207519. DOI: 10.1016/j.ijpara.2015.09.005. URL: https://linkinghub.elsevier.com/retrieve/pii/S002075191500260X (visited on 06/09/2023).

[4] Simon Brooker. "Estimating the global distribution and disease burden of intestinal nematode infections: adding up the numbers–a review". *International Journal for Parasitology* 40.10 (2010), pp. 1137–1144.

[5] Jae Im Choi, Kyoung-hye Yoon, Saraswathi Subbammal Kalichamy, Sung-Sik Yoon, and Jin Il Lee. "A natural odor attraction between lactic acid bacteria and the nematode *Caenorhabditis elegans*". en. *The ISME Journal* 10.3 (Mar. 2016), pp. 558–567. ISSN: 1751-7362, 1751-7370. DOI: 10.1038/ismej.2015.134. URL: https://www.nature.com/articles/ismej2015134 (visited on 06/08/2023).

[6] Deep Prakash, Akhil Ms, Buddidhathi Radhika, Radhika Venkatesan, Sreekanth H Chalasani, and Varsha Singh. "1-Undecene from *Pseudomonas aeruginosa* is an olfactory signal for flight-or-fight response in *Caenorhabditis elegans*". en. *The EMBO Journal* 40.13 (July 2021), e106938. ISSN: 0261-4189, 1460-2075. DOI: 10.15252/embj.2020106938. URL: https://www.embopress.org/doi/10.15252/embj.2020106938 (visited on 03/12/2025).

[7] Elizabeth Pradel, Yun Zhang, Nathalie Pujol, Tohey Matsuyama, Cornelia I. Bargmann, and Jonathan J. Ewbank. "Detection and avoidance of a natural product from the pathogenic bacterium *Serratia marcescens* by *Caenorhabditis elegans*". *Proceedings of the National Academy of Sciences* 104.7 (2007), pp. 2295–2300.

[8] Patricia Manosalva, Murli Manohar, Stephan H Von Reuss, Shiyan Chen, Aline Koch, Fatma Kaplan, Andrea Choe, Robert J. Micikas, Xiaohong Wang, Karl-Heinz Kogel, et al. "Conserved nematode signalling molecules elicit plant defenses and pathogen resistance". *Nature Communications* 6.1 (2015), p. 7795.

[9] Lin Zhang, Yuping Wei, Ye Tao, Suya Zhao, Xuyang Wei, Xiaoyan Yin, Suyao Liu, and Qiuhong Niu. "Molecular mechanism of the smart attack of pathogenic bacteria on nematodes". *Microbial Biotechnology* 13.3 (2020), pp. 683–705.

[10] Kristen E. Murfin, Amy C. Whooley, Jonathan L. Klassen, and Heidi Goodrich-Blair. "Comparison of Xenorhabdus bovienii bacterial strain genomes reveals diversity in symbiotic functions". en. *BMC Genomics* 16.1 (Dec. 2015), p. 889. ISSN: 1471-2164. DOI: 10.1186/s12864-015-2000-8. URL: https://bmcgenomics.biomedcentral.com/articles/10.1186/s12864-015-2000-8 (visited on 10/19/2023).

[11] P. S. Grewal, M. Matsuura, and V. Converse. "Mechanisms of specificity of association between the nematode *Steinernema scapterisci* and its symbiotic bacterium". *Parasitology* 114.5 (1997), pp. 483–488.

[12] Mathieu Sicard, Nathalie Le Brun, Sylvie Pages, Bernard Godelle, Noël Boemare, and Catherine Moulia. "Effect of native *Xenorhabdus* on the fitness of their *Steinernema* hosts: contrasting types of interaction". *Parasitology Research* 91 (2003), pp. 520–524.

[13] Erin E. Herbert and Heidi Goodrich-Blair. "Friend and foe: the two faces of *Xenorhabdus nematophila*". *Nature Reviews Microbiology* 5.8 (2007), pp. 634–646.

[14] John G. McMullen, Brittany F. Peterson, Steven Forst, Heidi Goodrich Blair, and S. Patricia Stock. "Fitness costs of symbiont switching using entomopathogenic nematodes as a model". *BMC Evolutionary Biology* 17 (2017), pp. 1–14.

[15] Dongjin Park, Kristin Ciezki, Ransome Van Der Hoeven, Swati Singh, Daniela Reimer, Helge B. Bode, and Steven Forst. "Genetic analysis of xenocoumacin antibiotic production in the mutualistic bacterium *Xenorhabdus nematophila*". *Molecular Microbiology* 73.5 (2009), pp. 938–949.

[16] Shobhi Chaudhary, Garima Singh, Nomita Gupta, Chaitali Ghosh, and Jitendra Singh Rathore. "New face in the row of bioactive compounds and toxin-antitoxin modules: *Xenorhabdus nematophila*". *Journal of Asia-Pacific Entomology* 26.4 (2023), p. 102148.

[17] Shabbir Ahmed and Yonggyun Kim. "Differential immunosuppression by inhibiting PLA2 affects virulence of *Xenorhabdus hominickii* and Photorhabdus temperata temperata". *Journal of Invertebrate Pathology* 157 (2018), pp. 136–146.

[18] Charles E. Cowles and Heidi Goodrich-Blair. "The *Xenorhabdus nematophila nilABC* genes confer the ability of *Xenorhabdus* spp. to colonize *Steinernema carpocapsae* nematodes". *Journal of Bacteriology* 190.12 (2008), pp. 4121–4128.

[19] Mengyi Cao. "CRISPR-Cas9 genome editing in *Steinernema* entomopathogenic nematodes". *bioRxiv* (2023), pp. 2023–11.

[20] Yan Yu, Ying K. Zhang, Murli Manohar, Alexander B. Artyukhin, Anshu Kumari, Francisco J. Tenjo-Castano, Hung Nguyen, Pratyush Routray, Andrea Choe, Daniel F. Klessig, and Frank C. Schroeder. "Nematode Signaling Molecules Are Extensively Metabolized by Animals, Plants, and Microorganisms". en. *ACS Chemical Biology* 16.6 (June 2021), pp. 1050–1058. ISSN: 1554-8929, 1554-8937. DOI: 10.1021/acschembio.1c00217. URL: https://pubs.acs.org/doi/10.1021/acschembio.1c00217 (visited on 10/17/2023).

[21] Andrew Renda, Stephanie Poly, Ying-Jung Lai, Archana Pannuri, Helen Yakhnin, Anastasia H. Potts, Philip C. Bevilacqua, Tony Romeo, and Paul Babitzke. "CsrA-Mediated Translational Activation of *ymdA* Expression in *Escherichia coli*". en. *mBio* 11.5 (Oct. 2020). Ed. by Pascale F. Cossart, e00849–20. ISSN: 2161-2129, 2150-7511. DOI: 10.1128/mBio.00849-20. URL: https://journals.asm.org/doi/10.1128/mBio.00849-20 (visited on 01/19/2024).

[22] Moonjeong Kim and Kwang-sun Kim. "Stress-responsively modulated *ymdABclsC* operon plays a role in biofilm formation and apramycin susceptibility in *Escherichia coli*". en. *FEMS Microbiology Letters* 364.13 (July 2017). ISSN: 1574-6968. DOI: 10.1093/femsle/fnx114. URL: https://academic.oup.com/femsle/article/doi/10.1093/femsle/fnx114/3861256 (visited on 06/06/2024).

[23] Ryan B. McLay, Hang N. Nguyen, Yuly Andrea Jaimes-Lizcano, Narendra K. Dewangan, Simone Alexandrova, Debora F. Rodrigues, Patrick C. Cirino, and Jacinta C. Conrad. "Level of fimbriation alters the adhesion of *Escherichia coli* bacteria to interfaces". *Langmuir* 34.3 (2018), pp. 1133–1142.

[24] Qingguo Liu, Jiaqing Zhu, Na Liu, Wenjun Sun, Bin Yu, Huanqing Niu, Dong Liu, Pingkai Ouyang, Hanjie Ying, Yong Chen, et al. "Type I fimbriae subunit *fimA* enhances *Escherichia coli* biofilm formation but affects L-threonine carbon distribution". *Frontiers in Bioengineering and Biotechnology* 10 (2022), p. 904636.

[25] Cheryl-Lynn Y Ong, Glen C. Ulett, Amanda N. Mabbett, Scott A. Beatson, Richard I. Webb, Wayne Monaghan, Graeme R. Nimmo, David F. Looke, Alastair G. McEwan, and Mark A. Schembri. "Identification of type 3 fimbriae in uropathogenic *Escherichia coli* reveals a role in biofilm formation". *Journal of Bacteriology* 190.3 (2008), pp. 1054–1063.

[26] Melissa A. Lasaro, Nina Salinger, Jing Zhang, Yantao Wang, Zhengtao Zhong, Mark Goulian, and Jun Zhu. "F1C fimbriae play an important role in biofilm formation and intestinal colonization by the *Escherichia coli* commensal strain Nissle 1917". *Applied and Environmental Microbiology* 75.1 (2009), pp. 246–251.

[27] Holly Snyder, Hongjun He, Heather Owen, Chris Hanna, and Steven Forst. "Role of Mrx Fimbriae of *Xenorhabdus nematophila* in Competitive Colonization of the Nematode Host". en. *Applied and Environmental Microbiology* 77.20 (Oct. 2011), pp. 7247–7254. ISSN: 0099-2240, 1098-5336. DOI: 10.1128/AEM.05328-11. URL: https://journals.asm.org/doi/10.1128/AEM.05328-11 (visited on 08/11/2024).

[28] Emilie Lefoulon, John G. McMullen, and S. Patricia Stock. "Transcriptomic analysis of Steinernema nematodes highlights metabolic costs associated to *Xenorhabdus* endosymbiont association and rearing conditions". *Frontiers in Physiology* 13 (2022), p. 821845.

[29] Gregory C. Bernard, Marceline Egnin, and Conrad Bonsi. "The impact of plant-parasitic nematodes on agriculture and methods of control". *Nematology-Concepts, Diagnosis and Control*. IntechOpen, 2017.

[30] Andrea Braun-Kiewnick, Nicole Viaene, Laurent Folcher, Fabrice Ollivier, Géraldine Anthoine, Björn Niere, Melanie Sapp, Bart van de Vossenberg, Halil Toktay, and Sebastian Kiewnick. "Assessment of a new qPCR tool for the detection and identification of the root-knot nematode Meloidogyne enterolobii by an international test performance study". *European Journal of Plant Pathology* 144 (2016), pp. 97–108.

[31] Ilker Kepenekci, Selcuk Hazir, Ercin Oksal, and Edwin E. Lewis. "Application methods of *Steinernema feltiae*, *Xenorhabdus bovienii* and *Purpureocillium lilacinum* to control root-knot nematodes in greenhouse tomato systems". *Crop Protection* 108 (2018), pp. 31–38.

[32] S. Manochaya, Shashikant Udikeri, B. S. Srinath, Mantri Sairam, Srinivas V. Bandlamori, and Krishnaveni Ramakrishna. "*In vivo* culturing of entomopathogenic nematodes for biological control of insect pests: A review". *Journal of Natural Pesticide Research* 1 (2022), p. 100005.

[33] Mengyi Cao, Hillel T. Schwartz, Chieh-Hsiang Tan, and Paul W. Sternberg. "The entomopathogenic nematode *Steinernema hermaphroditum* is a self-fertilizing hermaphrodite and a genetically tractable system for the study of parasitic and mutualistic symbiosis". *Genetics* 220.1 (2022), iyab170.

[34] Kristen E. Murfin, Adler R. Dillman, Jeremy M. Foster, Silvia Bulgheresi, Barton E. Slatko, Paul W. Sternberg, and Heidi Goodrich-Blair. "Nematode-Bacterium Symbioses—Cooperation and Conflict Revealed in the "Omics" Age". en. *The Biological Bulletin* 223.1 (Aug. 2012), pp. 85–102. ISSN: 0006-3185, 1939-8697. DOI: 10.1086/BBLv223n1p85. URL: https://www.

journals.uchicago.edu/doi/10.1086/BBLv223n1p85 (visited on 06/08/2023).

[35] Nicolas L. Bray, Harold Pimentel, Páll Melsted, and Lior Pachter. "Near-optimal probabilistic RNA-seq quantification". *Nature Biotechnology* 34.5 (2016), pp. 525–527.

[36] Michael I. Love, Wolfgang Huber, and Simon Anders. "Moderated estimation of fold change and dispersion for RNA-seq data with DESeq2". *Genome Biology* 15 (2014), pp. 1–21.

[37] Andrew D. Halleran, Anandh Swaminathan, and Richard M. Murray. "Single day construction of multigene circuits with 3G assembly". *ACS Synthetic Biology* 7.5 (2018), pp. 1477–1480.

[38] George A. O'Toole. "Microtiter dish biofilm formation assay". *Journal of Visualized Experiments: JoVE* 47 (2011), p. 2437.

Chapter 6

CONSTRUCTION OF A NEMATODE REPORTER BASED ON A TRANSCRIPTIONAL RESPONSE

The work described in this chapter is unpublished and was done by:
Elin M. Larsson, Carly R. Myers and Mengyi Cao.

Contributions: EML conceived the project idea; CRM and MC rendered and prepared nematodes for the trans-well experiment; EML designed and performed the experiments, analyzed and visualized the data, and wrote the text.

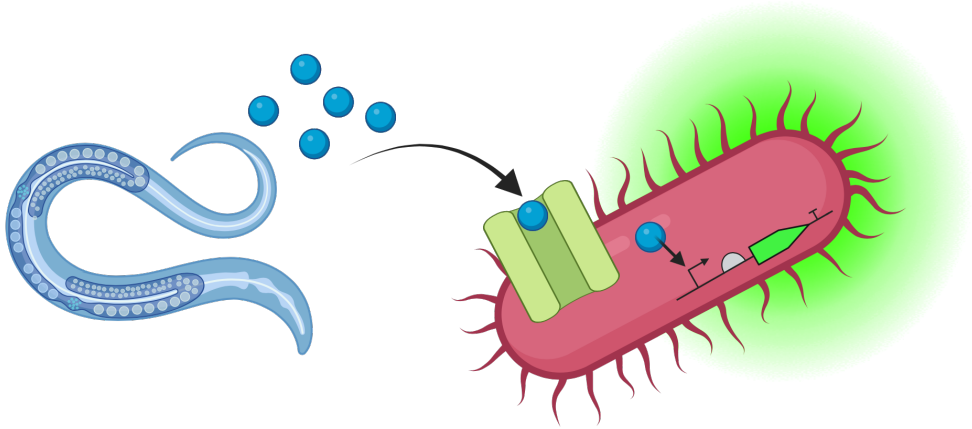

6.1 Introduction

As described in Chapter 5, the *Steinernema-Xenorhabdus* pair is an ecologically relevant model for mutualism and parasitism in the soil ecosystem. Another parasitic soil interaction is that of root-knot nematodes that infect food crops and cause losses worth billions of dollars every year [1].

The most common method to detect a nematode outbreak is by sampling soil and doing direct counts of nematodes per gram of soil. This requires knowledge about the morphological differences between different types of nematodes and is very time consuming. A more species specific method is qPCR. Although promising in multiple publications [2–4], this method has not yet reached commercial use.

It is difficult to work with root-knot nematodes in the lab, both because they are less well-studied than other classes of nematodes, but also because special regulations

make it harder to work with them. This is because of their high virulence and ability to be destructive to plants. For example, special sinks are needed in the lab when working with root-knot nematodes to ensure that any runoff gets autoclaved before release.

One question that we initially thought about when asking the question of whether *X. griffiniae* could sense *S. hermaphroditum* is "if this sensing does occur, how specific is it?". Can a specific species be sensed or is it broadly **all nematodes** or a **specific class** of nematodes? Given that *Xenorhabdus* spp. and *Steinernema* spp. release nematicidal compounds that can protect plants from root-knot nematodes [5], maybe they are also able to sense their presence. This made us wonder if a bacterial whole-cell nematode reporter can be developed for early detection of nematodes.

There is one paper describing a synthetic nematode reporter based on an elastase produced by a parasitic nematode to enable penetration of the skin barrier [6]. The elastase cleaves a specific motif that leads to the loss of a fluorescent particle on the cell surface. There is also a study describing a LAMP based biosensor for nematodes [7]. To our knowledge there are no whole-cell reporters for nematodes that are not based on surface displayed elements.

In previous chapters we described work on the model nematode-bacteria symbiosis of *S. hermaphroditum* and *X. griffiniae*. In this chapter we investigate the feasibility of turning *X. griffiniae* into a whole-cell biosensor for nematodes.

We found in Chapter 5 that *X. griffiniae* can sense *S. hermaphroditum* by the fact that genes were differentially regulated. This means that we can start to construct a whole-cell "nematode reporter" based on a transcriptional response for the first time. This distinction from other nematode reporters is important because it means that the sensing can be coupled to actuation, thereby paving the way towards sense-and-respond microbial products that can be use to deal with nematode outbreaks.

6.2 Results

To construct a nematode sensor, we first need to find a gene that is differentially regulated when nematodes are present couple that to an output, in this case a fluorescent protein. As described in Chapter 5, the gene with largest fold-difference in expression was *ymdA*. Since expression of this gene went down in the presence of the nematode, we need to make sure the output signal goes through active degradation so that the signal does not get obscured by pre-existing fluorescent protein.

We first made a part plasmid containing the entire intergenic region upstream of *ymdA*. The hypothesis being that the promoter region driving expression of *ymdA* would be in this region. We first tested this hypothesis by building a construct where P_{ymdA} drives expression of TurboRFP (Figure 6.1). We choose to use the fluorescent protein TurboRFP instead of GFPmut3, since the autofluorescence of the bacteria is very low for the RFP channel compared to the GFP channel (as seen in Chapter 4).

We then compared the RFP expression of this strain to an IPTG inducible strain constructed in Chapter 4, both when induced and non-induced (Figure 6.2). We saw that P_{ymdA} can drive expression of TurboRFP *in vitro* and that the expression strength is weak compared to RFP expression in the IPTG inducible strain at 1 mM inducer concentration.

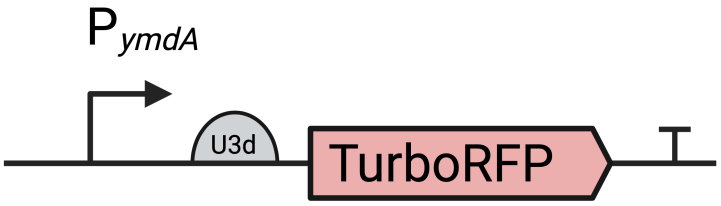

Figure 6.1: Circuit diagram of construct built to test P_{ymdA} *in vitro*.

As described above, since the gene expression is downregulated in the presence of nematodes, we need to make sure TurboRFP is actively degraded. It is not known whether the commonly used ssrA tags work in *Xenorhabdus griffiniae*, so the first thing we needed to do was to test if protein degradation occurs. We built four different constructs where P_{ymdA} drives expression of TurboRFP with no tag, an ASV, AAV or LAA-tag (Figure 6.3A). We then grew them overnight to compare their endpoint fluorescence (Figure 6.3). Although there is some spread between the replicates, the general rank order for the degradation using the different tags is the same as for *E. coli* [8].

Next, we wanted to know if these tags could be used to degrade TurboRFP enough to distinguish between cells grown alone vs. in the presence of nematodes. We therefore tried to replicate the experiment we set up for the RNA-sequencing screen in Chapter 5. We found a weak signal difference for one of the deg-tags — the ASV-tag. We saw a small subpopulation in the no nematode condition that has high expression of RFP (Figure 6.4). However, in this experiment the bacteria grew

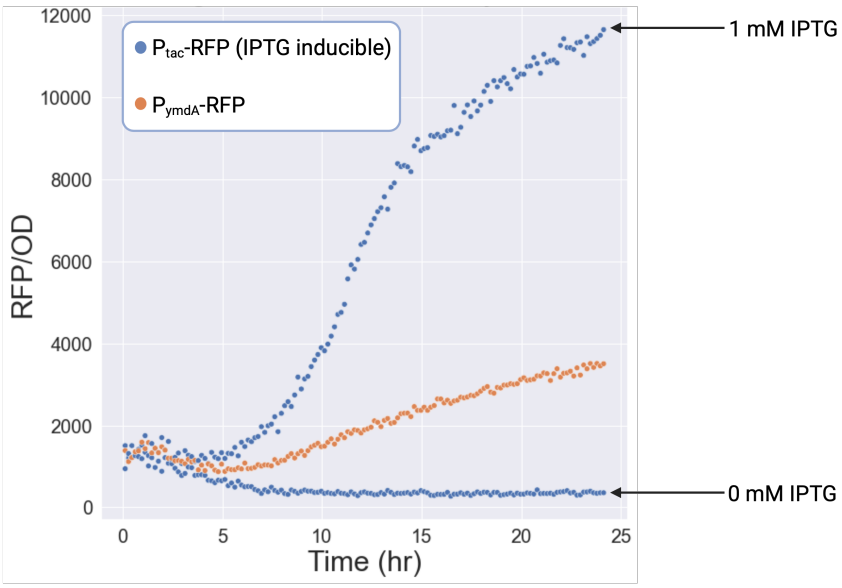

Figure 6.2: Normalized RFP trace for the IPTG inducible strain (on and off) and the P$_{ymdA}$-RFP construct.

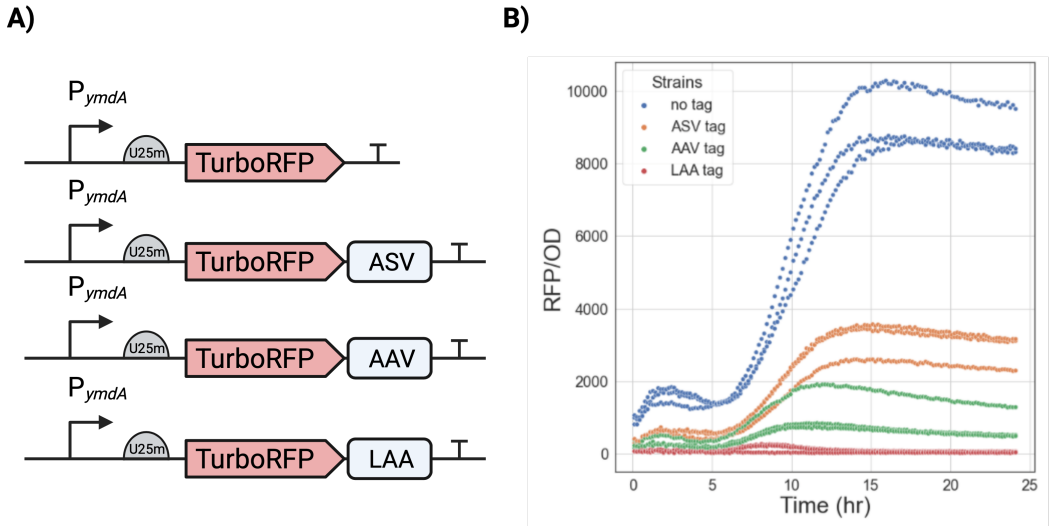

Figure 6.3: (A) Circuit diagrams of P$_{ymdA}$ driving expression of TurboRFP with and without degradation tags. (B) Plate reader experiment comparing degradation level of TurboRFP.

very poorly and in subsequent experiments where we tried to optimize the growth in

the minimal media without success, we decided to try the same experiment in rich media instead.

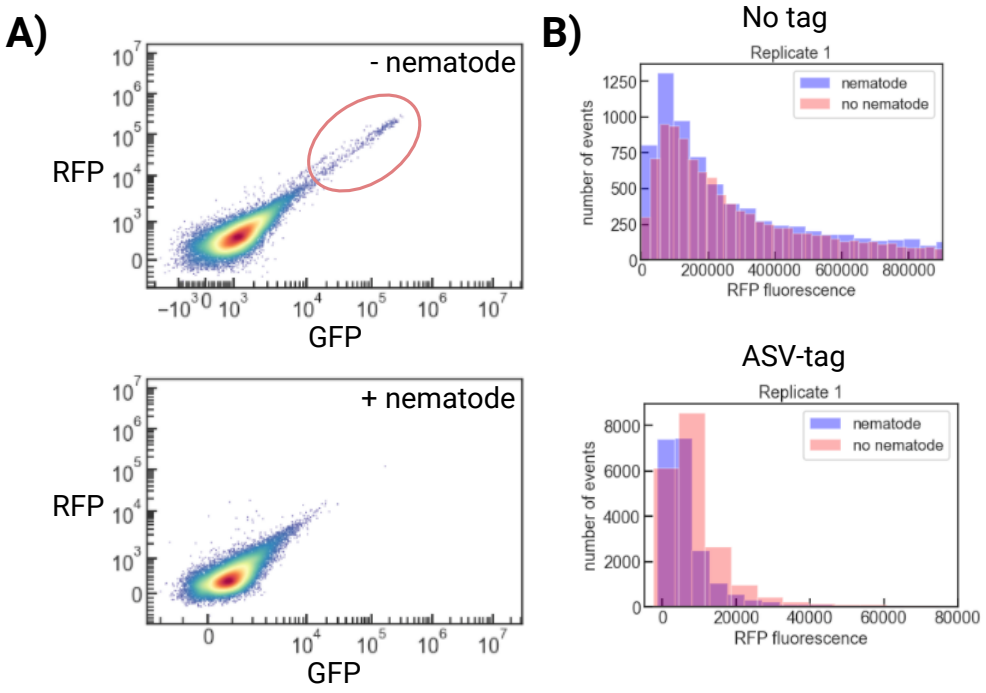

Figure 6.4: (A) Flow cytometry density plots for bacteria grown with and without nematodes. Subpopulation of high RFP-expressing bacteria circled. (B) Histograms for RFP events for bacteria expressing TurboRFP with no tag and with the ASV tag.

When grown in LB, we were able to see the same trend, where bacteria that were exposed to nematodes downregulated their expression of TurboRFP (Figure 6.5A-B), although the maximal RFP fluorescence is higher in minimal media than in rich media. We also measured the bulk RFP fluorescence with a plate reader (Figure 6.6).

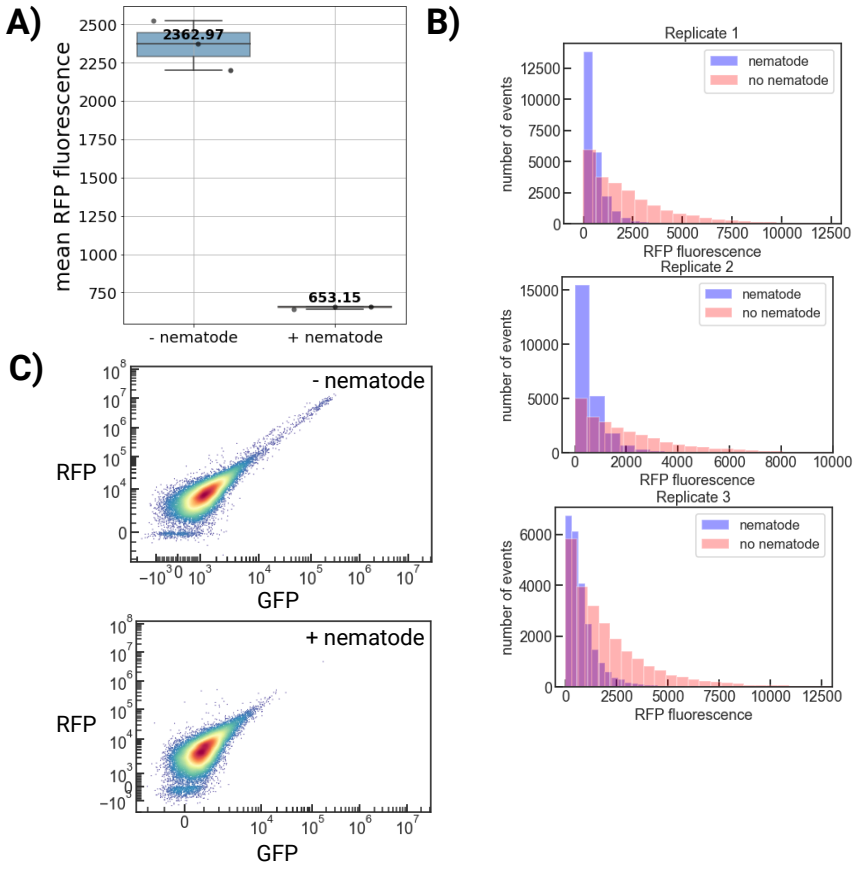

Figure 6.5: (A) Mean RFP fluorescence from flow cytometry measurements. Three replicates from one experiment plotted. (B) Histograms for each replicate showing the spread in RFP fluorescence for bacteria grown with and without axenic nematodes for 24 hours. (C) Flow cytometry density plots for bacteria grown with and without nematodes.

In the RNA-sequencing screen the log2 fold change was 2.33, meaning *ymdA* was about 5-fold more expressed when the bacteria were grown alone compared to when they were grown with the nematodes. From the flow cytometry measurements it seems like the no nematode condition has about 3.6-fold more fluorescence than the nematode condition. For the plate reader measurements, the fold change is only about 1.5.

With this, we have now shown the successful development of an initial transcriptional *S. hermaphroditum* reporter in *X. griffiniae*.

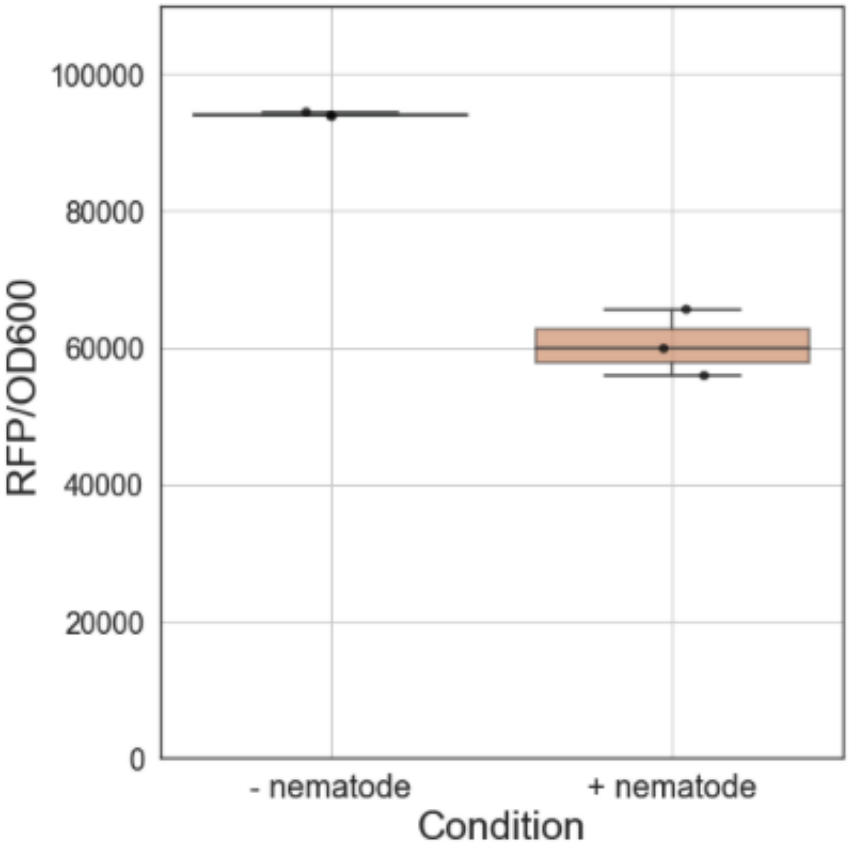

Figure 6.6: Normalized fluorescence measured by a Biotek plate reader after 24 hours of growth +/- nematodes in trans-wells.

6.3 Discussion

In this chapter, we leveraged a native *X. griffiniae* promoter and converted it into a transcriptional reporter for the presence of *S. hermaphroditum*.

The immediate next steps for the next iteration of this nematode reporter is to change the architecture of the reporter to a turn-on instead of a turn-off output (Figure 6.7). We propose a workflow for doing this that is outlined in Figure 6.8.

In this workflow, we avoid the lengthy process of rendering and preparing nematodes, for each iteration of the trans-well experiment, by replacing the nematodes with an inducer. Since we know how much the fluorescence is reduced by the nematodes, we can drive the test construct with a separate inducible promoter and show that by changing the induction level from X to Y, we match the fluorescence change observed in the test construct. So $P_{inducible}$ with inducer going from X to Y will be

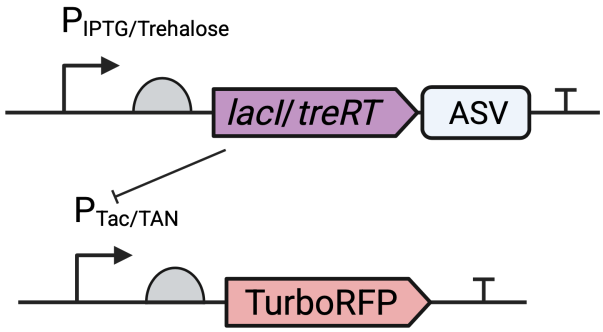

Figure 6.7: Architecture of a nematode reporter with ON-signal instead of OFF-signal.

the proxy for the presence/absence of the nematode, allowing us to iterate quickly and only test the final construct against the real nematodes.

As described in Chapter 4, to our knowledge, no inducible systems have been tested in *X. griffiniae*. In that chapter we identified IPTG as a functional inducer. Here, we also identified another option, trehalose (Figure 6.9). We tested rhamnose and tetracycline inducible systems without success (data not shown). Further experiments need to be done to obtain the complete induction curve for trehalose induction. Induction with rhamnose or tetracycline might be possible if the designs of the original inducible circuits are modified.

For the IPTG and trehalose inducible strains, we also tried *in vivo* induction. To do this, we colonized *S. hermaphroditum* with each strain, we then surface sterilized the nematodes to remove the outer cuticle before adding inducers to the surrounding media. We then waited for two days before imaging the nematodes to look for RFP expressing bacteria in the receptacle. For the IPTG-inducible strain, the observed RFP expression in the receptacle of the nematodes was very weak for the induced condition (Figure 6.10). We think there are at least three likely explanations for this:
1. The induction concentration was too low and/or IPTG degraded over time.
2. The inducer cannot penetrate the nematode inner cuticle.
3. The bacteria are in a dormant state where inducing synthetic constructs is not feasible.
4. Longer incubation time is needed to achieve higher expression levels.

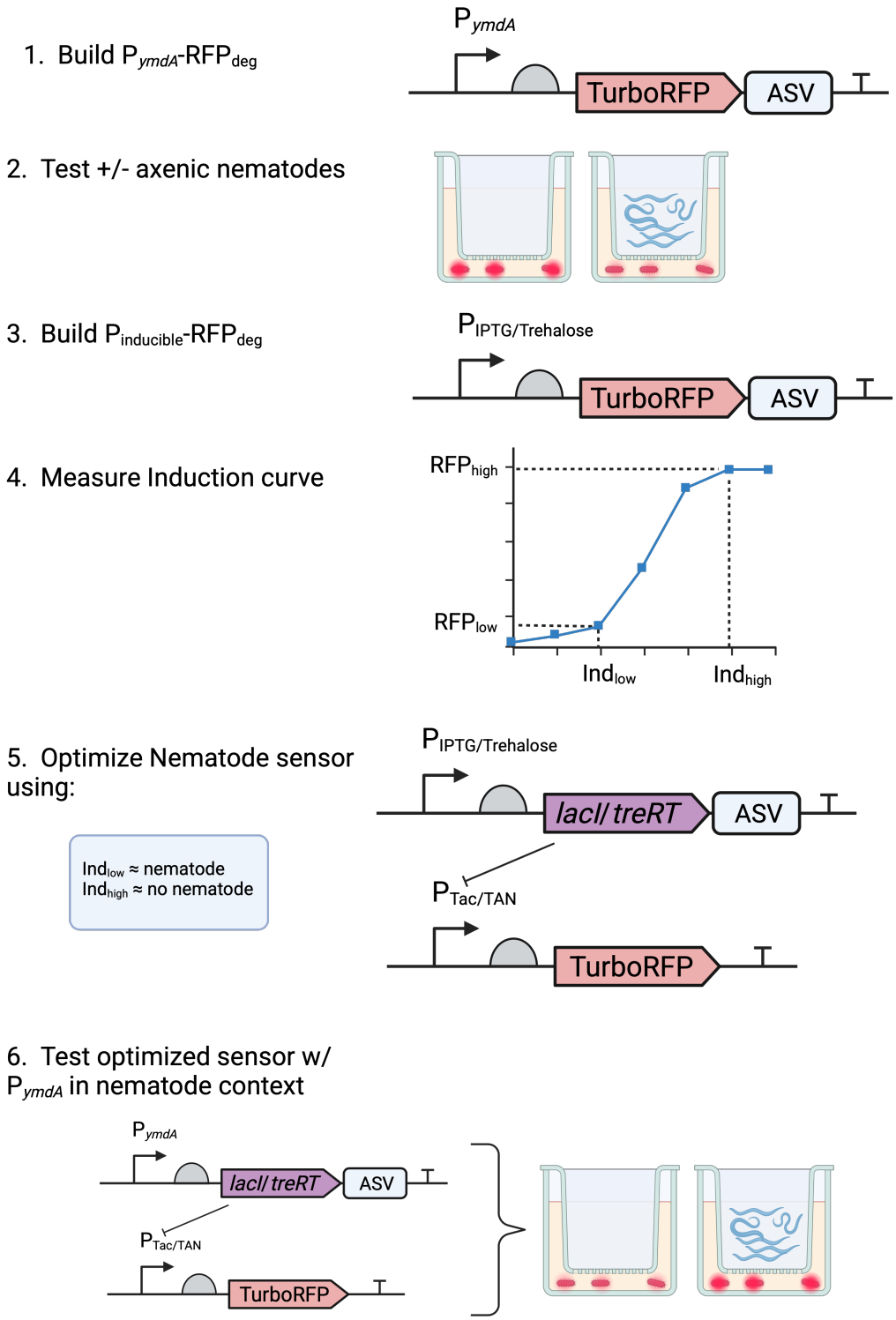

Figure 6.8: Proposed steps to construct a nematode reporter using the parts identified in Chapter 4,5 and 6.

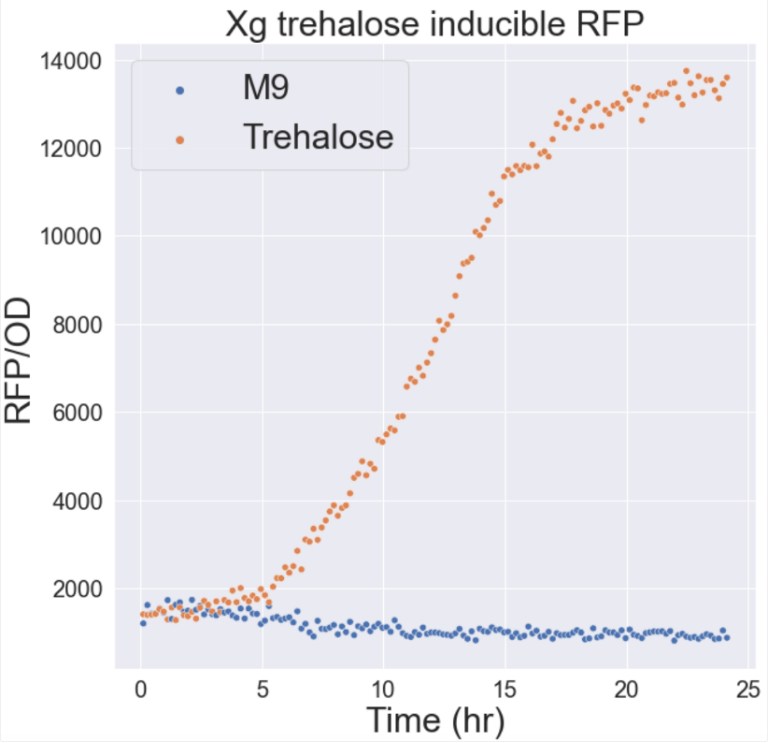

Figure 6.9: Normalized fluorescence of *X. griffiniae* in M9 minimal media +/- trehalose.

For the trehalose-inducible strain, we saw TurboRFP expression both when inducer was added and when it was not. This could either be because the expression is leaky under *in vivo* conditions, or because the trehalose produced by the nematodes is sufficient to induce expression in the "no inducer" control condition.

Even though the turn-on version of the reporter is preferable, we can still make use of the current version of the reporter to do some experiments that can help us understand the sensing mechanism *X. griffiniae* is using to detect *S. hermaphroditum*. For example, we can:

1. Test whether *X. griffiniae* can sense S. *hermaphroditum* in different media and matrices like soil and insect cadavers by separating the matrix from the bacteria before doing flow cytometry (as in Chapter 2).
2. Confirm the finding that only axenic nematodes, not colonized ones, can be sensed by *X. griffiniae*.
3. Test the specificity of the sensing mechanism by using other related nematodes species such as *S. nematophila* or *S. bovienii* in the trans-well set-up.
4. Test different purified molecules instead of whole nematodes (e.g., ascarosides).

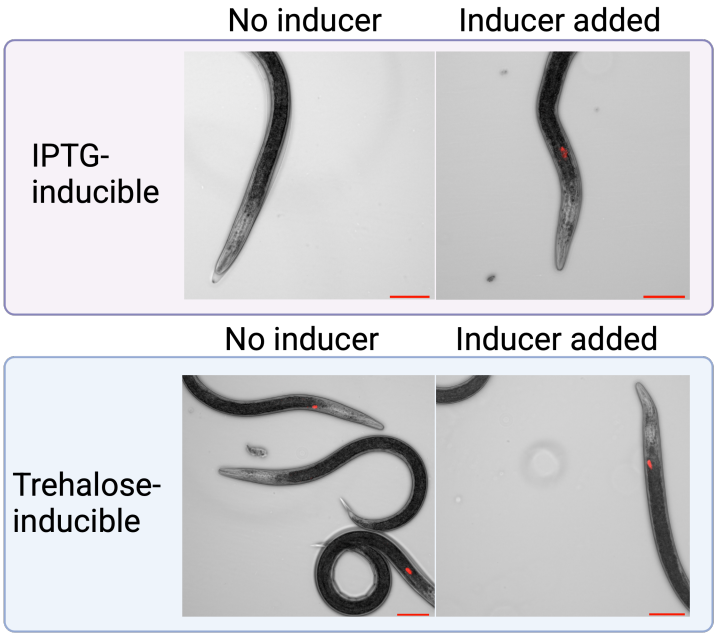

Figure 6.10: *In vivo* induction of IPTG and trehalose-inducible *X. griffiniae* in the *S. hermaphroditum* receptacle of infective juveniles. Scale bar 100 μm

.

In conclusion, having demonstrated the feasibility of the trans-well RNA-sequencing screen to engineered nematode bioreporter pipeline, the next step would be to test whether other genetically tractable soil microbes respond to the presence of root-knot nematodes in the trans-well setup, and try to engineer a biosensor for relevant nematodes via the same pipeline. A good first chassis candidate would be *P. synxantha* that makes phenazines and other molecules that are toxic to nematodes.

6.4 Methods

Cloning and transformation into *X. griffiniae*

Cloning and transformation was done as described as in Chapter 4. For the P_{ymdA} promoter region, we used the entire intergenic region between ymdA and the upstream gene (575 bp).

Trans-well experiments with nematodes

The trans-well set-up was the same as in Chapter 5 with the addition of one row of LB instead of M9 medium. The trans-well experiment was followed up by flow cytometry and plate reader measurements.

Plate reader experiments

For the *in vitro* characterization of the P_{ymdA}-RFP constructs (Figure 6.2 and 6.3) compared to P_{tac}-RFP, cells were inoculated into a 96-well plate from an LB overnight. Cells were then grown for 24 hours at 30 °C with linear continuous shaking in a Biotek plate reader with or without added IPTG (1 mM).

For the post trans-well measurement (Figure 6.6), OD and fluorescence was measured by transferring 200 μl from the trans-wells to a 96-well plate.

Flow cytometry

The flow cytometry and data analysis was done in the same way as in Chapter 2 with the exception of collecting 60000 events instead of 10000, as well as adding the 585 nm Yellow laser.

In vivo colonization and imaging

The same procedure as in Chapter 4 was followed, with the addition of the induction step where nematodes were collected from the water traps and surface sterilized with 1% bleach before adding the inducer. The nematodes were then incubated in room temperature for two days before imaging them.

Ackowledgements

The work in this chapter was made possible by key insights made by Olivia Wang in Chapter 4 and from numerous discussions with Dr. John Marken about experimental design.

References

[1] Gregory C. Bernard, Marceline Egnin, and Conrad Bonsi. "The impact of plant-parasitic nematodes on agriculture and methods of control". *Nematology-Concepts, Diagnosis and Control*. IntechOpen, 2017.

[2] Amanda K. Hodson, Tugce Celayir, and Alejandra Quiroz Alonso. "A Real-Time PCR assay to detect and quantify root-knot nematodes from soil extracts". *Plant Disease* 107.7 (2023), pp. 2169–2176.

[3] M Soule, A Peetz, H Baker, S Chavoshi, and IA Zasada. "Development of a Quantitative PCR Assays for Columbia Root-Knot Nematode (Meloidogyne chitwoodi) Diagnostics in the Pacific Northwest". *PhytoFrontiers* ja (2025).

[4] Andrea Braun-Kiewnick, Nicole Viaene, Laurent Folcher, Fabrice Ollivier, Géraldine Anthoine, Björn Niere, Melanie Sapp, Bart van de Vossenberg, Halil Toktay, and Sebastian Kiewnick. "Assessment of a new qPCR tool for the detection and identification of the root-knot nematode Meloidogyne enterolobii by an international test performance study". *European Journal of Plant Pathology* 144 (2016), pp. 97–108.

[5] Ilker Kepenekci, Selcuk Hazir, Ercin Oksal, and Edwin E. Lewis. "Application methods of *Steinernema feltiae*, *Xenorhabdus bovienii* and *Purpureocillium lilacinum* to control root-knot nematodes in greenhouse tomato systems". *Crop Protection* 108 (2018), pp. 31–38.

[6] A. J. Webb, R. Kelwick, M. J. Doenhoff, N. Kylilis, J. T. MacDonald, K. Y. Wen, C. McKeown, G. Baldwin, T. Ellis, K. Jensen, and P. S. Freemont. "A protease-based biosensor for the detection of schistosome cercariae". en. *Scientific Reports* 6.1 (Apr. 2016), p. 24725. ISSN: 2045-2322. DOI: 10.1038/srep24725. URL: https://www.nature.com/articles/srep24725 (visited on 06/01/2023).

[7] Maria João Camacho, Débora C Albuquerque, Maria L. Inácio, Verónica C. Martins, Manuel Mota, Paulo P. Freitas, and Eugénia de Andrade. "FTA-LAMP based biosensor for a rapid in-field detection of Globodera pallida—The pale potato cyst nematode". *Frontiers in Bioengineering and Biotechnology* 12 (2024), p. 1337879.

[8] Jens Bo Andersen, Claus Sternberg, Lars Kongsbak Poulsen, Sara Petersen Bjørn, Michael Givskov, and Søren Molin. "New unstable variants of green fluorescent protein for studies of transient gene expression in bacteria". *Applied and environmental microbiology* 64.6 (1998), pp. 2240–2246.

Chapter 7

CONCLUSION

There are advantages and disadvantages to choosing model bacteria versus less cooperative non-model bacteria from the environment for any given application. Environmental bacteria are well adjusted to their niche and often have interesting chemistries that have been lost in model organisms that have adapted to the laboratory environment. Although we are able to engineer many environmental bacteria, the design-build-test cycle is slower than for model organisms. This in combination with our poor understanding of the gene regulation, growth requirements, physiology, etc. of these species create challenges. In this thesis, we describe the engineering of two non-model bacteria that are important in the soil ecosystem.

In Chapter 2 we successfully design, build and thoroughly characterize the performance of a ratiometric reporter for phosphorus limitation in the wheat-colonizing bacterium *Pseudomonas synxantha* 2-79. We found that many of the promoter regions we tested from the RNA-sequencing screen were non-functional in the context of the P reporter construct. Although we predicted these sequences to be functional for driving the expression of GFP during phosphorus limitation, we often saw weak or no expression. There might have been interactions between those upstream regions and the other synthetic elements in the genetic construct that made them non-functional, or their regulation may be more complicated, making it hard for us to reproduce the response *in vitro*.

In Chapter 3, we produce and characterize cell-free extract from three soil Pseudomonads that make redox-active metabolites, phenazines, relevant to crop health. We then show that we can use these extracts for predicting constitutive promoter strengths *in vivo*. However, we found that the *in vivo* and *in vitro* expression does not perfectly match. Although using cell-free transcription-translation (TXTL) as a way to rapidly screen genetic parts for non-model organisms can be useful, it has limitations, not only because the *in vitro* and *in vivo* results are not always matching, but also because some genetic parts that we would like to screen are dependent on compartmentalization. For example, the PhoB/PhoR two component system that we leverage when building the P reporter cannot be tested using bulk TXTL, since the inner and outer membrane of the cell is crucial for this sensing mechanism.

Finally, another limitation is that certain compounds, that are not toxic to living cells that can adapt and use defense mechanisms, are known to inhibit transcription and translation in TXTL [1].

In Chapter 4, we build and characterize a genetic part library for *Xenorhabdus griffiniae*, the bacterial symbiont of the entomopathogenic nematode *Steinernema hermaphroditum*. One of the tested fluorescent proteins (mScarlet3) did not express well in *X. griffiniae*. In the same chapter, we also saw that adding RiboJ upstream of the RBS enhanced expression for one RBS (U4m) but not for another (U4d). Both this and the challenges in Chapter 2 and 3 highlight the issues related to unpredictable behavior and the need for methods that are high-throughput — in other words, we need to test many things in parallel since many variants are non-functional for reasons that are unknown. The functional parts characterized in this chapter are then used in Chapter 6 where we design, build and test a reporter for the presence of *S. hermaphroditum*.

Finally, one of the most substantive findings in this thesis is that bacteria living in nematodes have the ability to sense the presence of their host (Figure 7.1). This seems logical, but has not been reported before. We are expecting that the set-up we used to come to this conclusion will be used for other mutualistic partners in the future. The eventual goal would be to use this information to design functional nematode reporters, both for beneficial and harmful nematodes (e.g., root-knot nematodes).

Through the work in this thesis, we show that the process of constructing microbial bioreporters give new insights about the underlying biology of the chassis organism. For example, when looking for a way to construct a nematode reporter, we learned about one of the genes that *Xenorhabdus griffiniae* uses to improve its colonization efficiency and opened up for speculation and future studies about what roles the other differentially expressed genes might play in colonization and fitness. The constructed reporter itself has uses, not only as a tool for reporting on the presence or absence of a molecule or other organism but, as a tool to make further biological discoveries that helps uncover how bacteria interact with their environment, whether that is in a soil ecosystem acquiring nutrients, or in a symbiotic relationship with a host.

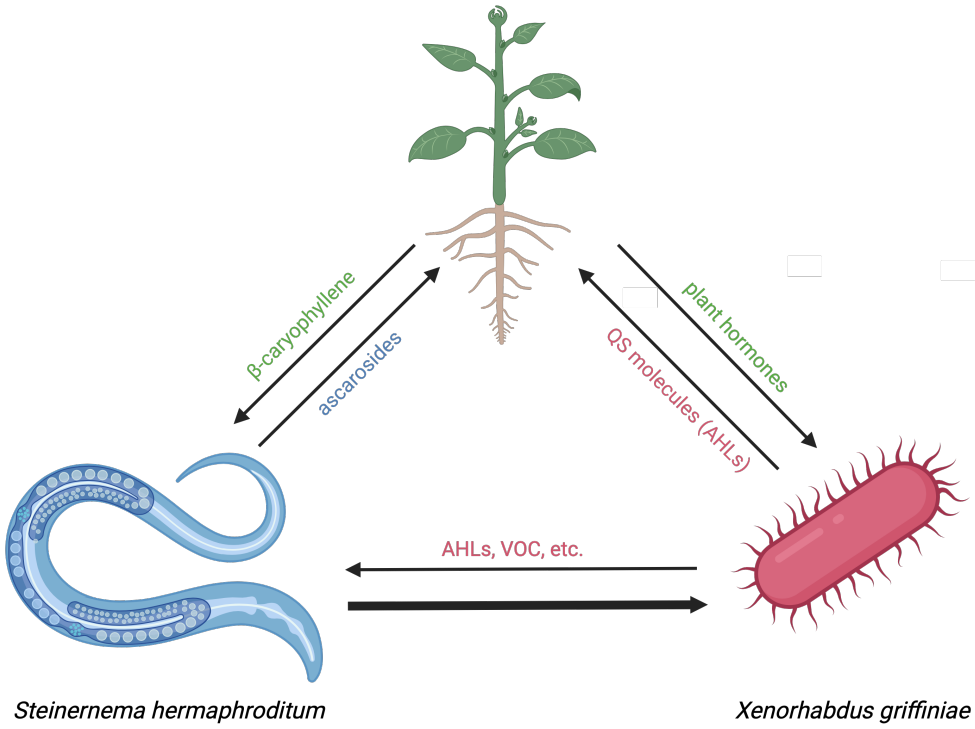

Figure 7.1: *Xenorhabdus griffiniae* is able to sense and respond to the presence of its nematode host *Steinernema hermaphroditum*.

Suggested next steps building on this thesis

Future work to address the mechanism behind the sensing we are observing in Chapter 5 include answering the following questions:

(1) What molecules are being sensed by the bacteria and who are secreting them?

(2) What is the molecular mechanism used by the bacteria to import and recognize these molecules?

We can answer these question by comparing the secreted molecules in colonized and axenic nematodes using untargeted metabolomics. By then using purified molecules, the exact sensing mechanism can be elucidated.

As described at the end of Chapter 6, the current nematode reporter (and future improved versions) can be used to address fundamental questions about the sensing and symbiosis with nematodes. For example:

(1) How specific is the sensing mechanism? Can the bacteria discriminate *S. hermaphroditum* from closely related *Steinernema* species?

(2) How is the sensing impacted by external factors?

In the same chapter, showing that we can induce gene expression when the bacteria

are already in the IJ receptacle opens up for new types of questions to be addressed without relying on resource intensive RNA-sequencing. This is particularly useful since RNA-sequencing of bacteria that are in the nematode receptacle is currently not feasible due to the limited amount of bacterial RNA that can be obtained compared to nematode RNA [2]. Questions you might be able to investigate while inducing genes in bacteria residing in the receptacle include:
(1) Are there genes that are detrimental to host fitness **after** colonization has occurred?
(2) Are there genes that can increase the efficiency of insect infection/killing?

The future of engineering non-model soil bacteria broadly

To leverage the untapped resource of environmental bacteria, we need to keep expanding the ways in which we grow bacteria in the lab by improving media optimization, co-culturing techniques, etc. This will enable study of the "dark" soil microbiome that have not yet been cultured in the lab. High-throughput screening of gene function/secreted molecules will be an important part in future discoveries that will benefit from using computational biology techniques that aid in initial predictions.

There are multiple groups working on challenges in this space. For example, Huang et al. developed a pipeline using automation and machine learning to isolate a diverse set of bacterial species from the human gut microbiome [3]. Another example is using dilution-to-extinction cultivation to isolate soil bacteria [4].

When engineering strains isolated from the environment, the same techniques that have been used for decades are often used in a "brute-force" manner. As described in the introduction chapter of this thesis: to engineer bacteria, we need to design DNA that can be used to express or delete genes in the species of choice. This DNA then needs to be delivered and/or reliably maintained in the bacterial cell. Cells then need to be screened for the desired phenotype followed by isolation of the engineered bacteria, if they were screened in a pool of variants. Going through this time-consuming design-build-test cycle for each organism is currently required as there is no one size fits all for engineering different bacterial species. There are some new frontiers in engineering of non-model bacteria: for example using genetic parts from bacteriophages [5], and developing CRISPR-Cas9 systems to edit the genomes of non-model bacteria [6]. However, in order to speed up the process of

engineering non-model bacteria there has to be some breakthrough that generalizes across many different species.

Aside from the technical challenges, a major hurdle that remains is regulatory obstacles and a lack of knowledge about *how* to safely deploy engineered bacteria [7]. Because of the complex nature of regulation of engineered microbes, and the lengthy process towards approval, it is difficult to deploy most of bacteria that are engineered in the lab today. Most innovations are still limited to proof-of-concept demonstrations in the lab or to industrial processes in closed-off reactor tanks. To use the untapped resources offered by engineered microbiology to solve problems in sustainability and medicine, we need to overcome some of these obstacles.

References

[1] Nan Jiang, Xuanwei Ding, and Yuan Lu. "Development of a robust *Escherichia coli*-based cell-free protein synthesis application platform". *Biochemical Engineering Journal* 165 (2021), p. 107830.

[2] Emilie Lefoulon, John G. McMullen, and S. Patricia Stock. "Transcriptomic analysis of Steinernema nematodes highlights metabolic costs associated to *Xenorhabdus* endosymbiont association and rearing conditions". *Frontiers in Physiology* 13 (2022), p. 821845.

[3] Yiming Huang, Ravi U. Sheth, Shijie Zhao, Lucas A. Cohen, Kendall Dabaghi, Thomas Moody, Yiwei Sun, Deirdre Ricaurte, Miles Richardson, Florencia Velez-Cortes, et al. "High-throughput microbial culturomics using automation and machine learning". *Nature Biotechnology* 41.10 (2023), pp. 1424–1433.

[4] Ryan P. Bartelme, Joy M. Custer, Christopher L. Dupont, Josh L. Espinoza, Manolito Torralba, Banafshe Khalili, and Paul Carini. "Influence of substrate concentration on the culturability of heterotrophic soil microbes isolated by high-throughput dilution-to-extinction cultivation". *mSphere* 5.1 (2020), pp. 10–1128.

[5] Eveline-Marie Lammens, Pablo Ivan Nikel, and Rob Lavigne. "Exploring the synthetic biology potential of bacteriophages for engineering non-model bacteria". *Nature Communications* 11.1 (2020), p. 5294.

[6] Daniel C. Volke, Enrico Orsi, and Pablo I. Nikel. "Emergent CRISPR–Cas-based technologies for engineering non-model bacteria". *Current Opinion in Microbiology* 75 (2023), p. 102353.

[7] Yonatan Chemla, Connor J. Sweeney, Christopher A. Wozniak, and Christopher A. Voigt. "Design and regulation of engineered bacteria for environmental release". *Nature Microbiology* 10.2 (2025), pp. 281–300.

Appendix A

XENORHABDUS GRIFFINIAE HAS TWO PHENOTYPIC VARIANTS

A.1 Introduction

Many bacteria are known to have two phenotypic variants that they can switch between, reversibly or irreversibly, to accommodate different lifestyles [1, 2]. In the early 80s, the first example of *Xenorhabdus* spp. typically having two phenotypic variants, or forms, that they can be in was described [3]. The primary form is characterized by antibiotic production, motility, fimbriae on the cell surface, larger cell size, the ability to bind blue dye on nitroblue tetrazolium (NBT) agar plates and agglutinate red blood cells, etc. [4]. These forms can be a reflection of the adaptation that is required to switch between being a nematode symbiont and a virulent insect killer.

If we want to develop a more comprehensive understanding of how the bacteria can shift between these forms, both in the lab and *in insecta*, the first step would be to do a comprehensive RNA-sequencing study, to try to figure out how this shift is regulated and what genes are causing the phenotypic differences described.

When I was making deletion strains for Chapter 5, my transconjugants had a lack of pigmentation, making me wonder if they had turned into secondary form or if this was a phenotype of deleting *ymdA*. After doing two complementary tests in addition to seeing lack of pigmentation, I could confirm that the transconjugants had indeed shifted into secondary form. Then I had to redo my conjugation to obtain transconjugants that were in primary form. Below I outline what we currently know about primary and secondary variants in *X. griffiniae*.

A.2 Results

There are several common phenotypic tests that can be done to determine whether *Xenorhabdus* is in its primary or secondary form. The first one we tested was to plate the bacteria on NBT agar plates. On these plates, the primary form cells appear blue after two days of growth, whereas secondary form bacteria appear red (Figure A.1)

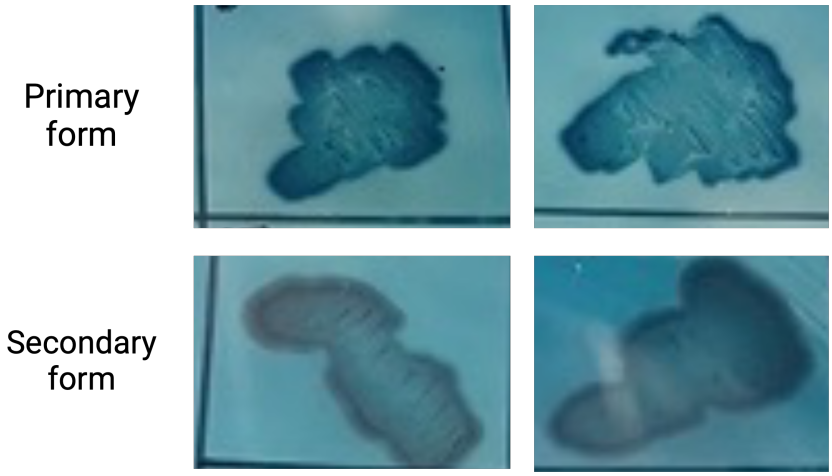

Figure A.1: Upper row: primary form bacteria appear blue after two days of growth. Lower row: secondary form bacteria appear red after two days of growth.

The second test we did was assessing the ability of the bacteria to produce antibiotics. This is tested by *E. coli* growth inhibition. Primary form cells inhibit a lawn of *E. coli* DH10β in a halo around the *Xenorhabdus* colony, whereas secondary form cells do not (Figure A.2)

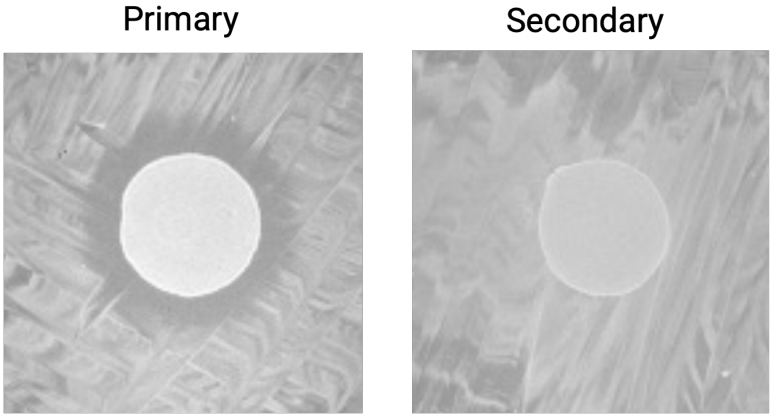

Figure A.2: Primary form bacteria produce antibiotics and will inhibit growth of an *E. coli* DH10β lawn, seen by a clearing around the *X. griffiniae* colony in the center. Secondary form bacteria do not produce antibiotics and will not inhibit growth of *E. coli*.

The last test we did was to grow the bacteria in liquid cultures (minimal and rich media). Secondary form bacteria reach a higher optical density in minimal media than primary form bacteria (Figure A.3).

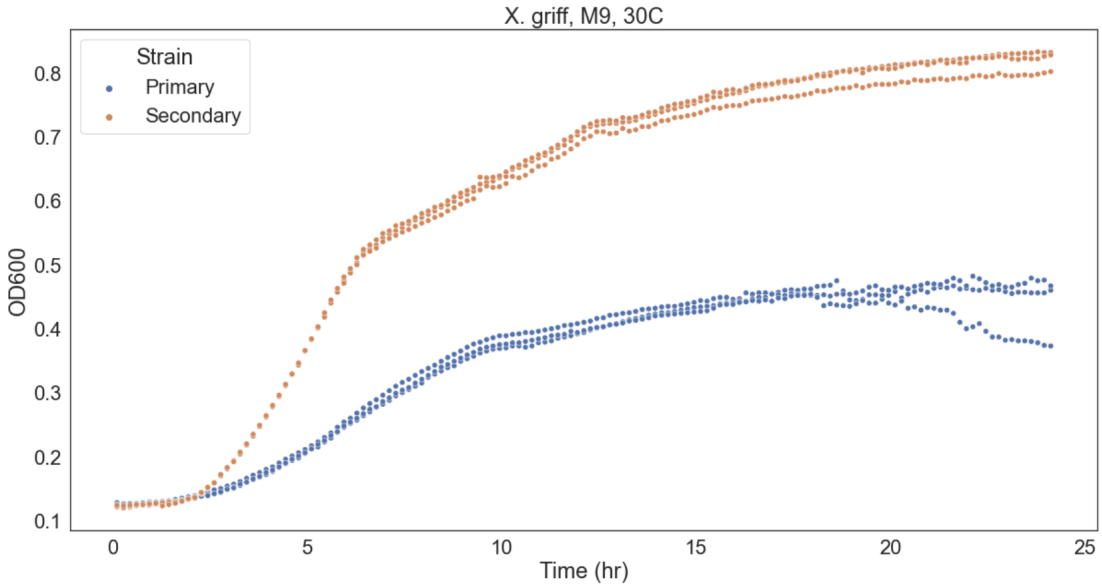

Figure A.3: Secondary form bacteria can reach a higher OD than primary form bacteria in minimal M9 glucose media. Time traces for three technical replicates per strain plotted.

Primary and secondary form bacteria reach the same optical density in rich growth medium (LB), but primary form bacteria have a longer lag time than secondary form bacteria (Figure A.4).

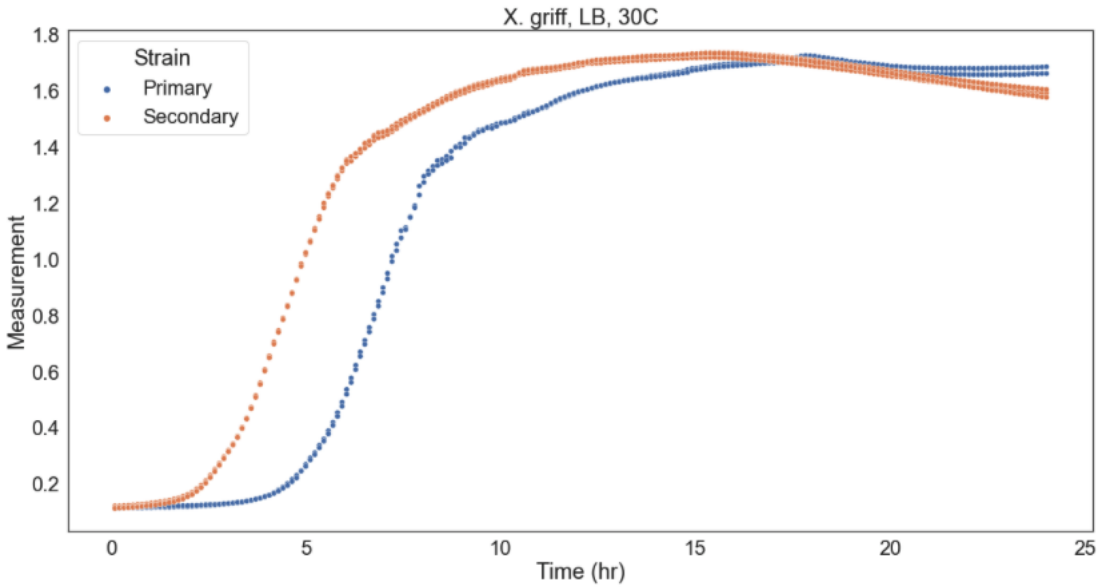

Figure A.4: Secondary form bacteria reaches the same OD as primary form bacteria in rich medium, but has a shorter lag time than primary form bacteria. Time traces for three technical replicates per strain plotted.

A.3 Materials and methods

Dye binding

NBT agar plates:

8 g LB broth

15 g agar

0.025 g bromothymol blue

1 g sodium pyruvate

1 L MilliQ water

Autoclave 20 min LIQ cycle and let cool. Add 0.04 g triphenyltetrazolium chloride.

Streak out bacteria from a glycerol stock or liquid culture onto the plates. After 2 days of growth primary form will be blue color and secondary form will be red.

Antibiotic production

E. coli DH10β were streaked out on an LB agar plate to cover the whole surface. The plate was then dried for 20 minutes. A spot of dense *X. griffiniae* culture was added to the center of the plate. The plate was then incubated over night at 30°C.

Growth rates

Primary and secondary form *X. griffiniae* were grown in a Biotek plate reader for 24 h at 30°C with continuous linear shaking.

References

[1] Neena Jain, Abraham Guerrero, and Bettina C. Fries. "Phenotypic switching and its implications for the pathogenesis of *Cryptococcus neoformans*". *FEMS yeast research* 6.4 (2006), pp. 480–488.

[2] Lucía García-Pastor, Elena Puerta-Fernández, and Josep Casadesús. "Bistability and phase variation in *Salmonella enterica*". *Biochimica et biophysica acta (BBA)-gene regulatory mechanisms* 1862.7 (2019), pp. 752–758.

[3] Raymond J. Akhurst. "Morphological and functional dimorphism in *Xenorhabdus* spp., bacteria symbiotically associated with the insect pathogenic nematodes *Neoaplectana* and *Heterorhabditis*". *Microbiology* 121.2 (1980), pp. 303–309.

[4] Antonia Volgyi, Andras Fodor, Attila Szentirmai, and Steven Forst. "Phase variation in *Xenorhabdus nematophilus*". *Applied and Environmental Microbiology* 64.4 (1998), pp. 1188–1193.